GEC87

40th Annual Gaseous Electronics Conference

October 13-16, 1987

Georgia Institute of Technology
Atlanta, Georgia

UNCLASSIFIED

SECURITY CLASSIFICATION OF THIS PAGE

REPORT DOCUMENTATION PAGE

1a. REPORT SECURITY CLASSIFICATION UNCLASSIFIED	1b. RESTRICTIVE MARKINGS
2a. SECURITY CLASSIFICATION AUTHORITY	3. DISTRIBUTION / AVAILABILITY OF REPORT Approved for public release; distribution is unlimited.
2b. DECLASSIFICATION / DOWNGRADING SCHEDULE	
4. PERFORMING ORGANIZATION REPORT NUMBER(S)	5. MONITORING ORGANIZATION REPORT NUMBER(S) AFOSR-TR- 88-1245
6a. NAME OF PERFORMING ORGANIZATION Georgia Tech Research Corporation 6b. OFFICE SYMBOL (If applicable)	7a. NAME OF MONITORING ORGANIZATION AFOSR/NP
6c. ADDRESS (City, State, and ZIP Code) Centennial Research Bdg, Rm 24 Atlanta, GA 30332-0420	7b. ADDRESS (City, State, and ZIP Code) Building 410, Bolling AFB DC 20332-6448
8a. NAME OF FUNDING / SPONSORING ORGANIZATION AFOSR 8b. OFFICE SYMBOL (If applicable) NP	9. PROCUREMENT INSTRUMENT IDENTIFICATION NUMBER AFOSR-87-0339
8c. ADDRESS (City, State, and ZIP Code) Building 410, Bolling AFB DC 20332-6448	10. SOURCE OF FUNDING NUMBERS PROGRAM ELEMENT NO. 61102F; PROJECT NO. 2301; TASK NO. A4; WORK UNIT ACCESSION NO.
11. TITLE (Include Security Classification) (U) THE FORTIETH ANNUAL GASEOUS ELECTRONICS CONFERENCE	
12. PERSONAL AUTHOR(S) Dr M R Flannery	
13a. TYPE OF REPORT FINAL 13b. TIME COVERED FROM 1 Sep 87 TO 31 Aug 88	14. DATE OF REPORT (Year, Month, Day) July 1988 15. PAGE COUNT 194
16. SUPPLEMENTARY NOTATION	
17. COSATI CODES FIELD / GROUP / SUB-GROUP 2008	18. SUBJECT TERMS (Continue on reverse if necessary and identify by block number)

19. ABSTRACT (Continue on reverse if necessary and identify by block number)

The Fortieth Annual Gaseous Electronics Conference was held 13-16 Oct, 1987 at the Georgia Institute of Technology. Thirty-one scientific sessions were held and approximately four hundred papers were presented.

20. DISTRIBUTION / AVAILABILITY OF ABSTRACT X ☐ UNCLASSIFIED/UNLIMITED X ☐ SAME AS RPT. ☐ DTIC USERS	21. ABSTRACT SECURITY CLASSIFICATION UNCLASSIFIED
22a. NAME OF RESPONSIBLE INDIVIDUAL R E KELLEY	22b. TELEPHONE (Include Area Code) (202) 767-4908 22c. OFFICE SYMBOL AFOSR/NP

DD FORM 1473, 84 MAR

83 APR edition may be used until exhausted.
All other editions are obsolete.

SECURITY CLASSIFICATION OF THIS PAGE
UNCLASSIFIED

40th Annual Gaseous Electronics Conference

GEC87

13-16 October 1987
Atlanta, Georgia

PROGRAM AND ABSTRACTS

A topical conference of The American Physical Society

Sponsored by

The Georgia Institute of Technology
The American Physical Society:
Division of Atomic, Molecular and Optical Physics

EXECUTIVE COMMITTEE

GEORGIA TECH COMMITTEE

School of Physics: M. R. Flannery, I. R. Gatland, M. M. Graff, E. W. McDaniel, E. J. Mansky II, A. Ralston, R. Roy and T. Uzer

School of Mechanical Engineering: T. L. Eddy

Education Extension Services: Chris Carter, Deidre Mercer, Irene Miller, Bettye Parker, Trish Stolton and Marcus Yarbrough

ACKNOWLEDGEMENTS

The Gaseous Electronics Conference gratefully acknowledges the support of The Georgia Institute of Technology where the Conference is held and The Georgia Tech Committee for the local arrangements. Financial support for the Gaseous Electronics Conference has been provided by:

The Air Force Office of Scientific Research

The National Science Foundation

The Office of Naval Research

The General Electric Company

GTE

Electromagnetic Sciences (Atlanta)

The System Works (Atlanta)

The Gaseous Electronics Conference is a Topical Conference of the American Physical Society with sponsorship by the Division of Electron and Atomic Physics.

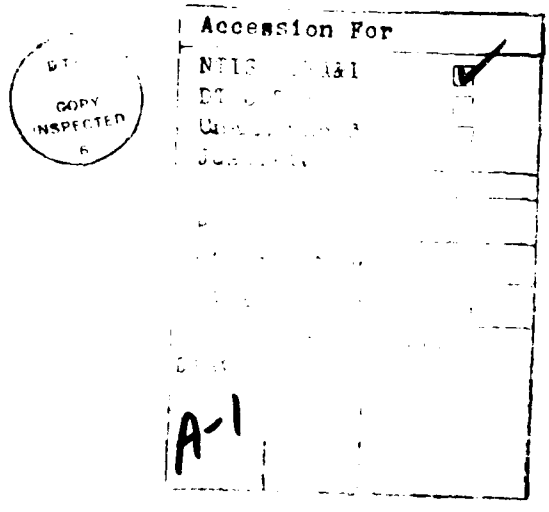

CONTENTS

PROGRAM

FORTIETH ANNUAL

GASEOUS ELECTRONICS CONFERENCE

October 12-16, 1987

All scientific sessions held in Paul Weber Building, Rooms 3-5, Space Science and Technology Center (SSTC), Georgia Institute of Technology, Atlanta, Georgia

Monday, October 12

6:30 PM - 9:30 PM		Reception and Registration	Pierremont Plaza Hotel

Tuesday, October 13

			SSTC-Room
8:00 AM - 8:10 AM	A	Welcome (Vice President John Hooper)	3-5
8:10 AM - 9:55 AM	A	Atomic Collisions and Recombination (T. F. Moran)	3-5
10:15 AM - 11:45 AM	BA	Breakdown and Switching (R. DeWitt)	5
10:15 AM - 11:45 AM	BB	Plasma Deposition (P. Hargis)	4
1:15 PM - 2:55 PM	CA	Electron-Impact Cross Sections I (B. Bederson)	5
1:15 PM - 3:15 PM	CB	Sheaths: Models and Experiments (K. Greenberg)	4
3:15 PM - 6:00 PM	D	Posters (A. Larson) posted from 12 Noon	3
	DA	Heavy Particle Collisions	3
	DB	Recombination and Attachment	3
	DC	Lamps and Arcs	3
	DD	Radiative Properties	3

Wednesday, October 14

8:00 AM - 10:05 AM	EA	Molecular Clusters (M.M. Graff)	5
8:00 AM - 10:00 AM	EB	RF Glows: Experiment (P.A. Miller)	4
10:25 AM - 11:55 AM	FA	Plasma Etching (J. Kramer)	5
10:25 AM - 11:55 AM	FB	High Field Discharges (T. Moratz)	4
1:15 PM - 3:10 PM	GA	Electron-Impact Cross Sections II (M. Inokuti)	5
1:15 PM - 3:10 PM	GB	Laser Diagnostics (T. Intrator)	4
3:15 PM - 6:00 PM	H	Posters (M. Menendez), posted from 9:00 AM - 6:00 PM	3
	HA	Electron-Impact Excitation: Experiment	3
	HB	Electron-Impact Excitation: Theory	3
	HC	RF Plasmas	3
4:00 PM - 6:00 PM		Physical Review Drop-In (B. Bederson and C. Kraner)	5
7:30 PM - 10:00 PM	I	Electron-Impact Theory Panel (J.N. Bardsley and M.R. Flannery)	5
7:30 PM - 10:00 PM	J	Posters (T. Eddy), posted from 6:00 PM	3
	JA	Swarms and Breakdown	3
	JB	D.C. Glows	3
	JC	Sheaths	3

Thursday, October 15

8:00 AM - 9:45 AM	KA	Recombination and Ion-Molecule Collisions (M. Mandich)	5
8:00 AM - 9:05 AM	KB	Beams and Radiation Produced Plasmas (K. Stalder)	4
10:00 AM - 11:30 AM	LA	Electron-Impact Cross Sections III (J. Ajello)	5
9:25 AM - 11:20 AM	LB	High Intensity Discharge Lamps (H. Witting)	4
11:30 AM - 12 Noon		Business Meeting (J. Proud)	4
1:30 PM - 3:25 PM	MA	Electron-Impact Cross Sections IV (W. Blumberg)	5
1:30 PM - 3:25 PM	MB	Microscopic Modeling of Discharges (J.P. Boeuf)	4
3:45 PM - 5:15 PM	NA	Laser Kinetics (K.Y. Tang)	5
3:45 PM - 5:30 PM	NB	Arcs (A. Bhattacharya)	4
6:30 PM -		Social Hour and Banquet	Pierremont Plaza Hotel

Friday, October 16

8:00 AM - 10:10 AM	O	Macroscopic Modeling of Discharges (V. Godyak)	3-5
10:30 AM - 12:10 PM	P	Electron-Impact Cross Sections V (L.C. Lee)	3-5

ROOM ALLOCATION

DATE	TIME	SSTC ROOMS		
		Room 5	Room 4	Room 3
Tuesday, October 13	8:00 AM	- - - - - - - - - -	A	- - - - - - - - -
	10:15 AM	BA	BB	--
	1:15 PM	CA	CB	--
	3:15 PM	--	--	D (Posters)
Wednesday, October 14	8:00 AM	EA	EB	--
	10:25 AM	FA	FB	--
	1:15 PM	GA	GB	--
	3:15 PM	--	--	H (Posters)
	4:00 PM	Phys. Rev.	--	--
	7:30 PM	I	--	J (Posters)
Thursday, October 15	8:00 AM	KA	KB	--
	10:00 AM	LA	LB	--
	11:30 AM	--	Business	--
	1:30 PM	MA	MB	--
	3:45 PM	NA	NB	--
Friday, October 16	8:00 AM	- - - - - - - - - -	O	- - - - - - - - -
	10:30 AM	- - - - - - - - - -	P	- - - - - - - - -

FORTY YEARS OF GASEOUS ELECTRONICS CONFERENCES

	Year	Hosts Location	Chairman Secretary	Number of Papers	Number of Authors
1.	1948	**Brookhaven National Laboratory** Upton, Long Island, NY	L. H. Fisher J. B. H. Kuper	38	34
2.	1949	**Mellon Institute** Pittsburgh, PA	W. P. Allis D. Alpert	49	48
3.	1950	**Bell Laboratories** Barbizon Plaza, New York, NY	W. P. Allis N. D. Hagstrum	68	50
4.	1951	**General Electric Research Lab.** Schnectady, NY	W. P. Allis H. W. Hull	30	48
5.	1952	**R. C. A. Laboratories** Princeton University, NJ	W. P. Allis L. Malter	35	47
6.	1953	**Office of Naval Research** Washington, DC	W. P. Allis W. R. Gruner	43	61
7.	1954	**New York University** New York, NY	W. P. Allis L. H. Fisher	45	59
8.	1955	**General Electric Research Lab.** Schnectady, NY	W. P. Allis J. D. Cobine	48	70
9.	1956	**Westinghouse Research Lab.** Pittsburgh, PA	W. P. Allis A. V. Phelps	48	70
10.	1957	**M.I.T. and Sylvania** Cambridge, MA	W. P. Allis S. C. Brown	42	59
11.	1958	**Bell Telephone Laboratories** Barbizon Plaza, New York, NY	W. P. Allis D. J. Rose	64	102
12.	1959	**National Bureau of Standards** Washington, DC	W. P. Allis L. M. Branscomb	51	91
13.	1960	**Naval Postgraduate School** Monterey, CA	W. P. Allis N. L. Oleson	61	93
14.	1961	**General Electric** Schnectady, NY	W. P. Allis C. J. Gallagher	55	116
15.	1962	**National Bureau of Standards** Boulder, CO	M. A. Biondi E. C. Beaty	81	146
16.	1963	**University of Pittsburgh and Westinghouse** Pittsburgh, PA	M. A. Biondi G. J. Schulz	53	102

17.	1964	**Army Electronics Laboratories** Atlantic City, NJ	M. A. Biondi S. Schneider	86	137
18.	1965	**University of Minnesota and Honeywell** Minneapolis, MN	A. V. Phelps L. M. Chanin	83	143
19.	1966	**Georgia Institute of Technology** Atlanta, GA	A. V. Phelps J. W. Hooper E. W. McDaniel	109	203
20.	1967	**Lockheed** Palo Alto, CA	L. H. Fisher R. N. Varney	113	184
21.	1968	**National Bureau of Standards** Boulder, CO	L. H. Fisher G. H. Dunn	69	208
22.	1969	**Oak Ridge National Laboratory** Gatlinburg, TN	G. J. Schulz G. F. Barnett	141**	279
23.	1970	**United Aircraft Research** Hartford, CN	G. J. Schulz R. H. Bullis	158**	283
24.	1971	**University of Florida** Gainesville, FL	G. H. Dunn T. L. Bailey	166**	264
25.	1972	**University of Western Ontario** London, Ontario, CANADA	G. H. Dunn J. W. McGowan	197**	217
26.	1973	**University of Wisconsin** Madison, WI	G. E. Weissler C. C. Lin	158**	281
27.	1974	**Rice University** Houston, TX	G. E. Weissler R. O. Rundel	172**	311
28.	1975	**University of Missouri** Rolla, MO	R. H. Bullis L. D. Schearer	149	169
29.	1976	**General Electric, Nela Park** Cleveland, OH	R. H. Bullis J. H. Ingold	169	285
30.	1977	**SRI International** Palo Alto, CA	F. C. Fehsenfeld J. R. Peterson	215	390
31.	1978	**SUNY** Buffalo, NY	F. C. Fehsenfeld D. M. Bennenson	195	355
32.	1979	**Westinghouse Res. & Development** Pittsburgh, PA	J. D. Schearer P. J. Chantry	154	262
33.	1980	**University of Oklahoma** Norman, OK	J. D. Schearer R. M. St.John	148	369

**Including Arc Symposium

34.	1981	**AVCO, Everett** Boston, MA	L. P. Harris M. L. Boness	142	309
35.	1982	**University of Texas** Dallas, TX	L. P. Harris C. B. Collins	129L 25P 154T	281
36.	1983	**State University of New York** Albany, NY	A. Garscadden G. A. Farrall	91L 34P 125T	245
37.	1984	**National Bureau of Standards & JILA** Boulder, CO	A. Garscadden E. C. Beaty	98L 72P 170T	323
38.	1985	**Naval Postgraduate School** Monterey, CA	J. T. Verdeyen O. Biblarz	101L 49P 150T	265
39.	1986	**University of Wisconsin** Madison, WI	J. T. Verdeyen L. W. Anderson	116L 84P 210T	396
40.	1987	**Georgia Institute of Technology** Atlanta, GA	J. M. Proud M. R. Flannery	128L 103P 231T	444

L: Lectures
P: Posters
T: Total Papers

TECHNICAL PROGRAM

FORTIETH ANNUAL

GASEOUS ELECTRONICS CONFERENCE

RECEPTION AND REGISTRATION

6:30 PM - 9:30 PM
Monday, October 12, 1987
Pierremont Hotel

WELCOMING REMARKS: Dr. John Hooper (Vice President, Georgia Tech)
8:00 AM - 8:10 AM, Tuesday, October 13, 1987
Space Science and Technology Center, Rooms 3-5

PLENARY SESSION A. ATOMIC COLLISIONS AND RECOMBINATION

8:[illegible]AM - 9:55 AM, Tuesday, October 13
Space Science and Technology Center, Rooms 3-5.
Chairman: T. F. Moran (Georgia Tech)

8:10 - 8:35	A-1.	THE THIRD WAVE: ATOMIC COLLISIONS SINCE 1963 E. W. McDaniel (Invited Paper)
8:35 - 9:00	A-2.	DISSOCIATIVE RECOMBINATION: FROM THE IONOSPHERE TO THE LABORATORY AND BACK AGAIN M. A. Biondi (Invited Paper)
9:00 - 9:25	A-3.	RECOMBINATION: CALCULATIONS, SIMULATIONS AND APPLICATIONS J. N. Bardsley (Invited Paper)
9:25 - 9:50	A-4.	TERMOLECULAR RECOMBINATION M. R. Flannery (Invited Paper)

SESSION BA. BREAKDOWN AND SWITCHING

10:15 AM - 11:46 AM, Tuesday, October 13
Space Science and Technology Center, Room 5
Chairman: R. DeWitt (Naval Surface Weapons Center)

10:15 - 10:28	BA-1.	CALCULATION OF ELECTRON TRANSPORT PARAMETERS AND CRITICAL FIELD STRENGTHS FOR THE GAS MIXTURES SF_6/CO_2, SF_6/Ar, SF_6/Ne, and SF_6/He Th. Aschwanden, R. J. Van Brunt and A. V. Phelps

10:28 - 10:41 BA-2. STREAMER PROCESS IN TRIGGERED BREAKDOWN
F. E. Peterkin and P. F. Williams

10:41 - 10:54 BA-3. MICRODISCHARGE PROPERTIES OF DIELECTRIC-BARRIER DISCHARGES
U. Kogelschatz and B. Eliasson

10:54 - 11:07 BA-4. CHARACTERIZATION OF METASTABLE NITROGEN IN THE EFFLUENTS OF OZONIZER-TYPE DISCHARGES
L. G. Piper and W. P. Cummings

11:07 - 11:20 BA-5. A SPARK GAP RECOVERY SIMULATION CODE
L. P. Rosen, M. Von Dadelszen and R. D. Milroy

11:20 - 11:33 BA-6. BREAKDOWN STRENGTH AND RECOVERY OF A STEAM INSULATED SPARK GAP
W. J. Thayer and V. C. H. Lo

11:33 - 11:46 BA-7. SIMULATION OF ELECTRON SCATTERING FROM DIELECTRICS IN SURFACE DISCHARGES
T. L. Peck and M. J. Kushner

SESSION BB. PLASMA DEPOSITION

10:15 AM - 11:45 AM, Tuesday, October 13
Space Science and Technology Center, Room 4
Chairman: P. Hargis (Sandia National Laboratories)

10:15 - 10:28 BB-1. ATTACHMENT IN SILANE-HELIUM RF DISCHARGES
L. J. Overzet and J. T. Verdeyen

10:24 - 10:41 BB-2. MASS SPECTROSCOPIC STUDIES OF SILANE AND SILANE-HYDROGEN GLOW DISCHARGES
J. R. Doyle, M. Z. He, G. H. Lin and A. Gallagher

10:41 - 10:54 BB-3. OPTICAL EMISSION AND MASS SPECTROMETRIC DIAGNOSTICS OF SILANE AND DISILANE RF DISCHARGES
H. Chatham and P. K. Bhat

10:54 - 11:19 BB-4. SIMULATION OF SUBSTRATE SURFACE PHYSICS IN RF SPUTTERING
W. L. Morgan
(Long Paper)

11:19 - 11:32 BB-5. HYDROGEN ISOTOPE CONCENTRATION INSIDE AMORPHOUS SILICON THIN FILMS PRODUCED BY Ar-SiH_4-D_2 MIXTURE GAS
X. Chan, J. S. Chang and A. A. Berezin

11:32 - 11:45 BB-6. HYDROGEN-REDUCED MULTILAYER DEPOSITION OF CARBON THIN FILMS
H. Sugai, S. Ohshita, S. Yoshida and T. Okuda

SESSION CA. ELECTRON-IMPACT CROSS SECTIONS I

1:15 PM - 2:55 PM, Tuesday, October 13
Space Science and Technology Center, Room 5
Chairman: B. Bederson (New York University)

1:15 - 1:40 CA-1. MEASUREMENTS OF ELECTRON IMPACT IONIZATION CROSS SECTIONS
R. S. Freund, R. C. Wetzel, T. R. Hayes, R. J. Shul and F. A. Baiocchi
(Invited Paper)

1:40 - 2:05 CA-2. ELECTRON EXCITATION OF THE ALKALIS
A. Gallagher
(Invited Paper)

2:05 - 2:30 CA-3. PROBING ELECTRON-IMPACT EXCITATION USING V.U.V. POLARIZATION ANALYSIS
J. W. McConkey
(Invited Paper)

2:30 - 2:55 CA-4. A TECHNIQUE FOR MEASURING ELECTRON EXCITATION CROSS SECTIONS FROM TRANSIENT SPECIES
L. W. Anderson, D. L. A. Rall, F. A. Sharpton, M. B. Schulman, J. E. Lawler and C. C. Lin
(Invited Paper)

SESSION CB. SHEATHS: MODELS AND EXPERIMENTS

1:15 PM - 3:15 PM, Tuesday, October 13
Space Science and Technology Center, Room 4
Chairman: K. Greenberg (Sandia National Laboratory)

1:15 - 1:28 CB-1. QUADRATIC STARK LASER SPECTROSCOPY DETERMINATION OF THE ELECTRIC FIELD DISTRIBUTION IN THE CATHODE SHEATH OF AN ELECTRON BEAM GLOW DISCHARGE
S. A. Lee, L.-U.A. Andersen, J. J. Rocca, M. C. Marconi and N. D. Reesor

1:28 - 1:41 CB-2. MEASUREMENT OF THE LOCAL ELECTRIC FIELD IN DISCHARGES USING LASER STARK SPECTROSCOPY OF NaK
J. Derouard, H. Debontride and N. Sadeghi

1:41 - 1:54 CB-3. CURRENT BALANCE AT THE SURFACE OF A COLD CATHODE
J. E. Lawler, E. A. Den Hartog and D. A. Doughty

1:54 - 2:07 CB-4. PLASMA-SHEATH PARAMETERS AT INTERMEDIATE PRESSURES
V. Godyak and N. Sternberg

2:07 - 2:20 CB-5. ELECTRON ENERGY DISTRIBUTION NEAR AN ORIFICE IN Hg-Ne LOW PRESSURE DISCHARGE
R. Lagushenko, V. Godyak and J. Maya

2:20 - 2:33 CB-6. A ONE DIMENSIONAL MODEL FOR THE INVESTIGATION OF AVALANCHING DC CATHODE SHEATHS
R. D. Milroy, M. Von Dadelszen and L. P. Rosen

2:33 - 2:46 CB-7. AN APPROXIMATE SELF-CONSISTENT SOLUTION FOR A COLLISIONAL PRE-SHEATH IN A FULLY IONIZED PLASMA
G. L. Main

2:46 - 2:59 CB-8. STUDY OF INTENSE PULSED GLOW DISCHARGES
B. Szapiro, H. F. Ranea-Sandouval, C. Murray and J. J. Rocca

2:59 - 3:12 CB-9. STUDY OF SOFT VACUUM ELECTRON BEAM GENERATION USING LASER OPTO-GALVANIC SPECTROSCOPY
S. Moriya, P. Zeller and G. J. Collins

SESSION D. POSTERS

3:15 PM - 6:00 PM, Tuesday, October 13
Chairman: A. Larson (Georgia Tech)
Space Science and Technology Center, Room 3

All posters may be assembled from 12 noon and manned from 3:15 PM

SESSION DA. HEAVY PARTICLE COLLISIONS

DA-1. THRESHOLD PHOTOIONIZATION STUDIES OF SILVER CLUSTERS
K. Laihing, P. Y. Cheng and M. A. Duncan

DA-2. LONG-LIVED, WEAKLY BOUND ELECTRONICALLY EXCITED COMPLEXES FORMED IN METAL BASED OXIDATIONS
M. J. McQuaid and J. L. Gole

DA-3. PRODUCTION AND STABILITY OF Ar_3^+ and Ar_4^+
P. Scheier, M. Lezius, T. D. Mark, C. R. Albertoni and R. Castleman, Jr.

DA-4. REACTIONS OF He_2^+ and $He(2^3S)$ WITH SELECTED ATOMIC AND MOLECULAR SPECIES AT ATMOSPHERIC PRESSURES
J. M. Pouvesle, A. Khacef, J. Stevefelt, H. Jahani, V. T. Gylys and C. B. Collins

DA-5. FINE STRUCTURE EFFECTS IN THE REACTIVE COLLISION $O+OH-O_2+H$
M. M. Graff, A. F. Wagner and A. C. Allison

DA-6. EXPERIMENTAL STUDY OF REACTIVE COLLISIONS OF HIGH-TEMPERATURE SYSTEMS
M. M. Graff

DA-7. FAST METASTABLE ARGON ATOMS FROM A HOT CATHODE DISCHARGE
J. W. Sheldon and K. A. Hardy

DA-8. FREE RADICAL PROCESSES IN SF_6/O_2 PLASMAS
K. R. Ryan and I. C. Plumb

DA-9. COLLISIONAL DESTRUCTION OF METASTABLE N_2 ($a''^1\Sigma_g^+$) MOLECULES BY N_2
A. B. Wedding and A. V. Phelps

DA-10. QUENCHING OF Ar METASTABLES IN RADIO FREQUENCY GLOW DISCHARGES
G. R. Scheller, R. A. Gottscho T. Intrator and D. B. Graves

DA-11. ZEEMAN MIXING INDUCED IN COLLISIONS OF 5^2P K ATOMS WITH NOBLE GASES
R. Berends, W. Kedzierski and L. Krause

DA-12. WALL VIBRATIONAL DEEXCITATION EFFECTS ON THE VIBRATIONAL TEMPERATURE IN WEAKLY IONIZED NITROGEN PLASMAS
S. Ono and S. Teii

DA-13. HIGHLY EXCITED MOLECULAR HYDROGEN CONFINED IN A SUPERFLUID HELIUM FILM COATED CELL
Y. M. Xiao, S. Buchman, L. Pollack, D. Kleppner and T. J. Greytak

DA-14. CONNECTIONS BETWEEN FAST ATOMIC COLLISIONS AND THREE BODY COULOMB STATES
M. G. Menendez and M. M. Duncan

SESSION DB. RECOMBINATION AND ATTACHMENT

DB-1. MEASUREMENT OF THE RECOMBINATION RATE OF Cs^+ and e^- IN HIGH PRESSURE MOLECULAR GASES
S. M. Jaffe, M. Mitchner and S. A. Self

DB-2. FINAL STATE ENERGY DISTRIBUTION PRODUCED BY HYDROGEN ATOM RECOMBINATION
M. L. Homer and A. E. Orel

DB-3. ELECTRON ATTACHMENT RATE CONSTANTS OF BROMINE COMPOUNDS
W. C. Wang, D. P. Wang and L. C. Lee

DB-4. ELECTRON ATTACHMENT TO SF_6 IN N_2, Ar and Xe BUFFER GASES
S. R. Hunter, J. G. Carter and L. G. Christophorou

DB-5. VIBRATIONAL ACCOMMODATION COEFFICIENTS AND DISSOCIATIVE ATTACHMENT 'THERMOMETRY'
C. Chu, K. L. Stricklett and P. D. Burrow

DB-6. DISSOCIATIVE ATTACHMENT OF ELECTRONS TO TRANSITION METAL SUPERACIDS
T. M. Miller, A. E. S. Miller, J. F. Friedman and D. J. Ewing

DB-7. EFFECT OF TEMPERATURE ON THE NONDISSOCIATIVE ELECTRON ATTACHMENT TO $n\text{-}C_4F_{10}$, $n\text{-}C_6F_{14}$, and $c\text{-}C_4F_6$
P. G. Datskos and L. G. Christophorou

SESSION DC. LAMPS AND ARCS

DC-1. DETERMINATION OF TEMPERATURE IN A HIGH PRESSURE Hg DISCHARGE BY PULSED LASER OPTOGALVANIC SPECTROSCOPY
J. Kramer

DC-2. A LASER-TRIGGERED HIGH VOLTAGE SWITCH USING A COMPOSITE TARGET PELLET
P. J. Brannon and D. F. Cowgill

DC-3. RADIATION TRAPPING IN SODIUM VAPOR
J. Huennekens, T. Colbert and H. J. Park

DC-4. ANALYTIC TEMPERATURE PROFILE FOR PLASMA DIAGNOSTICS
P. A. Vicharelli and L. C. Pitchford

DC-5. THE ELECTRICAL CONDUCTANCE OF HIGH PRESSURE MERCURY DISCHARGE LAMPS
B. Debbagh-Zriouil, C. Soriano, M. Aubes and J. J. Damelincourt

DC-6. APPLICATION OF GENERALIZED MULTI-THERMAL EQUILIBRIUM MODEL TO COLLISIONAL-RADIATIVE CALCULATIONS FOR NONEQUILIBRIUM HYDROGEN PLASMA
K. Y. Cho and T. L. Eddy

DC-7. SUPERCRITICAL VAPOR IN ARC CATHODE REGION
H. Minoo

DC-8. TRANSVERSE SPREADING MECHANISMS IN THE LOW-PRESSURE MERCURY-ARGON POSITIVE COLUMN
J. T. Dakin

DC-9. A MODEL FOR THE OPTOGALVANIC EFFECT INDUCED IN AN Hg-Ar DISCHARGE
W. Richardson, L. Maleki and E. Garmire

DC-10. PULSE TECHNIQUE FOR PROBE MEASUREMENTS IN GAS DISCHARGE
V. Godyak

SESSION DD. RADIATIVE PROPERTIES

DD-1. INTENSITY DISTRIBUTION OF ATOMIC HELIUM RYDBERG STATE STARK SPECTRA
J. R. Shoemaker, B. N. Ganguly, B. L. Preppernau and A. Garscadden

DD-2. LIFETIME OF He(2^1S) IN HIGH PRESSURE HELIUM ELECTRIC DISCHARGES
D. F. Hudson

DD-3. DETERMINATION OF THE TRANSITION PROBABILITY OF A SELF-REVERSED LINE
D. Karabourniotis, E. Krakakis and J. J. Damelincourt

SESSION EA. MOLECULAR CLUSTERS

8:00 AM - 10:05 AM, Wednesday, October 14
Space Science and Technology Center, Room 5
Chairwoman: M. M. Graff, Georgia Tech

8:00 - 8:25 EA-1. FORMATION AND PHOTODISSOCIATION DYNAMICS OF ANTIMONY AND BISMUTH METAL CLUSTER IONS
M. A. Duncan, M. E. Geusic and R. R. Freeman
(Long Paper)

8:25 - 8:50 EA-2. PHOTODISSOCIATION OF MASS SELECTED CLUSTER IONS
W. C. Lineberger, D. Ray and N. E. Levinger
(Long Paper)

8:50 - 9:15 EA-3. THEORETICAL STUDIES OF MOLECULAR CLUSTERS
D. A. Dixon
(Long Paper)

9:15 - 9:40 EA-4. SEQUENTIAL CLUSTERING REACTIONS OF Si^{+}_{1-7} with SiD_4: IDENTIFICATION OF BOTTLENECKS PREVENTING RAPID GROWTH OF HYDROGENATED SILICON PARTICLES
M. L. Mandich, W. E. Reents, Jr. and M. F. Jarrold
(Long Paper)

9:40 - 10:05 EA-5. PREPARATION, CHARACTERIZATION, AND OXIDATION OF SMALL METAL CLUSTERS
J. L. Gole, R. Woodward, T. C. Devore, S. H. Cobb and M. McQuaid
(Long Paper)

SESSION EB. RF GLOWS: EXPERIMENT

8:00 AM - 9:55 AM, Wednesday, October 14
Space Science and Technology Center, Room 4
Chairman: P. A. Miller (Sandia National Laboratories)

8:00 - 8:13 EB-1. SPATIAL VARIATIONS IN CAPACITIVE RF PLASMAS DUE TO SELF-GENERATED ELECTROMAGNETIC (TEM) SURFACE MODES
S. E. Savas

8:13 - 8:38 EB-2. AN EXPERIMENTAL VIEW OF THE PARALLEL PLATE RADIO FREQUENCY DISCHARGE
G. A. Hebner and J. T. Verdeyen
(Long Paper)

8:38 - 8:51 EB-3. IMPEDANCE CHARACTERISTICS AND ENERGY DEPOSITION IN RF PARALLEL PLATE DISCHARGES
P. Bletzinger

8:51 - 9:04 EB-4. USE OF LANGMUIR PROBES IN RF GLOW DISCHARGE PLASMAS
N. Hershkowitz, M.-H. Cho, C. H. Nam and T. Intrator

9:04 - 9:29 EB-5. METASTABLE AND ELECTRON KINETICS IN RADIO FREQUENCY DISCHARGES THROUGH MIXTURES OF RARE AND ATTACHING GASES
R. A. Gottscho, G. R. Scheller, T. Intrator and D. B. Graves
(Long Paper)

9:29 - 9:42 EB-6. LASER OPTOGALVANIC STUDY OF METASTABLE AND RESONANCE LEVELS OF ARGON IN RF GLOW DISCHARGE
D. E. Murnick, R. B. Robinson, F. A. Moscatelli and M. Colgan

9:42 - 9:55 EB-7. SPECTRAL LINE INTENSITIES IN LOW-PRESSURE SURFACE WAVE DISCHARGES
C. Beneking and P. Anderer

SESSION FA. PLASMA ETCHING

10:25 AM - 11:56 AM, Wednesday, October 14
Space Science and Technology Center, Room 5
Chairman: J. Kramer (GTE Laboratories)

10:25 - 10:38 FA-1. KINETICS OF SULFUR HEXAFLUORIDE PLASMA ETCHING DISCHARGES
K. E. Greenberg and P. J. Hargis, Jr.

10:38 - 10:51 FA-2. NEGATIVE IONS IN SF CORONA DISCHARGES
I. Sauers

10:51 - 11:04 FA-3. PREDICTING PLASMA/REACTIVE ION ETCH TOPOGRAPHY USING MONTE CARLO METHODS
T. J. Cotler, D. S. Grimard, M. S. Barnes and M. Elta

11:04 - 11:17 FA-4. ANISOTROPIC ETCHING IN ELECTRON BEAM GENERATED-PLASMAS
T. R. Verhey, J. J. Rocca and P. K. Boyer

11:17 - 11:30 FA-5. ACTIVATION ENERGY OF HYDROGEN PLASMA ETCHING OF AMORPHOUS BORON FILMS
H. Toyoda, H. Sugai and T. Okuda

11:30 - 11:43 FA-6. PULSED MICROWAVE PLASMA ETCHING OF POLYMERS FOR VLSI APPLICATIONA
T. H. Lin and Y. Tzeng

11:43 - 11:56 FA-7. LASER RAMAN DIAGNOSTICS OF PLASMA ETCHING DISCHARGES
P. J. Hargis, Jr. and K. E. Greenberg

SESSION FB. HIGH FIELD DISCHARGES

10:25 AM - 11:55 AM, Wednesday, October 14
Space Science and Technology Center, Room 4
Chairman: T. Moratz (University of Illinois)

10:25 - 10:38 FB-1. NON-EQUILIBRIUM MODELS FOR ELECTRONS IN AN IONIZED GAS AND INFLUENCED BY SPACE-TIME VARYING ELECTRIC FIELDS
E. E. Kunhardt, C. Wu and B. M. Penetrante

10:38 - 10:55 FB-2. IONIZATION RATES AND INDUCTION TIMES AT VERY HIGH FIELD STRENGTHS IN N_2, H_2, NO, Ne, AND Ar
J. T. Verdeyen, G. N. Hays, J. B. Gerardo, L. C. Pitchford and Y. M. Li

10:55 - 11:12 FB-3. A SIMPLE MODEL FOR ELECTRON TRANSPORT AND RATE COEFFICIENTS AT HIGH E/N
Y. M. Li and L. C. Pitchford

11:12 - 11:29 FB-4. EXCITATION OF N_2 IN PREBREAKDOWN DISCHARGES AT VERY HIGH E/N
V. T. Gylys and A. V. Phelps

11:29 - 11:42 FB-5. ELECTRICAL BREAKDOWN WAVES: EXACT NUMERICAL SOLUTIONS FOR THE QUASI-NEUTRAL REGION
M. Hemmati and R. G. Fowler

11:42 - 11:55 FB-6. NONEQUILIBRIUM ELECTRON KINETICS IN NITROGEN UNDER HIGH FREQUENCY ELECTRIC FIELD EXCITATION WITH OR WITHOUT A CROSSED D.C. MAGNETIC FIELD
Y. Tzeng, S. Govil and E. E. Kunhardt

SESSION GA. ELECTRON-IMPACT CROSS SECTIONS II

1:15 PM - 3:10 PM, Wednesday, October 14
Space Science and Technology Center, Room 5
Chairman: M. Inokuti (Argonne National Laboratory)

1:15 - 1:40 GA-1. APPLICATIONS OF ELECTRON SCATTERING DATA TO PLANETARY SCIENCE AND ASTROPHYSICS
J. P. Doering
(Invited Paper)

1:40 - 2:05 GA-2. THRESHOLD STUDIES OF H_2 IN THE VACUUM ULTRAVIOLET BY ELECTRON IMPACT
J. M. Ajello, G. K. James and D. E. Shemansky
(Long Paper)

2:05 - 2:30 GA-3. EMISSION OF RADIATION PRODUCED BY ELECTRON BEAM EXCITATION OF OXYGEN GAS
C. C. Lin, M. B. Schulman, R. S. Schappe, F. A. Sharpton, L. W. Anderson, W. A. M. Blumberg and B. D. Green
(Long Paper)

2:30 - 2:43 GA-4. LABORATORY STUDIES OF THE ELECTRON EXCITATION OF SINGLET AND TRIPLET ELECTRONIC STATES OF N_2
B. D. Green, B. L. Upschulte, K. W. Holtzclaw and W. A. M. Blumberg

2:43 - 2:56 GA-5. ANALYSIS OF SCATTERING OF LOW-ENERGY ELECTRONS BY ALKALI HALIDE MONOMERS
M. Zuo, T-Y. Jiang, L. Vuskovic, B. Stumpf and B. Bederson

2:56 - 3:10 GA-6. EFFECT OF TRACE CONCENTRATIONS OF SF_6 ON METASTABLE POPULATIONS IN ARGON RF GLOW DISCHARGE
D. E. Murnick, R. B. Robinson and R. A. Gottscho

SESSION GB. LASER DIAGNOSTICS

1:15 PM - 3:10 PM, Wednesday, October 14
Space Science and Technology Center, Room 4
Chairman: T. Intrator (University of Wisconsin)

1:15 - 1:40 GB-1. LASER-PRODUCED PHOTODETACHMENT AS A PROBE FOR NEGATIVE ION POPULATIONS IN OXYGEN
T. H. Teich
(Invited Paper)

1:40 - 1:53 GB-2. PHOTODETACHMENT MEASUREMENT OF H^- DENSITY PROFILE IN A PLANAR DIODE GLOW DISCHARGE
B. N. Ganguly and A. Garscadden

1:53 - 2:18 GB-3. RADIAL DEPENDENT DENSITY MEASUREMENTS OF Hg ($^3P_{0,1,2}$) IN A Hg-Ar DISCHARGE
L. Bigio
(Long Paper)

2:18 - 2:31 GB-4. BARIUM DENSITY MEASUREMENT IN THE VICINITY OF OXIDE COATED ELECTRODES
A. K. Bhattacharya and A. Awadallah

2:31 - 2:56 GB-5. DIRECT OBSERVATION OF Ba^+ VELOCITY DISTRIBUTION IN A DRIFT TUBE USING SINGLE-FREQUENCY LASER-INDUCED FLUORESCENCE
R. A. Dressler, H. Meyer, A. O. Langford,
V. M. Bierbaum and S. R. Leone
(Long Paper)

2:56 - 3:10 GB-6. OPTOGALVANIC SPECTRUM OF OH IN A WATER-NEON HOLLOW CATHODE DISCHARGE
S. P. Lee, S. Deshmukh, G. P. Reck and E. W. Rothe

SESSION H. POSTERS

3:15 PM - 6:00 PM, Wednesday, October 14
Chairman: M. Menendez (University of Georgia)
Space Science and Technology Center, Room 3

All posters may be assembled from 9:00 AM onwards, manned from 3:15 PM, and taken down at 6:00 PM.

SESSION HA. ELECTRON-IMPACT EXCITATION: EXPERIMENT

HA-1. QUANTITATIVE V.U.V. POLARIZATION DATA USING AN ELECTRON-IMPACT SOURCE
W. Karras, P. Hammond and J. W. McConkey

HA-2. LASER-INDUCED-FLUORESCENCE STUDIES OF ELECTRON-MOLECULE COLLISIONS
M. Darrach, P. Hammond and J. W. McConkey

HA-3. EXCITATION OF ($^1S_0$) FOLLOWING ELECTRON-IMPACT ON O_2
J. J. Corr, M. A. Khakoo, A. G. McConkey and J. W. McConkey

HA-4. DISSOCIATIVE EXCITATION OF CF_4 FOLLOWING ELECTRON IMPACT
S. Wang, J. L. Forand and J. W. McConkey

HA-5. POLARIZATION CORRELATIONS IN THE RARE GASES FOLLOWING CONTROLLED ELECTRON IMPACT
P. Plessis, P. Hammond, M. A. Khakoo, J. J. Corr and J. W. McConkey

HA-6. COLLISION CROSS SECTIONS AND EXCITATION RATE COEFFICIENTS IN NEON
L. Torchin, S. Mizzi and V. Puech

HA-7. COHERENCE IN ELECTRON-HEAVY RARE GAS COLLISIONS
K. E. Martus and K. Becker

HA-8. ACCURATE ABSOLUTE PHOTOEMISSION CROSS SECTIONS IN THE VUV
R. C. G. Ligtenberg, P. J. M. Van Der Burgt, W. B. Westerveld and J. S. Risley

HA-9. POSITRON AND ELECTRON DIFFERENTIAL ELASTIC SCATTERING BY ATOMS
W. E. Kauppila, S. J. Smith, G. M. A. Hyder, M. Mandavi-Hezaveh, C. K. Kwan and T. S. Stein

HA-10. ELECTRON BEAM GROWTH IN N_2
W. A. M. Blumberg, P. C. F. Ip, B. D. Green, W. J. Marinelli and J. Person

HA-11. LOW ENERGY CROSS SECTION MEASUREMENTS FOR INELASTIC SCATTERING OF ELECTRONS FROM DISILANE
H. Tanaka, Ludwig Boesten, M. A. Dillon and D. Spence

HA-12. PLASMA DOUBLE LAYERS IN ELECTRON IMPACT SPECTROSCOPY OF Hg
P. Nicoletopoulos

HA-13. SECONDARY ELECTRON ENERGY (1eV-200eV) AND ANGULAR DISTRIBUTIONS FOR ELECTRON IMPACT IONIZATION OF CO BY 800eV ELECTRONS
CE MA and R.A. Bonham

SESSION HB. ELECTRON-IMPACT EXCITATION: THEORY

HB-1. ELECTRON IMPACT IONIZATION CROSS SECTION OF ATOMS
H. Deutsch, P. Scheier and T. D. Mark

HB-2. ELECTRON SCATTERING BY Na
A. Z. Msezane

HB-3. ORIENTATION AND ALIGNMENT PARAMETERS FOR e^- + He ($2^{1,3}S$, $2^{1,3}P$) e^- + He($3^{1,3}P$, $3^{1,3}D$) COLLISIONS
E. J. Mansky II and M. R. Flannery

HB-4. A THEORETICAL INVESTIGATION OF ^2P SHAPE RESONANCES IN GROUP II ATOMS USING AN APPROXIMATE VERSION OF FANO'S THEORY
D. Chen and G. A. Gallup

HB-5. ELECTRON-IMPACT EXCITATION OF O-LIKE IONS
A. Z. Msezane, K. J. Reed and R. J. W. Henry

HB-6. ELECTRONIC EXCITATION OF $H_2(X\ ^1\Sigma_g^+, v'')$ MOLECULES TO YIELD $H_2(X\ ^1\Sigma_g^+, v'')$ MOLECULES VIA EXCITATIONS OF THE ELECTRONIC SINGLET SPECTRUM
J. R. Hiskes

HB-7. MOLECULAR STRUCTURE EFFECT ON MOMENTUM TRANSFER CROSS SECTIONS IN ELECTRON-POLYATOMIC MOLECULE COLLISIONS
M. Kimura, H. Sato and K. Fujima

HB-8. THEORETICAL STUDY ON THE TOTAL (ELASTIC + INELASTIC) CROSS SECTIONS FOR e-H_2O and NH_3 COLLISIONS AT 10-3000 eV
A. Jain

HB-9. SWARM-DERIVED SCATTERING CROSS SECTIONS OF CYCLO-C_4F_8
M. F. Frechette and J. P. Novak

HB-10. RESONANCE OVERLAP STRUCTURE IN THE MICROWAVE IONIZATION OF THE HYDROGEN ATOM
T. Uzer and D. Farrelly

HB-11. STUDY OF DEPENDENCE OF SCATTERING PHASE SHIFTS ON ATOMIC CHARGE AND MASS NUMBER
W. J. Romo and S. R. Valluri

SESSION HC. RF PLASMAS

HC-1. A PARTICLE MODEL OF A PLASMA-ETCHING DISCHARGE
W. N. G. Hitchon and G. J. Hofmann

HC-2. MODELING SPECIES TRANSPORT AND ETCHING KINETICS IN SF_6 DISCHARGES FOR PLASMA ETCHING
H. M. Anderson and J. A. Merson

HC-3. SELF-CONSISTENT STOCHASTIC ELECTRON HEATING IN HIGH FREQUENCY RF DISCHARGES
C. G. Goedde, A. J. Lichtenberg and M. A. Lieberman

HC-4. MEASUREMENTS AND MODELLING OF PLASMA PROPERTIES IN PLANAR MAGNETRON DISCHARGES
A. E. Wendt, L. Gu and M. A. Lieberman

HC-5. OPTICAL DIAGNOSTICS OF A HIGH POWER, RF DRIVEN, INDUCTIVELY COUPLED PLASMA
M. Trkula, N. S. Nogar, G. L. Keaton and J. E. Anderson

HC-6. PLASMA AND FREE RADICAL PARAMETERS IN AN Ar-NH_3 RF POSITIVE COLUMN
S. Ono, J. S. Chang, M. Yamada and S. Teii

HC-7. TUNABLE DIODE LASER DIAGNOSTICS OF MOLECULES IN PLASMA ETCHING SYSTEMS
J. Wormhoudt

HC-8. LASER-INDUCED FLUORESCENCE OF SiCL: SPECTROSCOPY AND COLLISION DYNAMICS FOR QUANTITATIVE MEASUREMENTS
J. B. Jeffries

HC-9. CHARACTERIZATION OF A LOW PRESSURE OXYGEN SURFACE-WAVE DISCHARGE
A. Granier, J. Marec, P. Supiot, C. Boisse-Laporte, R. Darchicourt, S. Pasquiers and P. Leprince

HC-10. RF PLASMA GENERATION USING INDUCTIVELY COUPLED LOOP ANTENNA
M. H. Cho, G. H. Kim, N. Hershkowitz and P. Nonn

HC-11. SHORT-PULSE MICROWAVE BREAKDOWN IN AIR
T. Armstrong, M. I. Buchwald, R. Karl
and R. A. Roussel-Dupre

SESSION I. ELECTRON COLLISIONS: THEORY PANEL

7:30 PM - 10:00 PM, Wednesday, October 14
Space Science and Technology Center, Room 5
Co-Chairmen: J. N. Bardsley (Lawrence Livermore Laboratory)
and M. R. Flannery (Georgia Tech)

I-1. DIFFERENTIAL AND INTEGRAL CROSS SECTIONS FOR ELECTRON IMPACT EXCITATION DETERMINED BY FOMBT/DW-TYPE THEORIES
D. C. Cartwright and G. Csanak
(Invited Paper)

I-2. MULTICHANNEL EIKONAL THEORY OF ELECTRON-METASTABLE ATOM COLLISIONS
E. J. Mansky II
(Invited Paper)

I-3. EFFECTIVE COLLISION STRENGTHS FOR EXCITATION OF HYDROGEN BY ELECTRONS
J. Callaway, K. Unnikrishnan and D. H. Oza
(Invited Paper)

I-4. OSCILLATOR STRENGTHS AND COLLISION STRENGTHS FOR COMPLEX ATOMS AND IONS
R. J. W. Henry
(Invited Paper)

I-5. IONIZATION IN COLLISIONS BETWEEN ELECTRONS AND COMPLEX IONS
C. Bottcher, D. C. Griffin and M. S. Pindzola
(Invited Paper)

I-6. THEORY OF RESONANT ELECTRON-MOLECULE COLLISIONS
A. Hazi
(Invited Paper)

I-7. ROTATIONAL AND VIBRATIONAL EXCITATION OF SIMPLE MOLECULES
D. W. Norcross and S. Alston
(Invited Paper)

I-8. AN ALGEBRAIC VARIATIONAL APPROACH TO ELECTRON-MOLECULE SCATTERING
T. N. Rescigno and B. I. Schneider
(Invited Paper)

I-9. STUDIES OF LOW-ENERGY ELECTRON-MOLECULE COLLISIONS
W. M. Huo, H. Pritchard. K. Watari, M. A. P. Lima and V. McKoy
(Invited Paper)

SESSION J. POSTERS

7:30 PM - 10:00 PM, Wednesday, October 14
Chairman: T. Eddy (Georgia Tech)
Space Science and Technology Center, Room 3

All posters may be assembled from 6:00 PM onwards and manned from 7:30 PM onwards.

SESSION JA. SWARMS AND BREAKDOWN

JA-1. ELECTRON DEGRADATION SPECTRA AND INITIAL YIELDS OF IONS IN BINARY MIXTURES
M. Kimura, M. Inokuti and M. A. Dillon

JA-2. SIMULATION OF ELECTRON SWARM MOTION IN CCl_2F_2 USING MONTE CARLO TECHNIQUE
V. K. Lakdawala, S. T. Ko and S. Albin

JA-3. TIME EVOLUTION OF ELECTRON AND POSITRON SWARMS IN NEON
P. J. Drallos and J. M. Wadehra

JA-4. LOW ENERGY ELECTRONS IN DEUTERIUM
W. Roznerski, K. Leja and Z. Lj. Petrovic

JA-5. A NEW SWARM DETERMINATION OF ELECTRON MOLECULE CROSS SECTIONS IN TETRAFLUOROMETHANE
P. Segur, M. Breznotits and J. P. Zurru

JA-6. EFFECT OF PULSE RISING RATE ON CURRENT EMISSION AND OZONE GENERATION IN A PULSED STREAMER CORONA DISCHARGE IN AIR
A. Mizuno and Y. Kamase

JA-7. SHORT-GAP BREAKDOWN AT LOW OVERVOLTAGE
J. P. Novak and R. Bartnikas

JA-8. THE STUDIES OF GAS BREAKDOWN PROCESSES IN A CAPILLARY GLOW DISCHARGE
Z. M. Yang, Z. N. Luo, J. R. Yu and G. J. Collins

SESSION JB. D. C. GLOWS

JB-1. PHOTOABSORPTION CROSS SECTION OF XeF_2 FROM 150 TO 275 nm BY FORWARD SCATTERING EELS
D. Spence, H. Tanaka and M. A. Dillon

JB-2. BUFFER GAS EFFECTS ON THE PERFORMANCE OF A SELF-SUSTAINED DISCHARGE ArF LASER
M Ohwa and M. Obara

JB-3. TWO DIMENSIONAL MODEL OF DC GLOW DISCHARGES
J. P. Boeuf and P. Segur

JB-4. OPERATING E/n AND METASTABLE PRODUCTION IN THE POSITIVE COLUMN OF AN H_2-Ar DISCHARGE
M. A. Islam and A. V. Phelps

JB-5. NUMERICAL ANALYSIS OF SELF-SUSTAINING BULK PULSED DISCHARGE IN NITROGEN
S. K. Dhali and L. H. Low

JB-6. SPATIALLY RESOLVED TEMPERATURE MEASUREMENTS IN A POSITIVE-COLUMN NITROGEN DISCHARGE USING PLANAR BOXCARS
D. D. Hodson, C. J. Emmerich, P. P. Yaney and S. W. Kizirnis

JB-7. CONTINUUM MODEL OF DC NEGATIVE GLOW DISCHARGES: ARGON AND NITROGEN
M. Surendra and D. B. Graves

JB-8. EXPERIMENTAL STUDY OF A DC NITROGEN DISCHARGE
K. E. Huffstater, G. M. Jellum and D. B. Graves

JB-9. MASS SPECTROMETER MEASUREMENTS OF DISILANE GLOW DISCHARGES
G. H. Lin, J. R. Doyle, M. Z. He and A. Gallagher

JB-10. SPECTROSCOPIC STUDY OF RESIST STRIPPING BY A GLOW DISCHARGE ELECTRON GUN
L. Li, Y. Hanwei, J. Krishnaswamy and G. J. Collins

SESSION JC. SHEATHS

JC-1. SPECTROSCOPIC DIAGNOSTICS IN THE CATHODE REGION OF A NITROGEN DISCHARGE
A. Margulis and J. Jolly

JC-2. ANALYSIS OF THE CATHODE FALL OF ABNORMAL GLOW DISCHARGES IN AN ELECTRONEGATIVE GAS
K. H. Schoenbach and H. Chen

JC-3. ON THE EFFECT OF CHARGE EXCHANGE COLLISIONS IN THE SPACE CHARGE SHEATH
K. U. Riemann

JC-4. THE BOUNDARY LAYER OF A WEAKLY IONIZED PLASMA WITH HOT NEUTRALS
S. Biehler and K. U. Riemann

JC-5. EFFECT OF ELECTRODE AREA RATIO ON RADIO FREQUENCY GLOW DISCHARGE SHEATH FIELDS
T. Intrator, G. R. Scheller and R. A. Gottscho

JC-6. PLASMA-SHEATH STRUCTURE FOR AN ELECTRODE CONTACTING A THERMAL PLASMA, INCLUDING ELECTRON ENERGY EFFECTS
L. D. Eskin and S. A. Self

JC-7. COLLISIONS OF ATOMS WITH A LIQUID METAL SURFACE IN A SPUTTERING ENVIRONMENT
W. L. Morgan

SESSION KA. RECOMBINATION AND ION-MOLECULE COLLISIONS

8:00 AM - 9:45 AM, Thursday, October 15, 1987
Space Science and Technology Center, Room 5
Chairwoman: M. Mandich (AT&T Bell Laboratories)

8:00 - 8:25 KA-1. DISSOCIATIVE RECOMBINATION OF ELECTRONS WITH H_2^+
A. P. Hickman
(Long Paper)

8:25 - 8:40 KA-2. DENSITY DEPENDENCE OF ION-ION RECOMBINATION IN HELIUM AND ARGON AT ATMOSPHERIC PRESSURES
H. S. Lee and R. Johnsen

8:40 - 8:53 KA-3. MEASUREMENT OF ION-ION RECOMBINATION IN HIGH-PRESSURE GASES USING A TWO-SLIT METHOD
C. R. Tenney, F. A. Dibianca, D. J. Wagenaar, J. E. Fetter, J. E. Vance, J. J. Brophy, D. L. McDaniel and P. Granfors

8:53 - 9:06 KA-4. THE REACTION OF N_2^+ WITH H_2O, D_2O, AND D_2O^{18}
F. J. Wodarczyk, R. H. Salter and E. Murad

9:06 - 9:19 KA-5. REACTION CROSS SECTIONS AND THERMOCHEMISTRY FOR THE REACTIONS OF Si^+ AND SiF^+_6 WITH SiF_4
M. E. Weber and P. B. Armentrout

9:19 - 9:32 KA-6. COLLISIONAL VIBRATIONAL QUENCHING OF $NO^+(v)$ IONS
R. A. Morris, A. A. Viggiano, F. Dale and J. F. Paulson

9:32 - 9:45 KA-7. QUENCHING OF $N_2(A^3\Sigma)$
R. A. Young, J. Blauer and R. Bower

SESSION KB. BEAM AND RADIATION PRODUCED PLASMAS

8:00 AM - 9:05 AM, Thursday, October 15, 1987
Space Science and Technology Center, Room 4
Chairman: K. Stalder (SRI International)

8:00 - 8:13 KB-1. ELECTRODE DESIGN AND DISCHARGE MODELING IN AN E-BEAM SUSTAINED DISCHARGE WITH A SPREADING SOURCE
M. Von Dadelszen

8:13 - 8:26 KB-2. KINETICS OF UV-SUSTAINED GLOW DISCHARGES
W. M. Moeny

8:26 - 8:39 KB-3. MODELING OF UNSTEADY NEGATIVE DIFFERENTIAL CONDUCTIVITY EFFECTS IN UV-SUSTAINED RADIAL GLOW DISCHARGES USING THE TETRA ELF COMPUTER CODES
W. M. Moeny

8:39 - 9:05 KB-4. ELECTRON PRODUCTION AND ENERGY SPECTRUM IN HEAVY ION PUMPED PLASMAS
T. J. Moratz and M. J. Kushner

8:39 - 9:05 KB-5. ELECTRON DISTRIBUTIONS AND EXCITATION RATES IN HEAVY ION PUMPED PLASMAS
T. J. Moratz AND M. J. Kushner

8:39 - 9:05 KB-6. HEAVY ION PUMPING OF EXCIMER LASERS
T. J. Moratz, T. D. Saunders and M. J. Kushner

SESSION LA. ELECTRON-IMPACT CROSS SECTIONS III

10:00 AM - 11:30 AM, Thursday, October 15, 1987
Space Science and Technology Center, Room 5
Chairman: J. Ajello (Jet Propulsion Laboratory)

10:00 - 10:25 LA-1. ELECTRON-IMPACT EXCITATION OF MOLECULES AND RARE GAS ATOMS
S. Trajmar
(Invited Paper)

10:25 - 10:50 LA-2. ELECTRON COLLISIONS IN THE COPPER VAPOR LASER
A. Hazi and K. Scheibner
(Long Paper)

10:50 - 11:03 LA-3. THE TOTAL ELECTRON-MOLECULE SCATTERING CROSS SECTIONS OF THE METHYL HALIDES
A. Benitez

11:03 - 11:16 LA-4. ELECTRON COLLISION CROSS SECTIONS FOR CH_4 FROM MEASURED SWARM DATA
L. E. Kline, D. K. Davies, W. E. Bies and T. V. Congedo

11:16 - 11:30 LA-5. CROSS SECTION MEASUREMENTS IN C_3F_8 AND C_2H_3Cl
P. J. Chantry and C. L. Chen

SESSION LB. HIGH INTENSITY DISCHARGE LAMPS

9:25 AM - 11:20 AM, Thursday, October 15, 1987
Space Science and Technology Center, Room 4
Chairman: H. Witting (General Electric-Corporate Research Division)

9:25 - 9:50 LB-1. ARC PHYSICS IN HIGH INTENSITY DISCHARGE LAMPS: THE PRESENT STATE OF THE ART AND CHALLENGES FOR THE FUTURE
J. F. Waymouth
(Invited Paper)

9:50 - 10:15 LB-2. CATAPHORESIS IN HIGH INTENSITY DISCHARGE LAMPS
J. H. Ingold
(Invited Paper)

10:15 - 10:28 LB-3. MODELS OF 2-D AND 3-D CONVECTIVE EFFECTS IN HIGH PRESSURE MERCURY DISCHARGES WITHOUT AND WITH ADDITIVES
J. T. Dakin and W. Shyy

10:28 - 10:41 LB-4. A SIMPLE LINESHAPE MODEL FOR RADIATION TRANSPORT CALCULATIONS IN HIGH INTENSITY DISCHARGES
P. A. Vicharelli and W. P. Lapotôvich

10:41 - 10:54 LB-5. DEVIATIONS FROM EXCITATION EQUILIBRIUM IN THE Hg 6^3P LEVELS IN A HIGH PRESSURE ARC
D. Karabourniotis and S. Couris

10:54 - 11:07 LB-6. PINPOINT LASER ABSORPTION MEASUREMENT OF SODIUM DENSITY IN A METAL-HALIDE LAMP
G. Allen

11:07 - 11:20 LB-7. PULSED LASER OPTOGALVANIC SPECTROSCOPY OF SCANDIUM AND SODIUM IN A HIGH PRESSURE METAL HALIDE DISCHARGE
J. Kramer

SESSION MA. ELECTRON-IMPACT CROSS SECTIONS IV

1:30 PM - 3:25 PM, Thursday, October 15, 1987
Space Science and Technology Center, Room 5
Chairman: W. Blumberg (Air Force Geophysics Laboratory)

1:30 - 1:55 MA-1. MEASUREMENTS OF ELECTRON-IMPACT IONIZATION CROSS SECTIONS FOR IONS
R. A. Phaneuf
(Invited Paper)

1:55 - 2:20 MA-2. ELECTRON-MOLECULE CROSS SECTIONS AND TEMPORARY NEGATIVE ION STUDIES
P. D. Burrow
(Invited Paper)

2:20 - 2:45 MA-3. ELECTRON IMPACT PHENOMENA USING QUASI-FREE ELECTRONS
T. J. Morgan
(Long Paper)

2:45 - 3:10 MA-4. MEASUREMENTS OF POSITRON- AND ELECTRON-ALKALI ATOM TOTAL SCATTERING CROSS SECTIONS
T. S. Stein, M. S. Dababneh, W. E. Kauppila, C. K. Kwan and Y. J. Wan
(Long Paper)

3:10 - 3:25 MA-5. ELECTRON-NOBLE-GAS SPIN-FLIP SCATTERING AT LOW ENERGY
T. G. Walker, K. D. Bonin and W. Happer

SESSION MB. MICROSCOPIC MODELING OF DISCHARGES

1:30 PM - 3:25 PM, Thursday, October 15, 1987
Space Science and Technology Center, Room 4
Chairman: J. Boeuf (Université Paul Sabatier)

1:30 - 1:55 MB-1. BEHAVIOR OF ELECTRON SWARMS IN METHANE AND MONOSILANE
H. Tagashira
(Invited Paper)

1:55 - 2:08 MB-2. MONTE CARLO CALCULATIONS OF ELECTRON TRANSPORT IN CH_4 WITH ANISOTROPIC SCATTERING
L. E. Kline, W. E. Bies and T. V. Congedo

2:08 - 2:33 MB-3. MONTE CARLO SIMULATIONS OF ION TRANSPORT THROUGH RF GLOW-DISCHARGE SHEATHS
B. E. Thompson and H. H. Sawin
(Long Paper)

2:33 - 2:46 MB-4. TRANSIENT AND STEADY STATE ELECTRON ENERGY DISTRIBUTION FUNCTIONS OBTAINED WITH A MONTE CARLO FLUX CODE
P. Hui and G. Schaefer

2:46 - 3:11 MB-5. MODELING OF GAS DISCHARGES DURING TRANSIENTS IN COMPLEX GEOMETRIES
M. J. Kushner
(Long Paper)

3:11 - 3:25 MB-6. ELECTRON ENERGY AND VIBRATIONAL DISTRIBUTION FUNCTIONS IN HIGH-FREQUENCY N_2 DISCHARGES
C. M. Ferreira and J. Loureiro

SESSION NA. LASER KINETICS

3:45 PM - 5:15 PM, Thursday, October 15, 1987
Space Science and Technology Center, Room 5
Chairman: K. Y. Tang (Western Research Corporation)

3:45 - 4:10 NA-1. UV EXCIMER RADIATION FROM DIELECTRIC-BARRIER DISCHARGES
B. Eliasson and U. Kogelschatz
(Long Paper)

4:10 - 4:23 NA-2. PHOTOABSORPTION MEASUREMENT OF Ar_2F EXCIMER AT 248 nm
K. Hakuta, S. Miki, T. Sugoh and H. Takuma

4:23 - 4:36 NA-3. ELECTRONIC STRUCTURE AND PHOTOABSORPTION CHARACTERISTICS OF Ar_3^+
H. H. Michels

4:36 - 4:49 NA-4. EXPERIMENTAL DETERMINATION OF THE EINSTEIN COEFFICIENTS FOR THE N_2 (B-A) TRANSITION
L. G. Piper, K. W. Holtzclaw, B. D. Green
and W.A.M. Blumberg

4:49 - 5:02 NA-5. A CHEMICAL PROCESS SHOWING LASER GAIN IN THE VISIBLE REGION
S. H. Cobb, R. Woodward and J. L. Gole

5:02 - 5:15 NA-6. A CHEMICALLY DRIVEN VISIBLE LASER USING FAST NEAR RESONANT ENERGY TRANSFER
R. Woodward, S. H. Cobb and J. L. Gole

SESSION NB. ARCS

3:45 PM - 5:30 PM, Thursday, October 15, 1987
Space Science and Technology Center, Room 4
Chairman: A. Bhattacharya (General Electric-Lighting Business Group)

3:45 - 3:58 NB-1. THE ELECTRICAL CONDUCTIVITY OF NON-IDEAL PLASMAS
R. J. Zollweg and R. W. Liebermann

3:58 - 4:11 NB-2. ON THE TRANSITION PROBABILITY SCALE MODIFICATION OF Ar I
A. Sedghinasab and T. L. Eddy

4:11 - 4:24 NB-3. TRANSIENT AND QUASI-STEADY NON-LTE DIAGNOSTICS OF A ROTATING ARGON ARC
R. V. Frierson and T. L. Eddy

4:24 - 4:37 NB-4. AN INVESTIGATION OF THE PULSED CESIUM-MERCURY-XENON ARC
H. L. Witting

4:37 - 4:50 NB-5. AN EFFECT OF MIXING PLENUM AND HYDROGEN CONCENTRATION ON THE DOWNSTREAM TEMPERATURE PROFILES OF DC PLASMA TORCH IN Ar-H_2 MIXTURE GAS PLASMAS
I. Ishii, J. S. Chang and F. Y. Chu

4:50 - 5:03 NB-6. TEMPERATURE MEASUREMENTS OF A FREE-BURNING PLASMA ARC BY A COMBINATION OF HOLOGRAPHIC INTERFEROMETRY AND EMISSION SPECTROSCOPY
A. Shah, M. S. Dassanayake and K. Etemadi

5:03 - 5:16 NB-7. INVESTIGATION OF ARC ROOT IGNITION ON OXIDIZED CATHODES
K. P. Nachtigall

5:16 - 5:30 NB-8. CONTROL OF SURFACE MELTING AND ABLATION VIA THE MVS MECHANISM: PROOF-OF-PRINCIPLE DEVICE
O. Hankins, O. Auciello, M. Bourham, J. Gilligan and B. Wehring

PLENARY SESSION O. MACROSCOPIC MODELING OF DISCHARGES

8:00 AM - 9:55 AM, Friday, October 16, 1987
Space Science and Technology Center, Rooms 3-5
Chairman: V. Godyak (GTE Electrical Products)

8:00 - 8:25 O-1. MODELING OF A D.C. OXYGEN GLOW DISCHARGE: COMPARISON WITH MEASUREMENT
C. M. Ferreira, G. Gousset, M. Touzeau and M. Vialle
(Long Paper)

8:25 - 8:38 O-2. A MODEL FOR ELECTRON BEAM SUSTAINED GLOW DISCHARGE FOR PLASMA ETCHING APPLICATIONS
A. P. Paranjpe and S. A. Self

8:38 - 8:51 O-3. EXPLICIT FINITE-DIFFERENCE METHODS FOR TIME-DOMAIN MODELING OF LOW PRESSURE RF GLOW DISCHARGES
M. S. Barnes, T. J. Cotler and M. E. Elta

8:51 - 9:04 O-4. FLUID MODELS AND DIAGNOSTICS OF GLOW DISCHARGES: PROSPECTS AND PROBLEMS
D. B. Graves, G. M. Jellum, M. Surendra and K. E. Hufstater

9:04 - 9:17 O-5. A NUMERICAL MODEL OF RF GLOW DISCHARGES
J. P. Boeuf

9:17 - 9:30 O-6. SCHOTTKY THEORY OF THE RECTANGULAR POSITIVE COLUMN
J. H. Ingold

9:30 - 9:55 O-7. THEORY OF POSITIVE AND NEGATIVE ELECTRICAL CORONA IN ELECTRONEGATIVE GASES
R. Morrow
(Invited Paper)

PLENARY SESSION P. ELECTRON-IMPACT CROSS SECTIONS V

10:30 AM - 12:10 AM, Friday, October 16, 1987
Space Science and Technology Center, Rooms 3-5
Chairman: L. C. Lee (San Diego State University)

10:30 - 10:55 P-1. ELECTRON COLLISIONS IN EXCIMER LASERS
D. C. Lorents
(Invited Paper)

10:55 - 11:20 P-2. APPLICATIONS OF ELECTRON CROSS SECTION DATA
A. V. Phelps
(Invited Paper)

11:20 - 11:45 P-3. MEASUREMENT OF ELECTRON-IMPACT EXCITATION AND IONIZATION CROSS SECTIONS RELEVANT TO IONIZED GAS SYSTEMS
D. Spence
(Invited Paper)

11:45 - 12:10 P-4. ELECTRON COLLISIONS WITH ETCHANT GAS PLASMA CONSTITUENTS
K. A. Blanks and K. Becker
(Invited Paper)

SESSION A

8:10 AM - 9:55 AM, Tuesday, October 13

Space Science and Technology Center, Rooms 3-5

ATOMIC COLLISIONS AND RECOMBINATION

Chairman: T. F. Moran (Georgia Tech)

A-1 "The Third Wave-Atomic Collisions Since 1963," by EARL W. MCDANIEL, Georgia Institute of Technology— Experimental research on Atomic Collisions began at about the beginning of the 20th century, and by 1930, good quantitative measurements had been made in several areas. Much of the field had been roughed out at the end of World War II, in 1945. The period between 1945 and 1963, say, saw the application of many important new experimental techniques and the acquisition of reliable data on most kinds of atomic collision phenomena. In the period between 1963 and the present, several new phenomena were discovered, and many kinds of collisions were studied at much higher resolution and with much greater accuracy than previously was possible. The striking developments during this time, and some projections into the future, are the subjects of this talk.

A-2 Dissociative Recombination: From the Ionosphere to the Laboratory and Back Again, MANFRED A. BIONDI, University of Pittsburgh - A brief history is given of the discovery and study of dissociative recombination, the highly efficient process whereby a molecular ion captures an electron to form an unstable molecule which dissociates to stabilize the reaction. The course of our understanding of this process -- from its postulation originally to explain electron loss in the Earth's ionosphere, to its discovery and confirmation in laboratory plasma-afterglow studies, to theoretical and experimental determinations of recombination coefficients for specific ions using a variety of techniques -- is outlined. The important role of dissociative recombination in determining the ionization levels attained in plasmas of such diverse types as planetary ionospheres, laser active media, plasma switches, interstellar clouds, etc. is touched on. Finally, the circle is closed by a discussion of recent recombination rate inferences from in-situ measurements in the ionosphere by satellites.

A-3 Recombination: Calculations, Simulations and Applications.* J.N. Bardsley, Lawrence Livermore National Laboratory. An overview will be given of the current status of our knowledge of electron-ion and ion-ion recombination processes. Recent theoretical progress will be reviewed and the need for further experimental data will be stressed. Studies of the state-dependence of the rates of dissociative recombination, and of the branching ratios for metastable state production will be discussed. Recent calculations of dielectronic recombination in multiply-charged ions will be reported. Special attention will be given to the density dependence of electron-ion and ion-ion recombination rates, and questions regarding non-equilibrium effects will be raised.

*Work performed under the auspices of the U.S. Department of Energy by Lawrence Livermore National Laboratory under contract #W-7405-Eng-48.

A-4 Termolecular Recombination*, M. R. FLANNERY, Georgia Tech - Theoretical description of termolecular ion-ion recombination and termolecular ion-atom association between atomic species in a gas will be presented. The underlying physics and dependence with gas density will be discussed. Results of various models - strong collision, diffusion and bottleneck - will be compared at low gas densities with the exact treatment.

*Research supported by AFOSR grant No. AFOSR-84-0233.

SESSION BA

10:15 AM - 11:45 AM, Tuesday, October 13

Space Science and Technology Center, Room 5

BREAKDOWN AND SWITCHING

Chairman: R. DeWitt (Naval Surface Weapons Center)

BA-1 Calculation of Electron Transport Parameters and Critical Field Strengths for the Gas Mixtures SF_6/CO_2, SF_6/Ar, SF_6/Ne, and SF_6/He, TH. ASCHWANDEN, Polytechnic University of New York, R. J. VAN BRUNT, A. V. PHELPS, National Bureau of Standards - The electron transport parameters for the gas mixtures SF_6/CO_2, SF_6/Ar, SF_6/Ne, and SF_6/He have been calculated from numerical solutions of the Boltzmann Transport Equation using the two term spherical harmonic expansion with an improved set of electron collision cross sections for SF_6. The critical electric field-to-gas density ratios at which the ionization rates in the gas equal the electron attachment rates were also determined and found to compare favorably with recent experimental data from swarm and breakdown measurements.[1] In the case of SF_6/Ne and SF_6/He, the calculated results provide insight into the maximum influence of Penning ionization on dielectric strength and the limitations of the maxwellian approximation[2] as apply to these mixtures.

1. Th. Aschwanden, Thesis, ETH, Switzerland (1985).
2. R. J. Van Brunt, J. Appl. Phys. 61, 1773 (1987).

BA-2* Streamer Processes in Triggered Breakdown*, F.E. Peterkin and P.F. Williams, University of Nebraska. - The initial processes causing triggered breakdown in an undervolted, N_2-filled, DC charged trigatron spark gap have been studied using time-resolved streak photography and two-dimensional shutter photography. We find clear evidence that classical streamers initiate the breakdown process and have an important influence on characteristics such as risetime, delay, and jitter in the final closure of the gap. Two dimensional shutter photos show that for a given breakdown event numerous streamers propagate in the gap, and the number and spatial characteristics can be varied by changing the triggering geometry and the gap voltage. The studies provide detailed empirical information about streamers which we compare with previous numerical modeling results.

*Research supported by NSWC and NSF.

BA-3 Microdischarge Properties of Dielectric-Barrier Discharges. U. KOGELSCHATZ AND B. ELIASSON, Brown Boveri Research Center, 5405 Baden/Switzerland - The dielectric-barrier discharge operated near atmospheric pressure is characterized by the presence of a large number of statistically distributed microdischarges of nanosecond duration. As it is possible to influence the electron energy and energy density by adjusting external discharge parameters one can use these short-lived microdischarge channels as a convenient medium for high pressure non-equilibrium processes. The generation of ozone in oxygen/nitrogen mixtures or the generation of excimers in rare gas mixtures are two examples of the application of such discharges. Each streamer initiated microdischarge consists of a nearly cylindrical current filament about 100 μm radius. In air or oxygen the current density can reach values of the order of kA/cm^2. The presence of the dielectric results in an almost immediate choking of the discharge. The energy deposition is so small that the filament remains close to room temperature. The electron energy lies in the range of 10eV. A pulse of electrons at these energies is ideally suited for molecular dissociation and atomic excitation and can initiate a number of plasma chemical reactions.

BA-4 Characterization of Metastable Nitrogen in the Effluents of Ozonizer-type Discharges.* L.G. PIPER and W.P. CUMMINGS, Physical Sciences Inc., Andover, MA, 01810. -- Several reports in the literature imply extremely large number densities of metastable nitrogen molecules can be found in the effluents of ozonizer or dielectric barrier discharges in flowing nitrogen. We have constructed an ozonizer-type discharge which operates at 1-10 kV in flowing nitrogen or mixtures of nitrogen in either argon or helium at total pressures between 0.3 and 6 Torr. Spectroscopic observations in the afterglow of this discharge indicates that virtually all observed excitation in region between 200 and 850 nm results from discharge streamers. All emissions are quenched upon adding a grounded loop down stream from the discharge. The absence of NO Gamma-band emission when NO is added downstream from the grounded loop indicates that $N_2(A)$ number densities in the afterglow are below 10^8 molecules cm^{-3}, some ten orders of magnitude below previous estimates.

* Performed under contract F19628-85-C-0032 with the Air Force Geophysics Laboratories and sponsored by AFOSR under Task 2310G4 and by DNA under project SA, task SA, work unit 115.

BA-5 A Spark Gap Recovery Simulation Code*, L. P. ROSEN, M. VON DADELSZEN, R. D. MILROY, Spectra Technology Inc. - The important phases in modeling spark gap recovery are breakdown, conduction and initial and long term recovery. The number of important parameters and timescales associated with these phases vary by orders of magnitude. The SPRAD code[1] is used to model the first three phases in a laser triggered gap with mixtures of H_2 and Ar out to the μs timescale. A local thermodynamic equilibrium (LTE) kinetics model was incorporated to supplement the two temperature kinetics in SPRAD, for better CPU efficiency. The final SPRAD timestep output is used as the initial conditions for a 2-D hydrodynamic code which models the long term 2-D gas recovery. Due to time and funding constraints, the code is presently restricted to rectangular geometries with no mean flow. We will describe the aspects of the code not previously reported, and show sample output.

*Work supported by NSWC
[1]M. J. Kushner et al., J. App. Phys. 58, 2988 (1985)

BA-6 Breakdown Strength and Recovery of a Steam Insulated Spark Gap*, WILLIAM J. THAYER AND VICTOR C. H. LO, Spectra Technology Inc.-DC breakdown experiments and analyses have been carried out to measure the breakdown strength of steam and to characterize the recovery processes of purged, steam insulated spark gaps. The voltage required for self breakdown of the gas between large radius electrodes was measured in steam, and in air for comparison, at pressures up to 5 atm and temperatures to 160°C. Air data at elevated temperatures agree well with past ambient temperature experiments when plotted as a function of nd rather than pd. The steam data at low nd agree with earlier experiments done at very low pressure[1]. The high pressure data indicate that high pressure steam has somewhat higher dielectric strength than air and will be a good dielectric medium for spark gap switches. Analysis shows that a steam purged spark gap will have low losses relative to alternate dielectric gases at high pulse repetition frequencies.

* Reasearch supported by the Department of Energy
[1] R. Hackman, J. Phys. D: Appl. Phys., 4, 1134 (1971).

BA-7 Simulation of Electron Scattering from Dielectrics in Surface Discharges.* Timothy L. Peck and Mark J. Kushner, University of Illinois--Surface discharges are typically initi- ated by electron emission from the vacuum/gas- cathode-dielectric triple point: and subsequent scattering of electrons from the dielectric. We report on a 3-D Monte Carlo particle simulation of the initiation of surface discharges across dielectrics. Arbitrary geometries and materials may be specified. Secondary electron emission from the dielectric, surface charging, gas de- sorption, and collisions with ambient or desorbed gas phase species are included in the model. The filamentary structure of surface discharges will be discussed and effective first Townsend coef- ficients for electron scattering from the surface will be presented. The role of desorbed gas early during the discharge will be discussed.

*Work Supported by NASA Lewis Research Center, Contract No. NAG 3-741

SESSION BB

10:15 AM - 11:45 AM, Tuesday, October 13

Space Science and Technology Center, Room 4

PLASMA DEPOSITION

Chairman: P. Hargis (Sandia National Laboratories)

BB-1 Attachment in Silane-Helium RF Discharges.
LAWRENCE J. OVERZET, AND JOSEPH T. VERDEYEN,
University of Illinois - The time evolution of the electron density and the optical emission intensity in response to a square wave modulated RF excitation of silane-helium mixtures has been studied. The optical emission intensity indicates that the number of high energy electrons is remaining nearly constant as a function of time in the modulated discharge even though the bulk electron density varies in a complex manner. An electron attachment process involving silane radicals, SiH_n (n = 1 to 3), has been identified as the probable cause for the complicated time dependence of the bulk electron density. One can estimate a diffusion time for the attaching specie(s) in the silane-helium discharge by comparing the peak electron densities caused by two consecutive rf pulses on a fresh gas mixture as a function of the elapsed time between the two pulses. An approximate Dp product is found by examining the dependence of the measured lifetimes on pressure.($\approx 110 \pm 20$ cm^2 Torr/second).

This work was supported by the Joint Services Electronics Program (U.S. Army, U.S. Navy, and U.S. Air Force under contract No. N00014-84-C-0149).

BB-2 Mass Spectrometric Studies of Silane and Silane-Hydrogen Glow Discharges.* J. R. DOYLE, M. Z. HE, G. H. LIN, and A. GALLAGHER,† JILA, Univ. of Colorado and NBS.—Mass spectrometric measurements of hydrogen and disilane production and silane depletion for silane glow discharges are reported. Substrate temperature, pressure, hydrogen dilution, discharge current (for dc discharges) and rf power were varied. A kinetic mechanism is discussed in which most of the disilane is produced by surface recombination of silyl radicals, consistent with other reports.[1,2] Comparison of dc and rf discharge chemistry is made, including the possible effects of ion bombardment. A simplified model of a-Si:H film growth is presented based on current and previous work.

*Work supported in part by the Solar Energy Research Institute.
†Staff member, Quantum Physics Division, National Bureau of Standards.
[1]R. Robertson and A. Gallagher, J. Appl. Phys. 59, 3402, (1986).
[2]P. A. Longeway, H. A. Weakliem, and R. D. Estes, J. Appl. Phys. 57, 5499, (1985).

BB-3 Optical Emission and Mass Spectrometric Diagnostics of Silane and Disilane RF Discharges*, H. CHATHAM, AND P.K. BHAT, Glasstech Solar, Inc. - The dependencies of SiH* and H* emission intensities and neutral mass spectrometric signals on pressure, flow rate, power, and substrate temperature have been determined in silane and disilane. These measurements have been performed in a deposition system designed to deposit device-quality hydrogenated amorphous silicon. Results for low and high rf powers suggest substantially different chemical kinetics for these two regimes. Variation of measured signals with substrate temperature suggest surface reactions with activation energies less than 0.1 eV. These results are interpreted in terms of a model of surface and gas phase neutral chemistry.

* Research supported by SERI Contract No. ZB-7-06002

BB-4 Simulation of Substrate Surface Physics in RF Sputtering, W. L. MORGAN, Lawrence Livermore National Lab* - Experiments by Rizzo, et al.[1] on sputtering of a Pu-4 at.% Ga target in a rare gas RF discharge have shown a substantial depletion of the Ga on the sputter substrate. In order to model this experiment I have developed a stochastic molecular dynamics simulation code based on a program of Tully's[2]. Using this simulation technique I have modeled the enhanced diffusion of a Ga atom on a Pu surface when bombarded by energetic Ar atoms[3] produced by neutralization at the target surface of the Ar^+ ions in the RF discharge. I will discuss this modeling and the generalization of these physical processes to other sputtering systems.

*Work performed under the auspices of the U.S. Department of Energy by the Lawrence Livermore National Laboratory under contract number W-7405-ENG-48.

[1]H.F. Rizzo, et al., J. Vac. Sci. Technol. A4, 518 (1986).
[2]J.C. Tully, J. Chem. Phys. 73, 1975 (1980).
[3]K.C. Kulander, unpublished TRIM calculations.

BB-5 Hydrogen Isotope Concentration inside Amorphous Silicon Thin Films Produced by Ar-SiH_4-D_2 Mixture Gas, X. CHAN, J.S. CHANG and A.A. BEREZIN, McMaster University, Canada - Stroge of the hydrogen isotopes in a solid phase becomes important in a processing of nuclear fusion fuel. In this work, the relationship between hydrogen isotope concentration inside thin film and plasma parameters for a-Si:D/H produced by Ar-SiH_4-D_2 mixture gas plasma has been investigated both experimentally and theoretically. The total concentration of the hydrogen isotopes inside a-Si is determined from the Urbach tail of the optical characteristics. Deutrium profiling was conducted independently by using an ion beam method. Plasma parameters are determined from the twin probe method and wall temperature is determined from IR image camera. The results show that: 1) the relatively uniform density of trapped deuterium inside the films has been observed; 2) the hydrogen concentration significantly influenced by the gas and substrate temperatures, and these temperatures are significantly influenced by discharge powers (or plasma density) and gas pressures; 3) the hydrogen concentration has a nonmonotonic dependence on the discharge powers and density is observed to be in between 10^{21} to 10^{22} (cm^{-3}); 4) the axial tube wall temperature profiles observed to be nonuniform in spite of relatively uniform plasma density profiles.

BB-6 Hydrogen-Reduced Multilayer Deposition of Carbon Thin Films, H. SUGAI, S. OHSHITA, S. YOSHIDA AND T.OKUDA Nagoya University, Japan. - Plasma assisted in-situ carbon coatings of the first wall of nuclear fusion devices have recently been noticed since the protective coatings drastically reduce the metal impurities in a high temperature fusion plasma. Besides the success of impurity control, however, there appeared a new problem of hydrogen gas desorption from the coated walls. In this paper, we present a novel coating technique to reduce the H-atom content of the films. The idea is based on the ion-induced desorption of hydrogens, and on the repeated multilayer deposition: In a helium glow discharge, a short(1 min) burst of methane is admixed at regular intervals of 20 min, where H atoms of films are desorbed by He^+ bombardment during the intervals. The hydrogen recycling test of the mutilayer films has verified the clear improvement in the response to hydrogen plasmas.

SESSION CA

1:15 PM - 2:55 PM, Tuesday, October 13

Space Science and Technology Center, Room 5

ELECTRON-IMPACT CROSS SECTIONS I

Chairman: B. Bederson (New York University)

CA-1 Measurements of Electron Impact Ionization Cross Sections. R. S. FREUND, R. C. WETZEL, T. R. HAYES, R. J. SHUL, and F. A. BAIOCCHI. AT&T Bell Laboratories -- Electron impact ionization is essential in initiating and sustaining gas discharges. Although ionization potentials for a large number of species are accurately known, ionization cross sections of many atoms and most molecules have never been measured and are difficult to even estimate, particularly the partial cross sections for formation of fragment ions and different charge states. This talk will outline our recent measurements of absolute cross sections of several highly reactive species, the halogen atoms and the free radicals SiF, SiF_2, and SiF_3. The experimental method crosses an electron beam with a fast beam of the reactive species which is prepared by charge transfer neutralization of a mass-selected ion beam. The accuracy of the measured absolute cross sections is estimated to be better than $\pm$15% over the energy range from threshold to 200 eV.

CA-2 Electron Excitation of the Alkalis. A. GALLAGHER,* JILA, Univ. of Colorado and NBS.--The alkalis have been, and continue to be, exceptionally useful for achieving an understanding of electron-atom collision phenomena. Many general characteristics of electron collisional excitation appear ideally in the alkalis, without complications that often occur for H and the noble gases. These will be discussed, from the threshold resonance-line polarization through tests of high-energy behavior and higher-state excitation. At least a half dozen different experimental methods have been devised to obtain spin and scattering-angle dependences. The simple alkali structure allowed excellent close-coupling calculations to be done in the 1970's, but new work emphasizing internal details is called for by these newer observations.

*Staff Member, Quantum Physics Division, National Bureau of Standards.

CA-3 Probing Electron-Impact Excitation Using V.U.V. Polarization Analysis* J.W. McCONKEY, University of Windsor--Polarization data can provide detailed information about the excitation process particularly if combined with electron-photon coincidence techniques. These measurements often provide a much more sensitive test of theory than differential cross-section measurements. In addition, accurate polarization data are required for proper calibration of optical equipment in the V.U.V. and for correction of optical excitation functions. Recent measurements of the polarization of resonance radiation from the rare gases and simple molecules taken in both coincidence and non-coincidence modes will be used to illustrate these points.

* Research supported by the Natural Sciences and Engineering Research Council of Canada.

CA-4 A Technique for Measuring Electron Excitation Cross Sections from Transient Species, L. W. ANDERSON, D. L. A. RALL, F. A. SHARPTON, M. B. SCHULMAN, J. E. LAWLER and CHUN C. LIN, Univ. of Wisconsin, Madison 53706--We have developed a technique for measuring the optical electron excitation cross section from transient species and have demonstrated the technique by measuring the optical cross section for the excitation of the 3^3P level of He from the 2^3S level. A beam containing some He atoms in the metastable 2^3S level is produced by flow from a hollow cathode discharge source. The metastable He beam is crossed by a low energy electron beam. The relative $3^3P \rightarrow 2^3S$ optical emission is detected as a function of the electron energy while modulating the electron beam current and the discharge current. The absolute cross section is obtained by measuring the ratio of the electron excitation cross section to the known optical absorption cross section. This is obtained by measuring with the same detection system the ratio of the optical emission produced by an electron beam of known current to the fluorescence integrated over the optical lineshape produced by a laser of known power. The optical electron excitation cross section is 4×10^{-16} cm^2.

SESSION CB

1:15 PM - 3:15 PM, Tuesday, October 13

Space Science and Technology Center, Room 4

SHEATHS: MODELS AND EXPERIMENTS

Chairman: K. Greenberg (Sandia National Laboratory)

CB-1 Quadratic Stark Laser Spectroscopy Determination of the Electric Field Distribution in the Cathode Sheath of an Electron Beam Glow Discharge*

S.A. Lee, L.-U.A. Andersen, J.J. Rocca, M. Marconi and N.D. Reesor. Department of Physics and Electrical Engineering. Colorado State University. We have measured the electric field distribution in the cathode sheath of a 5 KV D.C. electron beam He glow discharge. CW laser saturation spectroscopy was used to determine the quadratic Stark shifts of the HeI 2^1P_1-3^1D_2 transition produced by the electric field. Measurements were obtained for different discharge configurations and conditions. Values as large as 10 KV/cm were measured at the cathode surface. The experimental results are in good agreement with the calculations of a model of the cathode sheath that includes the creation of charged particle pairs.

*Work supported by U.S. Air Force & N.S.F.

CB-2 Measurement of the Local Electric Field in Discharges using Laser Stark Spectroscopy of NaK: J. DEROUARD, H. DEBONTRIDE, N. SADEGHI Univ. of Grenoble I, France -Electric field induced mixing between e and f $^1\Delta$ doublet levels of the NaK molecule excited in the $B^1\Pi$ state [1] has been used to map out the local electric field in D.C. discharges. Electric fields, from a few V/cm up to several kV/cm, can be measured with a spatial resolution of a 0.1 mm. This extends the technique introduced by Gottscho et al [2] to the study of discharges in electopositive gases such as rare gases or metallic vapors. We find that the field decreases roughly linearly with the position in the shieth, then falls fairly abrubptly just before the negative glow. Also, because of the very fast response (a few 10^{-9}s) of the NaK molecule to the electric field, R.F. or pulsed discharges can be studied as well.

1.J. Derouard and N. Sadeghi Opt. Com. 57 239 (1986)
2. C.A. Moore et al Phys. Rev. Lett. 52 538 (1984)

CB-3 Current Balance at the Surface of a Cold Cathode*, J. E. LAWLER, E. A. DEN HARTOG, and D. A. DOUGHTY, Univ. of Wisconsin—An electric field diagnostic based on optogalvanic detection of Rydberg atoms and an analytic treatment of ion transport in the cathode fall are combined to empirically determine the current balance in a He glow discharge. The ratio of ion current to electron current at the surface of a cold Al cathode is found to be 3.3 over a range of current densities from a near normal 173V cathode fall to a highly abnormal 600V cathode fall.[1] The absolute densities of He metastables are mapped using laser absorption spectroscopy. The ion to electron current ratio and maps of the metastable densities compare favorably to Monte Carlo simulations, based on the null collision technique, of electron avalanches in the cathode fall. The suppression of singlet metastable density in the negative glow is used to place limits on the density and temperature of the low energy electron gas in the negative glow.

[1] D. A. Doughty, E. A. Den Hartog, and J. E. Lawler, Phys. Rev. Lett. 58, 2668 (1987).

*Supported by ARO and AFOSR.

CB-4 Plasma-Sheath Parameters at Intermediate Pressures, V. GODYAK, GTE-Electrical Products, MA - N. STERNBERG, Clark University, Worchester, MA - The potential distribution and the low frequency and high frequency capacitancies of an electrode sheath at intermediate pressures have been calculated. The momentum transfer equation together with Poisson's equation have been used for numerical calculation of the sheath characteristics at different values of the parameter $\alpha = D_e/\lambda_i$: (where D_e is the electron Debye radius and λ_i is the ion mean free path). The results show that the small signal capacitance can be easily obtained from the static sheath model only for very low ($\omega << \omega_i$) and for very high ($\omega >> \omega_i$) frequencies (where ω_i is the ion plasma frequency). Otherwise, a dynamic sheath model must be developed. The problem has analytical solutions for collisionless ($\alpha << 1$) and for highly collisional ($\alpha >> 1$) sheaths. The static sheath model is not applicable to the RF discharge sheath at $\omega >> \omega_i$ because of strong nonlinearity of the sheath impedance in an RF discharge.

CB-5 Electron Energy Distribution Near an Orfice in Hg-Ne Low Pressure Discharge. R. Lagushenko, V. Godyak and J. Maya, GTE Electrical Products, Danvers, MA - Recent probe measurements [1] in the vicinity of an orifice in a low pressure Hg-Ne discharge have shown strong spatial dependence in the electron energy distribution function (EEDF). This can be explained by the non-equilibrium between electrons and the electric field (E). The EEDF has been calculated based on the solution of the one dimensional position dependent Boltzman equation. Assuming inelastic collisions with Hg atoms to be the only mechanism of electron energy loss we have obtained an analytical expression for the EEDF as a function of energy and distance from the orifice. Calculated shape of the EEDF is found to be in good agreement with experimental data [1]. The agreement between calculated and experimental average electron energy is within about 10-15%.

(1) V. Godyak, R. Lagushenko and J. Maya; Bull. of Am. Phys. Soc. 32, 1146 (1987)

CB-6 A One Dimensional Model for the Investigation of Avalanching DC Cathode Sheaths, R. D. MILROY, M. VON DADELSZEN, L. P. ROSEN, Spectra Technology Inc. - Stability in high pressure, avalanched, DC glow discharges is dependent upon the level of preionization and the avalanche conditions. One important mechanism for the glow-to-arc transition is the propagation of anode directed filaments from the cathode surface. These filaments appear to originate from the cathode sheath, frequently during the avalanche phase. Most previous DC discharge cathode sheath investigations are applicable to the steady state. We have developed a self-consistent, one dimensional model to investigate the nature of the cathode sheath during the avalanche phase. In order to obtain reasonable CPU efficiency, equilibrium discharge kinetics are assumed. This leads to qualitative results, but enables the investigation of a wide parameter space. As might be expected, important parameters are: volumetric preionization density; avalanche dV/dt; and secondary cathode electron flux due to external sources (UV, e-beam, X-ray, etc.) We will present a description of the model and a summary of the results.

CB-7 **An Approximate Self-Consistent Solution for a Collisional Pre-sheath in a Fully Ionized Plasma***, G. L. MAIN, **Georgia Institute of Technology** - Analytical calculations of collisional pre-sheath structure has centered on simplified collision terms[1,2,3] because of the difficulty in solving the equations with a collision term such as a Fokker-Planck term. Here, an approximate technique[4] is used to find a self-consistent solution for potential and the ion distribution function in the pre-sheath with a Fokker-Planck collision term that retains its full nonlinearity but is approximated in the direction perpendicular to the surface. The approximation yields an asymptotic series for potential that is accurate with only several terms.

*Research supported by AFOSR.
[1]G. A. Emmert et al., Phys. Fluids 23, 803 (1980).
[2]K. U. Riemann, Phys. Fluids 24, 2163 (1981).
[3]R. C. Bissel and P. C. Johnson, Phys. Fluids 30, 779 (1987).
[4]G. L. Main, Phys. Fluids 30, 1800 (1987).

CB-8 **Study of Intense Pulsed Glow Discharges**, B. SZAPIRO, H.F. RANEA-SANDOVAL, C. MURRAY, AND J.J. ROCCA, **Colorado State University** - Intense high voltage glow discharges (50-100 kV) that generate high current density (>10 A/cm^2) electron beams in the cathode sheath were studied. The dependence of electron emission on cathode materials and surface state was investigated. Electrostatic probe measurements show that the negative glow plasma density increases linearly with the discharge current and has spatial distribution that closely matches the electron beam current density profiles. Electron temperatures of 1 to 1.5 eV were measured at 7 cm from the cathode. In high current density discharges a denser and hotter plasma region was observed to develop at approximately 20 cm from the cathode.

*Work supported by the U.S. Air Force.

CB-9 Study of Soft Vacuum Electron Beam Generation Using Laser Opto-Galvanic Spectroscopy, S. MORIYA*, P. ZELLER*, G. J. COLLINS, Colorado State University - The 1-10 keV electron beams present in cold cathode glow discharges have already been used for microelectronic film processing and in pumping gas lasers[1]. However, beam generation optimization requires a deeper understanding of the cathode sheath and the influence of the cathode material. The electric field and its spatial variation has been measured for a wide range of discharge parameters and cathode materials using the established LOGS[2,3] method.

Research supported by NSF, ONR and DARPA.
*On leave from (resp.) Kawasaki Steel Corp. Japan, and University Paris-Sud, France.
[1]B. Shi, Z. Yu, J. Meyer and G. J. Collins, IEEE Tr. Plasma Science 14, 523 (1986).
[2]D. K. Doughty and J. E. Lawler, Appl. Phys. Lett. 45, 611 (1984).
[3]B. N. Ganguly et al, 39th GEC, Madison, WI (1986).

SESSION D

3:15 PM - 6:00 PM, Tuesday, October 13

Space Science and Technology Center, Room 3

POSTERS

Chairman: A. Larson (Georgia Tech)

SESSION DA

3:15 PM - 6:00 PM, Tuesday, October 13

Space Science and Technology Center, Room 3

HEAVY PARTICLE COLLISIONS

Chairman: A. Larson (Georgia Tech)

DA-1 Threshold Photoionization Studies of Silver Clusters, K. LAIHING, P. Y. CHENG AND M. A. DUNCAN, University of Georgia - Microclusters of silver containing up to 40 atoms are produced by laser vaporization in a pulsed molecular beam source, and studied with laser photoionization mass spectroscopy. Near threshold ionization is accomplished at a variety of UV excimer laser wavelengths (249, 193, 157 nm). Single-photon versus multiphoton ionization dynamics are studied by varying the laser wavelength and fluence. Under single-photon conditions, bracketing experiments establish ionization potentials as a function of size. An even-odd IP alternation is observed, with odd numbered clusters (N = 3,5,7...) having lower values than adjacent even numbered species. Multiphoton conditions result in extensive cluster fragmentation so that stable cations dominate mass spectral distributions. An even-odd alternation is again observed favoring odd-numbered cations. Similar studies are conducted on mixed-metal clusters (Ag/Mn, Ag/Cr, Ag/Mo) to examine the influence of added atoms on this ionization behavior.

DA-2 Long-lived, Weakly Bound Electronically Excited Complexes Formed in Metal Based Oxidations. M. J. Mc QUAID and JAMES L. GOLE, School of Physics, Georgia Institute of Technology, Atlanta, Georgia 30332 - Chemiluminescence from the oxidation of transition metal and Group III A atoms and clusters entrained in helium and argon at varying temperature have been associated with the formation of diatomic metal oxides[1] and metal cluster oxides[2]. The extension of this work through CO entrainment provides a means of evaluating metal carbonyl bonding and for initiating studies of surprisingly long-lived electronically excited metal oxide carbonyl complexes. Preliminary results appear to demonstrate a periodicity which correlates well with anticipated trends in transition metal-carbonyl binding and first row transition metal oxide bond strengths.

DA-3 Production and Stability of Ar_3^+ and Ar_4^+.* P. SCHEIER, M. LEZIUS, T.D. MÄRK, Universität Innsbruck, Austria, C.R. ALBERTONI, R. CASTLEMAN, Jr. Penn State University, University Park, Pa. - Rare gas cluster ions are of particular interest because of their simplicity (allowing comparison with theory), their possible role in power loss phenomena in excimer lasers and their role in understanding condensation phenomena (magic numbers). In the present work Ar_3^+ (and Ar_4^+) has been produced by two different nozzle expansion techniques, one involving electron impact ionization of the neutral cluster early and one late in the expansion process. In both cases metastability is observed to depend on the ion formation process. Moreover, it is found that the observed metastable reaction rate is a strong function of time. Furthermore, photodissociation of Ar_3^+ at ca. 540nm leads solely to Ar^+.

*Work supported by United States Austria Cooperative Science Program (NSF And FWF) : project Nr. 5692 and grant Nr. INT-842 0823.

DA-4 Reactions of He_2^+ and $He(2^3S)$ with Selected Atomic and Molecular Species at Atmospheric Pressures*, J. M. POUVESLE, A. KHACEF, AND J. STEVEFELT, University of Orleans, France, H. JAHANI, V. T. GYLYS, AND C. B. COLLINS, University of Texas at Dallas - Measurements of rate coefficients for the two-body and three-body non associative reactions of energy storing helium species have been extended to a wider set of reactants, using preionized pulsed discharge excitation in high pressures (1-6 atm) of helium gas diluent and over a wide range (0.1-6 Torr) of reactant gas partial pressures. Reaction rates in far excess of the Langevin limit have been found for the reactions of He_2^+ with molecular gases and must be expected at still higher pressures for the monatomic species, since there is no evidence of saturation at 6 atm pressure of diluent. For the reactions of $He(2^3S)$, three-body channels have been well characterized, and they occur at rates of the order of $10^{-31} cm^6 s^{-1}$.

*Supported by NSF grant ECS 83-14633 and NATO grant 655/84.

DA-5 Fine Structure Effects in the Reactive Collision $O+OH-O_2+H$*, M.M. Graff, Georgia Institute of Technology, A.F. Wagner, Argonne National Laboratory, and A.C. Allison, University of Glasgow. - The role of fine structure in the reactive collision $O+OH-O_2+H$ has been studied using coupled equations and adiabatic capture (AC) techniques. Adiabatic long-range potential curves and couplings have been obtained for the eighteen states correlating to the reactant ground states. A half-collision treatment in the adiabatic basis was chosen for consistency with an AC calculation of the cross section. Most reactive flux originates from the lowest fine structure levels; transitions occur primarily at avoided crossings of excited states. The rate constant has been calculated for the range 10-2000 K. Fine structure populations are suggested as a source of the negative temperature dependence in the rate constant at low temperatures.

*Supported by the Division of Chemical Sciences, Office of Basic Energy Sciences, U.S. Department of Energy.

DA-6 Experimental Study of Reactive Collisions of High-Temperature Systems*, M.M. GRAFF, Georgia Institute of Technology - A new experiment is being developed to study the energy dependence of reactivity in high-temperature neutral species. The double mass spectrometer design includes the formation of mass- and velocity-selected neutrals by photodetachment of negative ions in a beam. Radicals travel through a temperature-controlled collision cell containing stable reactants. Reaction products will be detected by ionization and mass analysis. The cooled reaction cell allows rotational state selectivity and improves energy resolution for the measurement of apparent cross sections. Accessible center-of-mass collision energies will range from threshold through tens of eV. Initial experiments will examine reactions of ionic and neutral species with H_2.

*Supported by Research Corporation and by the Division of Chemical Sciences, Office of Basic Energy Sciences, U.S. Department of Energy.

DA-7 Fast Metastable Argon Atoms from a Hot Cathode Discharge J.W. Sheldon and K.A. HARDY Florida International University Metastable Ar($^3P_{2,0}$) effusing from the anode of a hot cathode Ar discharge produce two peaks in the time of flight distribution. The slow peak is typical of the thermal velocity distribution of Ar($^3P_{2,0}$) in the discharge. The fast peak is much lower in intensity and corresponds to a velocity about four times thermal. The velocity dependent total elastic scattering cross sections for atoms in the fast peak on ground state rare gas targets are shown to be characteristic of fast Ar($^3P_{2,0}$) atoms. We propose these fast metastable atoms are formed from $^4S^e_{3/2}$ Ar^- ions by collisional detachment. These ions are known to form in collisions of Ar($^3P_{2,0}$) atoms with Cs atoms and lie just below the Ar($^3P_{2,0}$) states with an auto-detachment lifetime of 0.35 μs.[1]

[1]Y.K. Bae, J.R. Peterson, A.S. Schlachter and J.W. Sterns, Phys. Rev. Lett. 54, 789 (1985)

DA-8 Free Radical Processes in SF_6/O_2 Plasmas. K.R. RYAN and I.C. PLUMB. CSIRO Division of Applied Physics, Lindfield, NSW 2070, Australia. Processes which occur in SF_6 when subjected to an electric discharge are of interest in applications ranging from high voltage insulation to the plasma etching of semiconductor material. Because of this considerable efforts have been made to understand the basic chemical physics of these discharges. Nevertheless the neutral gas-phase chemistry is still poorly understood, a fact which prevents detailed modelling of these systems. This paper reports rate coefficients for the reaction of SF_x frangments from SF_6 with F, O and O_2. The experimental values obtained show quite plainly that current models of the chemistry of SF_6/O_2 plasmas need to be revised. The production of SOF_4, SOF_2, SO_2F_2 and SO_2 are discussed in terms of the rate coefficients obtained.

DA-9 Collisional Destruction of Metastable N_2 ($a''^1\Sigma_g^+$) Molecules by N_2 #, A.B. WEDDING and A. V. PHELPS, JILA, U. of Colo. and NBS.— Using CW laser absorption of the $N_2(c_4{}^1\Pi_u \leftarrow a''^1\Sigma_g^+)$ transition and the density perturbation technique of Tischer and Phelps[1] we have measured the collisional destruction of the a''-state. The a''-state metastables are generated in the positive column of a pulsed discharge (2 A cm^{-2}, 5 μs, 0.5 torr) and probed by CW laser absorption. The a''-state density is then perturbed by pulsed laser excitation and the destruction frequency determined from the recovery of transmission. Typical metastable lifetimes were 200ns. After linear extrapolation to zero discharge current, the density dependence of the destruction frequency yielded a collisional destruction rate coefficient by neutral N_2 of approximately 2.0×10^{-16} $m^3 s^{-1}$.

Supported in part by the Air Force Wright Aeronautical Laboratories and NSF.

[1] H. Tischer and A.V. Phelps, Chem.Phys. Letters 117, 550 (1985)

DA-10 Quenching of Ar Metastables in Radio Frequency Glow Discharges, G.R. SCHELLER, R.A. GOTTSCHO, T. INTRATOR, D.B. GRAVES, AT&T Bell Laboratories - Modulation spectroscopy is used to measure quenching rates for Ar metastables in radio frequency discharges containing both Ar and one of the molecular gases N_2, BCl_3, Cl_2, and SF_6. Except for BCl_3, quenching rates for these gases have been measured previously.[1,2] By comparing *in situ* quenching rates with those determined downstream, the effects of dissociation and charged particle collisions are assessed. Because the degree of dissociation increases with increasing rf power, the metastable quenching rate decreases with power: daughter molecules are less efficient quenchers than parent molecules. Extrapolation to zero power yields rate constants in good agreement with those measured downstream.

[1] J.E. Velazco, J.H. Kolts, D.W. Setser, J. Chem. Phys. 69, 4357 (1978).
[2] M. Bourene and J. Le Calve, J. Chem. Phys. 58, 1452 (1973).

DA-11 Zeeman Mixing Induced in Collisions of 5^2P K Atoms with Noble Gases.* R. BERENDS, W. KEDZIERSKI and L. KRAUSE, University of Windsor - Potassium vapor contained together with a noble gas in a fluorescence cell located in a 7T magnetic field, was irradiated with pulsed dye laser light which excited the K atoms to either the $5^2P_{1/2,-1/2}$ or the $5^2P_{3/2,-3/2}$ Zeeman substate. Collisions of the excited and polarized K atoms and noble gas atoms populated the entire 5^2P Zeeman manifold and resulted in the emission of a fluorescence spectrum which was resolved with a polarizer and a scanning F-P interferometer. Measurements of the relative spectral intensities yielded cross sections for multipole relaxation and Zeeman mixing, which are compared with theoretical predictions[1] and with the results of previous zero-field experiments.[2]

* Research supported by the Natural Sciences and Engineering Research Council of Canada.

1 Spielfiedel et al. J. Phys. B 12, 3693 (1979).
2 Berends et al. JQSRT 37, 157 (1987).

DA-12 Wall vibrational deexcitation effects on the vibrational temperature in weakly ionized nitrogen plasmas, S. ONO and S. TEII, Musashi Inst. Tech., Japan - Molecular gas plasma has been applied to many applications, for example, plasma reaction chamber or gaseous lasers. It is necessary to understand the behaviour of the molecule vibrational temperature Tv inside plasmas which surrounded by container walls for controlling molecule plasma at optimum operating condition, since the excitation rates or chemical reaction rates in plasmas depend on Tv. The effect of wall vibrational deexcitation on the nitrogen Tv is investigated both experimentally and theoretically. Tv was measured using 3 cm, 2 cm, 0.8 cm I.D. Pyrex glass cylindrical discharge tubes by side light emission intensity of N_2 2nd Pos. sys. B, and plasma parameters were measured by electrostatic probe. Theoretical calculation has been conducted at same condition to clarify plasma parameter dependences on the Tv by assuming the appropriate wall deexcitation probabilities between 0% to 100%. Experimental and theoretical Tv observed to decrease with decreasing discharge tube I.D. at fixed plasma conditions due to the vibrational wall deexcitation. The experimental values of Tv show good agreement with the theoretical one by assuming wall deexcitation probability around 20%.

DA-13 Highly Excited Molecular Hydrogen Confined In A Superfluid Helium Film Coated Cell.* Y.M. XIAO, S. BUCHMAN, L. POLLACK, D. KLEPPNER and T.J. GREYTAK, M.I.T. **- We have produced molecular ortho-hydrogen from a gas of doubly polarized atomic hydrogen[1]. The recombination reaction is initiated by flipping the electron spin by millimeter microwave resonance. The nuclear spin evolution of the resultant molecule is monitored by pulse NMR. The experiment is carried out in a magnetic field of 6.7 Tesla at temperatures below 1 Kelvin. Contrary to original expectations[2], the nuclear spin polarization is lost one second after the molecule is formed. We propose that a highly rotation-vibration excited molecular hydrogen gas is formed in the superfluid helium film coated cell, and the high angular momentum states are responsible for the loss of the polarization in a short time. We will discuss the possibilities of testing many of the untested theories[3] in this unique gas system.

*Submitted by Y. M. Xiao.

**Research supported by DOE grant DE-AC02-76ET03069

[1] R.W.Cline, T.J.Greytak and D.Kleppner, Phys. Rev. Lett. 47, 1195(1981)

[2] D.Kleppner, and T.J.Greytak AIP Conference Proceedings 95, 546 (1983)

[3] N. C. Blais and D. G. Truhlar, in Potential Energy surface and Dynamics Calculations, edited by D. G. Truhlar (Plenum, New York, 1981).

DA-14 Connections Between Fast Atomic Collisions and Three Body Coulomb States, M. G. MENENDEZ and M. M. DUNCAN, University of Georgia - Preliminary data on two types of measurements on fast (~0.5MeV/u) collisions between ions and atoms that lead to three-body final states will be discussed. In one case, collisions of H^- with He, the three body final state of interest is e^--H^+-e^-, which is produced by the double electron detachment process. Preliminary electron-electron coincidence measurements indicate general agreement with threshold theory predictions for two electrons escaping slowly from a positive ion. In the other case, collisions of H^+ with Kr and Ar, we have examined certain (energy) continuum electrons that are between the two Coulombic centers, i.e., H^+-e^--$Kr^+(Ar^+)$. These electrons display a sharp angular dependence that suggests a three body dynamical behavior. In addition, we have examined Auger electrons ejected by Kr^+ during these collisions and find an angular behavior that is similar to the above mentioned continuum electrons.

SESSION DB

3:15 PM - 6:00 PM, Tuesday, October 13

Space Science and Technology Center, Room 3

RECOMBINATION AND ATTACHMENT

Chairman: A. Larson (Georgia Tech)

DB-1 Measurement of the Recombination Rate of Cs^+ and e^- in High Pressure Molecular Gases. S.M. JAFFE, M. MITCHNER, AND S.A. SELF, Mech. Engr. Dept., Stanford Univ. - A xenon flashlamp is used to photoioinize Cs vapor in atmospheric pressure N_2 or H_2. Depletion of the ground state Cs population is monitored by absorption in the plasma afterglow. By relating this depletion to the concentration of Cs^+, fractional ionization (>20%) and recombination rates have been measured over a range of conditions: $10^{10} < [Cs] < 10^{14}$ cm^{-3}, $10^{19} < [N_2,H_2] < 5 \times 10^{19}$ cm^{-3}, $500 < T < 700$K. A kinetics model indicates that in this range of conditions, ion molecule reactions dominate the recombination rate. At higher temperatures (1200K) measurement of the rate of the reaction $Cs^+ + e^- + N_2 \rightarrow Cs + N_2$ is possible.

*Work supported by the AFOSR, Grant No. 83-0108.

DB-2 Final State Energy Distribution Produced by Hydrogen Atom Recombination. M. L. Homer and A. E. Orel, The Aerospace Corp.* -- The nascent vibrational/rotational distribution produced by the reaction $H + H + M \rightarrow H_2(v, J) + M$, M=He, Ar was calculated using the resonance complex theory of Roberts. Details of the reaction probability as a a function of impact parameter were determined and the total cross-sections compared to other calculations.

*Work supported by the Aerospace Sponsored Research Program.

DB-3 Electron Attachment Rate Constants of Bromine Compounds*, W. C. WANG, D. P. WANG, and L. C. LEE, San Diego State Univ. - The electron attachment rate constants of HBr and CH_3Br published in literature have a large discrepancy. We remeasured these data using a parallel-plate drift-tube apparatus. The electron attachment rate constants of HBr, CH_3Br, and C_2H_5Br have maximum values of $1x10^{-9}$, $1x10^{-11}$, and $9x10^{-11}$ cm^3/s at mean electron energies of 0.55, 0.4, and 0.8 eV, respectively. The electron attachment rate constants were measured as a function of mean electron energy, and they will be compared with the values determined from the electron impact attachment cross sections using the known electron energy distribution functions of N_2 and Ar at various E/N. The measurements for the electron impact attachment cross sections of the above bromine compounds are in progress in our laboratory.

* Work supported by AFOSR and ONR

DB-4 Electron Attachment to SF_6 in N_2, Ar and Xe Buffer Gases*, S. R. HUNTER, J. G. CARTER, AND L. G. CHRISTOPHOROU, Oak Ridge National Laboratory - We have measured the electron attachment rate constant k_a ($\langle\epsilon\rangle$) for vanishingly small quantities of SF_6 ($\geq$ 3 parts in 10^9) in N_2 and Ar buffer gases over the energy $\langle\epsilon\rangle$ range 0.04 eV $\leq\langle\epsilon\rangle\leq$ 4.5 eV using a high pressure swarm technique.[1] The electron drift velocity w and electron attachment coefficient η/N_a for small quantities of SF_6 ($\geq$ 5 parts in 10^{10}) have been measured in Ar and Xe buffer gases over the E/N range $4 \times 10^{-20} \leq E/N \leq 10^{-17}$ V cm^2 in a separate pulsed Townsend experiment.[2] The thermal $(k_a)_{th}$ in the SF_6/N_2 gas mixture is $(2.30 \pm 0.1) \times 10^{-7}$ cm^3 s^{-1} and in SF_6/Xe $(k_a)_{th} = (2.23 \pm 0.1) \times 10^{-7}$ cm^3 s^{-1}. The k ($\langle\epsilon\rangle$) and η/N_a measurements have been used in a Boltzmann analysis to obtain the total electron attachment cross section $\sigma_a(\epsilon)$ for $\epsilon \leq 10$ eV. These measurements are compared with the literature data.

*Research sponsored by OHER, USDOE under contract DE-AC05-840R21400 with Martin Marietta Energy Systems.

[1]S. R. Hunter and L. G. Christophorou, J. Chem. Phys., 80, 6150 (1984).

[2]S. R. Hunter, J. G. Carter, and L. G. Christophorou, J. Appl. Phys., 60, 24 (1986).

DB-5 Vibrational Accommodation Coefficients and Dissociative Attachment 'Thermometry'*, S.C. CHU, K.L. STRICKLETT and P.D. BURROW, U. of Nebraska, Lincoln -- The dissociative attachment cross section of N_2O is well known to be strongly temperature dependent for electrons with low incident energies.[1] The sensitivity of the O^- yield is attributed to thermal excitation of the bending mode. Conversely, a measurement of the yield allows the vibrational temperature of the gas in this mode to be determined. We have used this method to characterize the vibrational temperature of N_2O emerging from a cylindrical oven with a length-to-diameter ratio of 45. Monte Carlo calculations[2] are used to estimate the average number of wall collisions for the effusing molecules. With our preliminary data, we derive a vibrational accommodation coefficient of 0.001 on a stainless-steel surface at 470 °C.

*This work was supported by NSF.
[1]P.J. Chantry, J. Chem. Phys. 51, 3369 (1969).
[2]H.C.W. Beijerinck, M.P.J.M. Stevens and N.F. Verster, Physica 83C, 209 (1976).

DB-6 Dissociative Attachment of Electrons to Transition Metal Superacids,* T.M. MILLER, A.E.S. MILLER, J.F. FRIEDMAN, and D.J. EWING, U. of Oklahoma--We will report on measurements of electron attachment rates at 300 K for transition-metal compounds. We are especially interested in "superacid" molecules of the type $HCo(PF_3)_4$. The flowing afterglow/Langmuir probe technique[1] has been used in this work. Previous research has led to the conclusion that exothermic electron attachment reactions with strong acid molecules are likely to be exceptionally fast.[1] We found the electron attachment rate for $HCo(PF_3)_4$ to be surprisingly low, about 500 times lower than for $Fe(CO)_5$. The latter rate is known[2] to be fast (2×10^{-7} cm^3/s). Supporting mass spectrometric results and ion-molecule reaction data will be presented.

*Supported by the US Air Force and the ACS-PRF.
[1]N.G. Adams, D. Smith, A.A. Viggiano, J.F. Paulson, and M.J. Henchman, J. Chem. Phys. 84, 6728 (1986).
[2]P.M. George and J.L. Beauchamp, J. Chem. Phys. 76, 2959 (1982).

DB-7 Effect of Temperature on the Nondissociative Electron Attachment to $n\text{-}C_4F_{10}$, $n\text{-}C_6F_{14}$, and $c\text{-}C_4F_6$*. P. G. DATSKOS AND AND L. G. CHRISTOPHOROU, Oak Ridge National Laboratory and University of Tennessee - The total electron attachment rate constant, $k_a(\langle\epsilon\rangle,T)$, for $n\text{-}C_4F_{10}$, $n\text{-}C_6F_{14}$, and $c\text{-}C_4F_6$ has been measured (in a buffer gas of Ar or N_2) using an electron swarm technique over the temperature, T, range 300 to 750 K and in the mean electron energy, $\langle\epsilon\rangle$, range 0.41 to 4.81 eV for $n\text{-}C_4F_{10}$ and $n\text{-}C_6F_{14}$ and 0.046 to 0.911 eV for $c\text{-}C_4F_6$. The nondissociative component of $k_a(\langle\epsilon\rangle,T)$, $k_{nd}(\langle\epsilon\rangle,T)$, for $n\text{-}C_4F_{10}$ and $n\text{-}C_6F_{14}$ extends from $\langle\epsilon\rangle$ = 0.41 to $\langle\epsilon\rangle \lesssim 4.81$ eV and decreases precipitously with increasing T, for $T \gtrsim 400$ K. Similarly, the $k_{nd}(\langle\epsilon\rangle,T)$ for $c\text{-}C_4F_6$, which attaches electrons only nondissociatively below ~0.911 eV, decreases with T by three orders of magnitude between 400 and 650 K. The measured attachment rate constants and the cross sections unfolded from these, will be presented, and possible causes for these profound decreases in nondissociative electron attachment with increasing T will be discussed.

*Research sponsored by OHER, USDOE under contract DE-AC05-840R21400 with Martin Marietta Energy Systems.

SESSION DC

3:15 PM - 6:00 PM, Tuesday, October 13

Space Science and Technology Center, Room 3

LAMPS AND ARCS

Chairman: A. Larson (Georgia Tech)

DC-1 Determination of Temperature in a High Pressure Hg Discharge by Pulsed Laser Optogalvanic Spectroscopy. JERRY KRAMER GTE Labs --Pulsed laser irradiation of a high pressure mercury discharge tuned to excite the 7 $^3S_1 \leftarrow 6\ ^3P_{2,1,0}$ transitions in Hg at 546, 436, and 405 nm, respectively decreased the voltage across the discharge with respect to its unperturbed value. The optogalvanic signals had a non-linear dependence on laser intensity which was attributed to stimulated emission. Negative optogalvanic signals were also observed at 408 nm ($7\ ^1S_0 \leftarrow 6\ ^3P_1$), 577 nm ($6\ ^3D_2 \leftarrow 6\ ^1P_1$), and 590 nm ($6\ ^1D_2 \leftarrow 6\ ^1P_1$). The shape of the radial temperature profile was obtained by inverting the optogalvanic signals at 546 nm for various chords through the discharge and assuming that the optogalvanic signals depended on temperature through the spatial dependence of the $6\ ^3P_2$ state and a weak $T^{-1/2}$ dependence from the conductivity. The shape of the radial temperature profile calculated from the emission intensity of the Hg 577 nm line was in good agreement with the optogalvanic results.

DC-2 A Laser-Triggered High Voltage Switch Using a Composite Target Pellet, P. J. BRANNON AND D. F. COWGILL, Sandia National Laboratories - A laser-triggered high voltage vacuum switch with a unique composite target pellet has been developed. The target pellet is fabricated from a compressed mixture of equal weights of 8-μm titanium and 300-μm KCl powders. The switch triggers reliably for 532-nm laser input energies of 20 μJ corresponding to a peak irradiance of 1 MW/cm^2. Jitter times of less than $\pm$ 15 ns are observed. The delay time of the switch increases as the gap voltage decreases. A delay time of less than 100 ns is observed for a gap voltage of 6000 V and a gap spacing of 0.5 mm. The trigger energies and peak irradiances reported here are smaller by an order of magnitude or more than previously reported[1-3] for laser-triggered vacuum switches.

[1]R. G. Fellers, F. T. Warren, Jr., and J. E. Thompson, in Proceedings of Southeastcon '80, (IEEE, New York, NY, 1980), p. 315.

[2]A. A. Makarevich and V. A. Rodichkin, Instrum. Exp. Tech. (USSR) 16, 1716 (1973).

[3]V. S. Bulygin, V. B. Lebedev, G. A. Pryanikova, V. V. Ryukkert, S. S. Tsitisiahvili and V. A. Yakovlev, Sov. Phys. Tech. Phys. 20, 561 (1976).

DC-3 Radiation Trapping in Sodium Vapor*, J. Huennekens, T. Colbert, and H. J. Park, Lehigh University - We report measured values of sodium D line effective radiative rates in sodium - noble-gas mixtures. Sodium atoms in a stainless steel and sapphire cell were excited with a short pulse laser, and the time-resolved fluorescence emerging from the cell was recorded. Due to the well defined geometry and equilibrium conditions of our cell, we can make accurate comparisons with radiative rates predicted by the Holstein theory. In particular, we have studied the relationship between radiation trapping and collisional broadening of spectral lines. In all cases, Holstein theory results agree well with our measured values. Using this result, we demonstrate that measurements of effective radiative rates can, in some cases, yield unknown impact-regime line-broadening rates. In addition, we plan to present new data on sodium - mercury mixtures.
Research supported by NSF, GTE Laboratories, and General Electric Corporate R & D.

DC-4 *Analytic Temperature Profile for Plasma Diagnostics*, P.A. VICHARELLI and L.C. PITCHFORD, *GTE Laboratories Incorporated, Waltham, MA* -- Lineshape plasma diagnostics are usually based on the solution of the radiation transport equation with the aid of some analytic temperature profile with adjustable parameters.[1,2] This paper presents a simple analytic profile that may be used for this purpose. The derivation of this formula is based on an exact solution of the one-dimensional energy balance equation with a two-zone description of the radial dependence of the material properties such as electrical and thermal conductivities, and net emission coefficients. A parabolic temperature profile is obtained in the first zone, characterized by the arc core. The second zone, which corresponds to the arc mantle, is described by a second parabola and a logarithmic term. The two zones are connected by requiring temperature and heat flux continuity at the zone boundary. The application of this analytic profile to arc lamps is discussed.

1. H.-P. Stormberg and R. Schafer, J. Quant. Spectrosc. Radiat. Transfer 33, 27 (1985).

2. P. A. Vicharelli, W. P. Lapatovich, and C. Struck, 39th GEC. Paper JB-4, Madison, WI, 1986.

DC-5 The Electrical Conductance of High Pressure Mercury Discharge Lamps , B. DEBBAGH-ZRIOUIL, C. SORIANO, M. AUBES, J.J. DAMELINCOURT , C.P.A.T. , University Paul Sabatier (Toulouse- France) - The electrical conductance has been studied for a high pressure mercury discharge lamp operated under square wave conditions. From arc voltage measurements and optical observations we have evaluated the axial distribution of electric field and the unit length plasma conductance in the positive column and in the regions of voltage drop near the electrodes. In these regions radial temperature profiles have been determined from spectroscopic measurements. Electrical conductivity and plasma conductance have also been calculated in the framework of the Chapman-Enskog formalism[1]. The impact on the computation of both the values chosen for electron-mercury momentum-transfer cross section[2] and of the temperature distribution is evaluated. On the basis of a comparison between experimental and theoretical results the accuracy of cross section data and temperature determination are discussed.

[1]J.O. Hirschfelder et al., Molecular theory of gases and liquids, John Wiley & Sons, New York (1964).
[2]S.D. Rockwood, Phys. Rev. A 8, 2348 (1973)

DC-6 Application of Generalized Multithermal Equilibrium Model to Collisional-Radiative Calculations for Nonequilibrium Hydrogen Plasma,* K.Y. Cho and T.L. Eddy, Georgia Institute of Technology - To Analyze transport processes in plasma, it is very important to get the chemical compositions correctly. The collisional-radiative calculations are used to compensate the production of electrons by convection or ambipolar diffusion, in an effort to find out the effect of radiative transfer on nonequilibrium plasma. It was found that the steady state compositions of collisional-radiative calculations are strongly dependent on the methods of the detailed balance for recombination coefficients by 3-body collision. The compositions of Generalized Multi-Thermal Equilibrium (GMTE) Model are compared to collisional-radiative calculations for steady optically thick hydrogen plasma. Some methods of the detailed balance give the steady state compositions that are different from those of GMTE by orders of magnitude. And the results at LTE condition by those methods are different from those of Saha equilibrium. To ensure the consistency of collisional-radiative calculations at steady optically thick plasma and GMTE model, the detailed balance for recombination coefficients by 3-body collisional are made by GMTE equation.

*Sponsored in part by NSF Grant CPE 8311325.

[1] K.Y.Cho, T.L. Eddy, 39th GEC, EA-4, Madison, Wisconsin (1986)

DC-7 Supercritical Vapor in Arc Cathode Region. H. MINOO, Univ. Paris-Sud - At sufficiently high current densities J, using the energy balance, it is found that the metallic vapor in the arc cathode region is in a supercritical state.

cathode	Cu		Hg	
I (A)	10	100	10	100
J_b ($A.m^{-2}$)	$1,4 \times 10^9$	$1,4 \times 10^8$	$1,2 \times 10^5$	$1,2 \times 10^4$
J_c ($A.m^{-2}$)	$1,8 \times 10^{10}$	$1,8 \times 10^9$	$8,4 \times 10^6$	$8,4 \times 10^5$

As is shown in the table, for example with a Cu cathode and an arc current I = 10 A, the cathode reaches the boiling temperature T_b when the arc current density $J_b \gtrsim 1,4 \times 10^9$ $A.m^{-2}$, and the critical temperature T_c when $J_c \gtrsim 1,8 \times 10^{10}$ $A.m^{-2}$. Based on a continuous change of the mean local density in passing through the transition region, from the liquid phase to the gas phase[1], the continuous phase transition model is then introduced and the current transfer in the arc cathode spot is examided in this model.

1 T.L. Hill"Stat. Thermo.". Addison-Wesley (1960) p 318
2 The existense of a very dense metallic vapor layer was recognized as early as 1949 J. Rothstein, P. R. 73,1214

DC-8 Transverse Spreading Mechanisms in the Low-Pressure Mercury-Argon Positive Column, J.T. Dakin, GE Corporate R&D - A model[1] of radial variations in the low-pressure Hg-Ar positive column is viewed in the light of recent measurements[2] of radial variations in the Hg $6^3 P_{0,1,2}$ densities. Discharge conditions in the vicinity of 3 torr Ar pressure, 0.007 torr Hg pressure, 0.4 A current, and 34 mm tube diameter are considered. The electron energy distribution is paramaterized using a two-temperature approximation, and the bulk and tail temperatures are functions of radius. Mechanisms contributing to transverse discharge spreading include the diffusion of electrons, the diffusion of excitation (radiation trapping), radial cataphoresis, and axial electric field. The relatively high Ar momentum cross section for electrons above the Hg inelastic threshold is seen to diminish the role of electron diffusion in spreading the discharge.

1 J.T. Dakin, J. Appl. Phys., 60, p. 563 (1986)
2 L. Bigio, 40th Gaseous Electronics Conf., Atlanta, GA (1987).

DC-9 A Model for the Optogalvanic Effect Induced in an Hg-Ar Discharge, W. RICHARDSON, L. MALEKI, AND E. GARMIRE, Jet Propulsion Laboratory, California Institute of Technology - The optogalvanic effect induced in an Hg-Ar discharge by light at 546.1 nm is studied experimentally and theoretically. The plasma and its response to a disturbance in the atomic level populations is described entirely in terms of electron collision cross sections and other fundamental parameters. In a detailed description of the laser interaction with the atomic system, it was necessary to take into account velocity changing collisions (VCC). These collisions (VCC) strongly modify the interaction between the Doppler broadened system and the optical field. Measurements of the magnitude of the optogalvanic signal confirm most of the theoretical results.

DC-10 Pulse Technique for Probe Measurements in Gas Discharge, V. GODYAK, GTE Electrical Products, Danvers, MA - We report on an improved electron energy distribution function (EEDF) measurement technique and associated hardware design. The system is based on a combination of fast pulse technique, noise supression feedback circuits and automated cleaning of the probe during the measurement. It is shown that state of the art analog and digital electronics allow probe measurements as fast as tens of μS. This enables us to obtain the EEDF with high energy resolution and in a dynamic range of 30-50 db for single-shot and 60-80 db for repetitive processes. EEDF's measured in the positive column, cathode region and under conditions of artificial plasma perturbation are presented. Furthermore, experiments to explore the effect of the bandwith on energy resolution and dynamic range, as well as some fundamental and technological limitations of the fast EEDF measurement, are discussed.

SESSION DD

3:15 PM - 6:00 PM, Tuesday, October 13

Space Science and Technology Center, Room 3

RADIATIVE PROPERTIES

Chairman: A. Larson (Georgia Tech)

DD-1 Intensity Distribution of Atomic Helium Rydberg State Stark Spectra, J. R. Shoemaker, B. N. Ganguly, B. L. Preppernau and Alan Garscadden, APL, Wright-Patterson Air Force Base. -- Intensity distribution of atomic helium Stark manifolds with principal quantum number n=13 up to 22 have been measured with both $\Delta m_j=0$ and $\Delta m_j=\pm 1$ polarizations in plasma electric fields < 1000 v/cm, in the cathode sheath region. The spectra were observed by optogalvanic spectroscopy in a low pressure discharge and tunable laser excitation from the metastable 2^3S state. The $\Delta m_j=0$ polarization spectra exhibit distinctly non-hydrogenic intensity distribution for all n states up to the n mixing Stark manifold, whereas the $\Delta m_j=\pm 1$ polarization spectrum becomes hydrogenic for $n \gtrsim 16$ at electric field $\simeq 700$ v/cm.

DD-2 Lifetime of $He(2^1S)$ in High Pressure Helium Electric Discharges,*, D. F. HUDSON, Naval Surface Weapons Center, White Oak, MD - Recent experiments and studies, indicate the possibility of longer $He(2^1S)$ lifetimes in high pressure discharges than previously thought. To further clarify this problem, we are conducting an experiment which simultaneously measures the lifetimes of the $He(2^1S, 2^3S)$ metastables in the afterglow of high (100 - 760 torr) pulsed discharges. We obtain time resolved absorption curves from two dye lasers tuned to the 389 and 501 nm lines. Preliminary results appear to verify an increase in the 2^1S lifetime with increasing pressure. We will present our latest data and interpertation.

*Research supported by the NSWC IR program

DD-3 Determination of the Transition Probability of a Self-reversed Line.* D. KARABOURNIOTIS, Physics Department, University of Crete (Greece), AND E. DRAKAKIS AND J.J. DAMELINCOURT, C.P.A.T., University of Toulouse (France) - The aim of this study is to propose and test a method for determining the absolute value of the transition probability for a self-reversed line. The measuring technique is based on the determination of the optical depth at the line center and the line maximum and requires knowledge of the line-level temperatures. The multiparameter method is used.[1,2] The results obtained for the mercury self-reversed lines emitted by ac 50-Hz mercury arcs at different mercury pressures, are in good agreement among them, as well as with the published ones. Using the $Y(\tau, p)$ Bartel's function[3] satisfactoty results have been found only at the moment of current zero-crossing.

*Research performed as part of a J.R.P. between the Univrsity of Toulouse and the University of Crete.

[1] D. Karabourniotis, J. Phys. D, 16, 1267 (1983).
[2] D. Karabourniotis, Opt. Commun, 61, 38 (1987).
[3] P.A. Vicharelli and L.C. Pitchford, paper 66, 4th Inter. Conf. Light Sources, Karlsruhe, 1986.

SESSION EA

8:00 AM - 10:05 AM, Wednesday, October 14

Space Science and Technology Center, Room 5

MOLECULAR CLUSTERS

Chairwoman: M. M. Graff (Georgia Tech)

EA-1 Formation and Photodissociation Dynamics of Antimony and Bismuth Metal Cluster Ions, M. A. DUNCAN, M. E. GEUSIC*, AND R. R. FREEMAN**, University of Georgia - Ionized metal clusters of antimony or bismuth are produced by Nd:YAG laser vaporization in a pulsed nozzle source. Size distributions and relative abundances of both positive and negative ions are probed by time-of-flight mass spectroscopy sampling of the laser vaporization plasma. Magic numbers are observed at certain cluster sizes in these distributions, following similar patterns for both antimony and bismuth, which indicate stable cation (e.g. M_3^+, M_5^+, M_7^+) and anion (e.g. M_2^-, M_5^-, M_7^-) cluster species. Cation clusters are mass selected and photodissociated at 248 nm, with subsequent mass analysis of photofragment ions. Dissociation patterns for both metals suggest the preferential elimination of stable neutral dimers and tetramers and the formation of stable fragment cations.

*Battelle Northwest Laboratories, Richland, WA.
**AT&T Bell Laboratories, Murray Hill, NJ.

EA-2 Photodissociation of Mass Selected Cluster Ions*, W. C. LINEBERGER, D. RAY and N. E. LEVINGER, JILA, University of Colorado - We report photodissociation spectra of mass selected cluster ions containing as many as 100 atoms. The ions are formed by electron impact in a pulsed supersonic expansion and the large cluster ions are grown by ion-molecule association reactions. A tandem time-of-flight mass spectrometer selects the ion of interest and provides secondary mass analysis for all of the ionic photoproducts. The spectrum of photodissociation products provides clear evidence for an evaporative dissociation mechanism, while at the same time shedding light on the issue of "magic numbers" in mass spectra. The photodissociation cross-sections are observed to change significantly from one cluster size to the next, even in the case of large clusters. These and other results will be described in some detail.

*Research supported by the National Science Foundation.

EA-3 Theoretical Studies of Molecular Clusters, D. A. DIXON, E. I. du Pont de Nemours & Company, Inc. - Great strides have been made in the application of molecular orbital theory to important chemical systems due to recent advances in both hardware and software. Applications of these techniques to alkali metal systems will be discussed. These applications include the electron affinities of alkali dimers and trimers, the proton affinities of alkali dimers and alkali hydrides, and the Li^+ and Na^+ binding affinities of small molecules such as LiH, NaH, H_2, N_2 and CO. The proton affinities of the dimers and hydrides are very large due to charge transfer from the proton to the dimer or hydride. Essentially exact six-electron calculations on the model cluster H_6 will be discussed as will the structure of the trimer of HF.

EA-4 Sequential Clustering Reactions of Si_{1-7}^+ with SiD_4: Identification of Bottlenecks Preventing Rapid Growth of Hydrogenated Silicon Particles, M. L. Mandich, W. D. Reents, Jr., and M. F. Jarrold, AT&T Bell Laboratories -- Gas phase nucleation of hydrogenated silicon dust is a pernicious problem in silane CVD of high quality silicon films. Despite extensive studies of silane CVD chemistry, there is little understanding of how these particulates form. We have observed growth of subcritical size $Si_xD_y^+$ nuclei during sequential clustering of atomic and cluster silicon cations with SiD_4 at room temperature in an ion trap. The clustering reactions proceed in a highly specific fashion. Si^+ grows by addition of three $-SiD_2$ units and then reaches a terminal size which can only aggregate further by attachment of SiD_4. Bare Si_n^+ clusters show analogous growth. Si_n^+ clusters containing more than five atoms do not cluster exothermically with SiD_4 at all. The fundamental mechanisms and energetics for many of the reaction pathways have been calculated using *ab initio* electronic structure theory[1] in conjuction with phase space transition state theory. These calculations permit us to explain why infinite polymerization does not occur for these clusters.

[1]K. Raghavachari, submitted to J. Chem. Phys.

EA-5 Preparation, Characterization, and Oxidation of Small Metal Clusters. JAMES L. GOLE, R. WOODWARD, T.C. DEVORE, S.H. COBB, and M. MCQUAID, School of Physics, Georgia Institute of Technology, Atlanta, Georgia 30332- Clusters of the alkali, coinage, and transition elements are generated in agglomerating flows and supersonic expansions and characterized using laser fluorescent techniques and mass spectrometry. The unique dynamics of cluster oxidation is being characterized using a combination of chemiluminescence and mass spectrometry. An intense copper trimer source allows (1) the study of florescence from strongly dissociating levels and (2) the observation of substantial temperature dependent dynamic changes in spectral features associated with the fluxional nature of copper trimer. In an extrapolation of this study, we obtain the first fluorescence spectra of nickel trimer which, in conjunction with the results of other workers, provides insight into why higher order transition metal clusters have not been observed by resonant two-photon ionization techniques. The oxidation of coinage, Group III and IVA, and transition metal clusters formed in agglomeration flow has been found to produce the metal cluster oxides; the diverse dynamics already observed with limited reactant variation portends of an intriguing gas phase chemical physics.

SESSION EB

8:00 AM - 9:55 AM, Wednesday, October 14

Space Science and Technology Center, Room 4

RF GLOWS: EXPERIMENT

Chairman: P. A. Miller (Sandia National Laboratories)

EB-1 **Spatial Variations in Capacitive rf Plasmas due to Self-Generated Electromagnetic (TEM) Surface Modes.**
STEPHEN E. SAVAS*, Applied Materials, Santa Clara, Calif.
Higher harmonics (n>4) in the voltage of the 13.56 MHz excitation signal have been found to be generated with large amplitudes in some capactively coupled rf discharges used for plasma etching. These harmonics are found to accompany large electric potential variations across the surface of the powered electrode . These phenomena are shown to be due to electromagnetic (TEM) modes,generated by sheath impedance non-linearity, which form standing waves on the electrode surface. This is similar to the behavior of a short,terminated section of transmission line. Since the wavelengths of these modes, which are in approximate resonance with higher harmonics of the excitation signal, can be smaller than the electrodes there may be appreciable variations in rf amplitude across the electrode. This results in plasma density and ion current variations which may affect semiconductor processes.

*** Participating Guest at Lawrence Berkeley Laboratory**

EB-2 An Experimental View of the Parallel Plate Radio Frequency Discharge*, G. A. HEBNER and J. T. VERDEYEN, University of Illinois at Urbana-Champaign. - Microwave diagnostic techniques have been used to measure the radiation temperature and electron density in parallel plate capacitively coupled radio frequency (2.5 MHz) discharges. Evidence is presented for the existence and importance of an energetic electron beam, apparently produced by the large cathode sheath voltage, which sustains and excites the plasma. The measured radiation temperature of the bulk electrons is 500 K for helium and 800 K for argon. An upper limit on the radiation temperature is established for nitrogen (1200 K) and CF_4 (3000 K) discharges. Measurements of the electron density in Helium as a function of electrode spacing show a peak in the electron density that is compatible with the theory of ionization by beam electrons. The electric fields required to carry the RF current by drift in the bulk of the glow are extremely low and consistent with the measured radiation temperatures.

*Work supported by Joint Services Electronics Program (U.S. Army, U.S. Navy, U.S. Air Force) and Army Research Office for Advanced Construction Technology Center.

EB-3

Impedance Characteristics and Energy Deposition in rf Parallel Plate Discharges, P.Bletzinger, APL, Wright-Patterson Air Force Base.-- Detailed measurements of rf-parallel plate discharge characteristics reported previously indicated an ohmic component constant below about 1 Torr and increasing with pressure above 1 Torr. The increasing resistance is representative of collisional losses; the constant resistance indicates a different energy deposition process at the lower pressures. Processes suggested are acceleration of secondary electrons in the electrode sheaths and the "wave riding" process, where electrons gain energy from their reflections by the oscillating, negatively charged sheaths. Measurements of the impedance at different electrode spacings show that the impedance varies with electrode distance only above 1 Torr, again indicating that collisional processes in the discharge volume decrease in importance below 1 Torr. The frequency characteristics of the equivalent resistance and measurements with various electrode materials indicate that the wave riding process is probably the dominant energy deposition process.

EB-4 Use of Langmuir Probes in RF Glow Discharge Plasmas,* N. HERSHKOWITZ, M.-H. CHO, C.H. NAM, AND T. INTRATOR, University of Wisconsin-Madison--Details of the electron "saturation" current portion of a current-voltage characteristic of a collecting Langmuir probe in an rf glow discharge plasma can be combined with data from capacitive and emissive probes in order to determine plasma parameters. The observed time averaged I-V characteristic is sensitive to the time variation of the plasma potential and is also sensitive to the probe circuit. Data from capacitive probes provides an estimate of the time variation. It is demonstrated that ionization makes a significant contribution to the I-V characteristic and results in a false knee at $V_p + \varepsilon_i$, where V_p is the plasma potential and ε_i is the ionization potential. This feature tends to eliminate the value of data obtained with bias voltages that are much more positive ($\geq \varepsilon_i$) than V_p. Emissive probe data are complicated by the possibility of ionization when the probe is biased ε_i more negative than the plasma potential. Prescriptions are provided for determining plasma parameters.

*This work was supported by NSF ECS-8314488.

EB-5 Metastable and Electron Kinetics in Radio Frequency Discharges through Mixtures of Rare and Attaching Gases, R.A. GOTTSCHO, G.R. SCHELLER, T. INTRATOR, D.B. GRAVES, AT&T Bell Laboratories - Because glow discharges through gas mixtures are used in applications ranging from excimer lasers to plasma processing, we have studied the consequences of diluting Ar discharges with BCl_3. Using laser-induced fluorescence and plasma-induced emission spectroscopy, space-time resolved changes in Ar excited state and BCl ground and excited state densities were measured as a function of gas composition, power, pressure, and flow-rate. As Ar is diluted with BCl_3, the Ar metastable and BCl ground state densities increase by 30 - 50%, while the BCl excited state density increases by more than an order of magnitude. We will present a quantitative model that accounts for these observations in terms of quenching of Ar metastables, electron attachment to BCl_3, electron-impact dissociation of BCl_3, and superelastic collisions of electrons with Ar metastables.

EB-6 Laser Optogalvanic Study of Metastable and Resonance Levels of Argon in rf Glow Discharge.
D. E. MURNICK and R. B. ROBINSON, AT&T Bell Laboratories- F. A. MOSCATELLI, Swarthmore College and M. COLGAN, Rutgers University- The laser optogalvanic (LOG) effect from the $^3P_1(1s_4-2p_1$ at 667.7 nm) and $^3P_2(1s_5-2p_2$ at 696.5 nm) levels of argon in a weak rf discharge were studied as a function of pressure in the range .1 to 1.5 torr using a single frequency cw laser. The LOG response was obtained as a function of time using a Pockels cell chopper and a boxcar integrator. Above about 170 mtorr, the transition from the $^3P_1$ resonance level showed characteristics expected for a metastable state whereas the transition from the $^3P_2$ metastable exhibited nonmetastable character at pressures less than approximately 440 mtorr. Signals indicative of a decreased conductivity were always preceded by a transient increased conductivity at turn-on of the laser at the lower pressures. A detailed analysis indicates that trapping of resonance radiation and resonance-metastable interconversion are the major contributors to the effects observed.

EB-7 Spectral Line Intensities in Low-Pressure Surface Wave Discharges, C. BENEKING, AND P. ANDERER, Philips Research Laboratories, Aachen, F.R.G. - The axial structure of Ar and Hg-Ar plasma columns excited by radio-frequency surface waves has been studied with emission spectroscopy. The wave frequency was 300 MHz. A surfatron-type coupling structure as described by Moisan et al.[1] was used. The Ar filling pressures of the 23 mm (internal) diameter discharge tubes ranged between 0.04 torr and 12 torr. With the Hg-Ar discharges, the cold spot temperature was varied between 30°C and 80°C, resulting in a Hg vapor pressure range from about 3×10^{-3} torr to 9×10^{-2} torr. Within this parameter range, the side-on intensities of the visible Ar lines (around 800 nm) and all important Hg lines (including both 184.9 nm and 253.7 nm resonance lines) were measured as a function of axial position and RF input power.

[1] M. Moisan et al., IEEE Trans. Plasma sci. PS-3, 55 (1975).

SESSION FA

10:25 AM - 11:56 AM, Wednesday, October 14

Space Science and Technology Center, Room 5

PLASMA ETCHING

Chairman: J. Kramer (GTE Laboratories)

FA-1 Kinetics of Sulfur Hexafluoride Plasma Etching Discharges, K.E. Greenberg and P.J. Hargis, Jr., Sandia National Laboratories — Pulsed-ultraviolet laser Raman spectroscopy was used to measure the percent dissociation of sulfur hexafluoride in a small plasma etching reactor operating at 13.56 MHz. Measurements were made in the loaded and unloaded reactor at rf powers between 0.5 and 2.5 W/cm². Published model predictions of sulfur hexafluoride dissociation, under similar discharge conditions, are approximately a factor of 3 higher than the experimentally measured dissociation. Optical emission and laser-induced fluorescence spectra recorded in conjunction with the Raman measurements show that gas phase chemistry is important and cannot be neglected in modeling these discharges. At rf powers in excess of 1.0 W/cm² a loading effect was observed which caused the discharge to operate in a bimodal fashion — a stable discharge could be obtained with the brightest part of the glow above either the substrate or the bare electrode. Optical emission spectra are significantly different for the two modes of operation.

FA-2 Negative Ions in SF_6 Corona Discharges.* I. SAUERS, Oak Ridge National Laboratory, Oak Ridge Tennessee--Recent work in modelling by-product formation in SF_6 via corona discharges [Van Brunt et al., Plasma Chem. Plasma Proc. (to be published)] has indicated that SF_6^- is not the only negative charge carrier in SF_6 corona. Reactions of SF_6^- with neutral by-products of SF_6 corona lead to other stable negative ions such as SOF_5^- which is formed by reactions of SF_6^- with SOF_4. Furthermore, clustering reactions occur as well which influence the reactivity of the negative ions with by-products. Experiments have been made in which ions generated by corona discharges in SF_6 at p = 100 torr have been identified mass spectrometrically. The major negative ions observed, in addition to SF_6^-, SF_5^- and F^-, include the product ions SOF_5^-, SOF_4^-, $SO_2F_2^-$, and SO_2F^- and the cluster ions $F^-(HF)_n$, $SF_6^-(HF)$, $SOF_5^-(HF)$, and $SF_5^-(HF)$. No dimer $SF_6^-(SF_6)$ ions nor trimer $SF_6^-(SF_6)_2$ ions were detected. The relationship of the ions to the modelling of SF_6 by-product formation will be discussed.

*Research supported by the Division of Electric Energy Systems, USDOE, under contract DE-AC05-840R21400 with Martin Marietta Energy Systems, Inc.

FA-3 Predicting Plasma/Reactive Ion Etch Topography using Monte Carlo Methods* T. J. COTLER, D. S. GRIMARD, M. S. BARNES and M. ELTA, University of Michigan - A two dimensional microstructure etch simulation using Monte Carlo methods[1] is applied to plasma/reactive ion etching. The simulation predicts the topography of an arbitrary profile, periodic semiconductor surface after (ion assisted) plasma etching. The dependency of the etched structure on the etch chemistry, the ion energy and the physical bombardment mechanism is investigated. Simulation results are compared with experimental profiles and trends are shown to be correct. Furthermore, it will be demonstrated how this simulation can be used to investigate the mechanism responsible for general trends in plasma etching and particular features present in an etched structure.

*Research supported by SRC.
[1]T. J. Cotler et al, submitted to J. Vac. Sci. B.

FA-4 Anisotropic Etching in Electron Beam Generated-Plasmas, T.R. VERHEY, J.J. ROCCA, AND P.K. BOYER, Colorado State University - Anisotrpic etching of SiO_2 and Si has been achieved using a plasma generated by a broad-area low energy (150-300 eV) electron beam in a He + CF_4 atmosphere. A novel hollow cathode electron source was used to decompose CF_4 molecules into reactive radicals and provide a directed flux of energetic electrons to the sample surface. The fluxes of energetic charged particles to the sample is discussed in relation to their possible contribution to the etching process.

*This work was supported by N.S.F.

FA-5 Activation Energy of Hydrogen Plasma Etching of Amorphous Boron Films, H. TOYODA, H. SUGAI, AND T. OKUDA, Nagoya University, Nagoya, Japan - Etching processes of boron thin films in a DC glow-discharge hydrogen plasma have been studied in veiw of an application to boron coatings[1] in nuclear fusion devices. The hydrogen plasma gives rise to B_2H_6 with the chemical etching of the films. The etching speed is measured as a function of the film temperature T_s, the result of which shows an increase with T_s(<500 K) and the saturation at T_s=550 K. The measured activation energy, 0.12eV, turned out to be comparable to that of amorphous carbon films. To clarify the ion flux contribution to the film etching processes, we electrostatically removed the hydrogen ion flux to the boron films. This experiment indicated that the etching scarcely proceeds without hydrogen ion flux, and that the ion flux has an important role in the film etching process.

[1]H. TOYODA, et al., submitted to Appl. Phys. Lett.

FA-6 Pulsed Microwave Plasma Etching of Polymers for VLSI Applications*, T. H. LIN AND Y. TZENG, Auburn University - Gaseous Plasma generated by a microwave oven power supply is applied to the etching of photoresist, polyimide and other polymers. A magnetron supplies a 1.5 kW peak power at 2.45 GHz through a rectangular waveguide to a two-inch-diameter quartz tube, in which gases such as oxygen and air are flowing at a pressure between 0.1 Torr and 10 Torr, and generates the pulsed plasma at a rep-rate of 60 Hz. The plasma is studied by a Langmuir double probe and an optical emission detector. Polymers placed in the downstream of the plasma tube are etched at very high rates especially when additional heating is applied to the polymers to raise the sample temperature. The plasma characteristics and the etching results will be reported.

*Research supported by NSF (ECS-8504781).

FA-7 Laser Raman Diagnostics of Plasma Etching Discharges, P.J. Hargis, Jr. and K.E. Greenberg, Sandia National Laboratories — Pulsed ultraviolet laser Raman spectroscopy is ideally suited for measuring the dissociation of feed gases in the rf-discharges used for plasma etching. The capabilities of this technique were demonstrated by measuring the percent dissociation of nitrogen, oxygen, sulfur hexafluoride, freon-23, and nitrogen trifluoride in a small plasma etching reactor operating at 13.56 MHz. Nitrogen trifluoride was found to dissociate approximately 60% at rf powers as low as 0.4 W/cm^2. Conversely, rf powers in excess of 2.0 W/cm^2 were required to dissociate 60 to 80 percent of the sulfur hexafluoride. Measurements made with a static gas fill suggest that recombination is important for sulfur hexafluoride and negligible for nitrogen trifluoride.

SESSION FB

10:25 AM - 11:55 AM, Wednesday, October 14

Space Science and Technology Center, Room 4

HIGH FIELD DISCHARGES

Chairman: T. Moratz (University of Illinois)

FB-1 Non-Equilibrium Models for Electrons in an Ionized Gas and Influenced by Space-Time Varying Electric Fields,* E.E. Kunhardt, C. Wu and B.M. Penetrante, Weber Research Institute, Polytechnic University -- In this paper, non-equilibrium models for electrons in a weakly ionized gas and influenced by space-time varying fields are presented. The equations of evolution in space-time are obtained through a multi-time scale perturbation theory. Expressions for the distribution function and parameters that appear in the equations of evolution and examples of the non-equilibrium space-time behavior of the electrons are also presented.

*Work supported by the Office of Naval Research

FB-2 Ionization Rates and Induction Times at Very High Field Strengths in N_2, H_2, NO, Ne, and Ar*, J. T. VERDEYEN, U. of Illinois, G. N. HAYS AND J. B. GERARDO, Sandia Laboratories, L. C. PITCHFORD AND Y. M. LI, GTE Laboratories - Previously we developed and reported a microwave technique for measuring the ionization rate and the induction times for values of an effective E/N up to 10kTd (10^{-13} V-cm^2), and we showed the equivalence of this technique to an applied DC field at this value. Our technique utilizes a low-power (10 mW) microwave interferometer to sense the time-dependent electron density subsequent to a high-power (200 watt) heating pulse, with nanosecond resolution. We have extended our measurements to E/N values up to 35kTd for some gases. We find that the equality between the induction times and the inverse of the density-normalized ionization rate, τ (induction) = ν_i^{-1}, is very good in nitrogen but poor in hydrogen and neon. For selected cases we will also present and discuss data for induction times and excitation rates of excited states, obtained by monitoring the emission from these states simultaneously with the electron density measurements.

*Work performed at Sandia Laboratories supported by USDOE under contract no. DE-AC04-76DP00789.

FB-3 A Simple Model for Electron Transport and Rate Coefficients at High E/N,* Y.M. LI and L.C. PITCHFORD, GTE Laboratories, – The multiple beam model proposed last year[1] has been evaluated by comparisons with full time-dependent Monte Carlo calculations of electron ionization rate coefficients, ν_i, average energies, ϵ, and drift velocities, v_d up to 30 kTd in nitrogen. This model describes each electron born in ionization events as a monoenergetic beam whose energy and momentum are given by single-particle moment equations. Comparisons of ν_i, ϵ, and v_d, from this model and from our Monte Carlo calculations show increasingly better agreement with increasing E/N, and at 30 kTd, the multi-beam model predicts these quantities to within 5%. Anisotropic electron scattering is included in the model via the momentum transfer cross section. The model has also been used to describe the transient behavior of the electrons as a result of a rapidly rising electric field.

[1]L.C. Pitchford, Y.M. Li, G.N. Hays, J.B. Gerardo and J.T. Verdeyen, 39th GEC, Paper BB-2.

*This work was supported in part by Sandia National Laboratories, Albuquerque, NM.

FB-4 Excitation of N_2 in prebreakdown discharges at very high E/n*. V.T. GYLYS and A.V. PHELPS**, JILA, U. of Colo. and NBS -- Pulsed laser irradiation at 266 nm of the semitransparent cathode of a drift tube was used to obtain 10 mA peak current and < 10 ns width. The E/n were from 380 Td to 52 kTd at N_2 densities from 1.6×10^{22} to 9.6×10^{20} m^{-3}. Current transients suggest that the principal ion produced by the electrons is N_2^+, but that the N^+ flux at the cathode increases as E/n is increased. Emission from the 1st and 2nd positive band systems of N_2 and the 391.4 nm band of N_2^+ was monitored. At E/n < 3000 Td the production of all excited states is concurrent with the electron pulse and increases with distance from the cathode as expected for an electron current avalanche. At all E/n the 391.4 nm excitation occurs by electron impact. At E/n > 10 kTd production of the 1st and 2nd positive bands near the cathode is delayed relative to the electron pulse and is larger than near the anode as expected for excitation by fast N_2 or fast N_2^+.

* Supported in part by Lawrence Livermore Laboratories.
** Staff Member, Quantum Physics Division, NBS.

FB-5 E lectrical Breakdown Waves: Exact Numerical Solutions For The Quasi-Neutral Region, M. HEMMATI, Arkansas Tech University, AND R.G.FOWLER, University Of Oklahoma- The propagation of electrical breakdown waves in a gas which is primarily driven by electron gas, is described by fluid-dynamical equations. An electron wave is composed of two regions: 1- The thin Debye sheath region. This region had been discussed extensively in the previous papers. 2- The broad Quasi-Neutral region behind the sheath in which the electric field is negligible. In this region electrons and heavy particles have the same velocity and electron and ion densities are equal. Using a set of boundary conditions at the end of the Debye sheath, electron fluid dynamical equations for the Quasi-Neutral region have been formulated. Computer solutions of these equations has now been investigated, and the results conform to the boundary conditions at the end of the Quasi-Neutral region.

FB-6 Nonequilibrium Electron Kinetics In Nitrogen Under High Frequency Electric Field Excitation With OR Without A Crossed D.C. Magnetic Field*, Y. TZENG AND S. GOVIL, Auburn University, AND E.E. KUNHARDT, Polytechnic University - Microscopic simulation of electron kinetics is performed by means of the Monte Carlo technique. We will report such time-varying electron kinetic parameters as electron energy and ionization rate during both the initial stage of a pulsed high frequency electric field excitation and the following evolution of the electron assembly. The application of a D.C. crossed magnetic field to the high frequency electric field excitation, especially under the electron cyclotron resonance condition, greatly enhances the electron energy and the ionization rate. The influence of electron-neutral scattering angles on the average electron energy and the ionization rate will also be discussed.

*Research supported by NSF (ECS-8504781).

SESSION GA

1:15 PM - 3:10 PM, Wednesday, October 14

Space Science and Technology Center, Room 5

ELECTRON-IMPACT CROSS SECTIONS II

Chairman: M. Inokuti (Argonne National Laboratory)

GA-1 Applications of Electron Scattering Data to Planetary Science and Astrophysics. J. P. DOERING, Dept. of Chemistry, Johns Hopkins Univ.--Some recent developments in techniques of electron scattering cross section determinations and the applications of such data to planetary science and astrophysics will be discussed. For example, the disagreement between theory and experiment on the intensity of the earth's daytime ambient ionospheric photoelectron flux has been greatly reduced by new laboratory cross sections. Observed differences in intensity ratios of visible atomic oxygen emissions from the earth's auroral zone atmosphere can now be understood quantitatively on the basis of different exciting electron energy distributions using laboratory cross sections. However, much more data are needed since, for example, it is suspected that interstellar masing of species such as SiO may be produced by electron impact excitation; but experiments to study such difficult species have not yet been performed.

GA-2 Threshold Studies of H_2 in the Vacuum Ultraviolet by Electron Impact*, J. M. Ajello, G. K. James, Jet Propulsion Laboratory, and D. E. Shemansky, University of Arizona - The excitation cross section of the singlet and triplet states of H_2 have been studied in a crossed beam experiment. The competition between VUV emission by the band systems of the singlet and triplet states and dissociative production of fast H(1s) atoms by the triplet states is compared in threshold region from 0 to 100 eV. We have studied in the laboratory three major processes for Lyman band emission. Excitation function measurements of Lyman band features place these processes into 3 energy regions: 1) resonant excitation of H_2^- from 11 eV to 14 eV, 2) E, F cascading from 14 to 18 eV, 3) direct excitation above 18 eV. We report cross section of the $a^3\Sigma_u^+ \longrightarrow b^3\Sigma_g^-$ continuum emission. We have measured the dissociative excitation cross section for Lyman-α from H_2 and have found structure at 32 eV due to production of fast H(2p) atoms from doubly excited states.

*Research supported by NASA, NSF, and AFOSR.

GA-3 Emission of Radiation Produced by Electron Beam Excitation of Oxygen Gas*, CHUN C. LIN, M. BRUCE SCHULMAN, R. SCOTT SCHAPPE, FRANCIS A. SHARPTON, L. W. ANDERSON, U. of Wisconsin, W. A. M. BLUMBERG, Air Force Geophysics Laboratory, and B. D. GREEN, Physical Sciences, Inc.--The emission of molecular and atomic species produced by electron impact on O_2 in the energy range of 60-400 eV results largely from simultaneous ionization-excitation. The optical cross sections for the $A^2\Pi_u(v') \rightarrow X^2\Pi_g(v'')$ emission of O_2^+ (the second negative band system) have been measured. Apparent ionization- excitation cross sections of the $A^2\Pi_u(v')$ levels of O_2^+ with $v' = 0$-8 are determined and compared with calculations based on a Franck-Condon model. Emission cross sections for O and O^+ lines in the 3,500-11,000Å range have also been measured. By combining these measurements with theoretical Einstein coefficients, cross sections for IR emission lines of O and O^+ are obtained. These cross sections are used to analyze the oxygen fluorescence observed in the AFGL LABCEDE facility in which O_2 was irradiated with keV electrons.

*Supported by AFGL, AFOSR, and DNA.

GA-4 LABORATORY STUDIES OF THE ELECTRON EXCITATION OF SINGLET AND TRIPLET ELECTRONIC STATES OF N_2, B.D. Green, B.L. Upschulte, K.W. Holtzclaw, Physical Sciences Inc., Research Park, P.O. Box 3100, Andover, MA 01810 and W.A.M. Blumberg, Air Force Geophysics Laboratory, Hanscom AFB, MA 01731--We report here our laboratory observations of the fluorescence from electron irradiated N_2 in the 0.2-7 μm spectral region. States observed include the N_2 a, B, C, W, w, and N_2^+ A and B. At low pressures (less than 1/2 mtorr) few collisions occur during a radiative lifetime and the fluorescense reflects energetic electron impact (Franck-Condon) followed by radiative decay. The spectrally resolved fluorescence is compared to theoretical spectrum of each state and the relative total state productions are obtained. Variations are observed as a function of pressure. Extrapolation to the zero-pressure provides the distributions formed by electron impact at 4.5 keV. Differences from models in state production and internal distributions will be discussed. This information will be useful in refining auroral and discharge models of N_2. This work was supported by the Air Force Office of Scientific Research and the Defense Nuclear Agency.

GA-5 Analysis of Scattering of Low-Energy Electrons by Alkali Halide Monomers*. M.ZUO, T-Y. JIANG, L. VUŠKOVIĆ, B. STUMPF**, AND B. BEDERSON, New York University--We will present a detailed analysis of the deconvolution of data for the scattering of electrons by LiBr and CsCl at 5 and 20 eV, the data being obtained using the molecular beam recoil method[1]. This analysis is generic, in the sense that it attempts to take into account quantitatively the contributions due to scattering in and scattering out from the detector, using as parameters the known scattering geometry, including both electron and molecular beam shapes, detector characteristics, and other beam parameters. The results are compared, without normalization, to computed differential cross sections, over a range of angles ranging from a few degrees to very large angles (>90°), for results from Born Approximation, semi-classical impulse approximation, and quantum mechanical calculations[2].

*Supported by DOE and NSF **U. of Windsor

[1]B. Jaduszliwer, A. Tino, and B. Bederson, Phys. Rev. A, 30, 1269 (1984).

[2]D.W. Norcross and L.A. Collins, in Advances in Atomic and Molecular Physics (Academic, NY, 1982) 18, p241.

GA-6 Effect of Trace Concentrations of SF_6 on Metastable Populations in Argon rf Glow Discharge, D. E. MURNICK, R. B. ROBINSON and R. A. GOTTSCHO, AT&T Bell Laboratories- Laser optogalvanic (LOG) studies of the lowest resonance and metastable levels in an Argon rf glow discharge indicated the importance of inelastic scattering of low energy electrons in maintaining discharge equilibrium.[1] The (LOG) effect from the $^3P_1$ ($1s_4-2p_1$ at 667.7 nm) and $^3P_2$($1s_5-2p_2$ at 696.5 nm) levels of argon in a weak rf discharge at 200 mtorr were then studied as a function of concentration of the electron getter SF_6 in the range 0 to·3% SF_6. The response on the $^3P_1$ level changed from a positive (lower conductivity) signal to negative (higher conductivity) signal at about 1% SF_6. This effect is due to quenching of the slow electrons which normally deactivate metastable $^3P_2$ atoms. The LOG effect from the $^3P_2$ level, however, remained negative and was only weakly perturbed in amplitude in the SF_6 concentration range studied.

1. D. E. Murnick et al. this meeting and to be published.

SESSION GB

1:15 PM - 3:10 PM, Wednesday, October 14

Space Science and Technology Center, Room 4

LASER DIAGNOSTICS

Chairman: T. Intrator (University of Wisconsin)

GB-1 Laser-produced Photodetachment as a Probe for Negative Ion Populations in Oxygen. T.H. TEICH, Swiss Fed. Inst. Technol., Zürich. - The reaction scheme for discharge development in oxygen is relatively complicated and competing processes make conventional determination of basic discharge data more difficult, especially detachment data which are closely linked to the O^- and O_2^- populations require further scrutiny. Synchronized irradiation of an axial section of a moving ion swarm in a homogeneous field, initiated by photoelectrons from a UV laser pulse, produces an optogalvanic signal with components due to photodetachment from O^- and O_2^-, each component is proportional to the density of these ions in the irradiated volume. In combination with conventional discharge current analysis*, temporal and spatial scanning by choice of irradiation location and time has been applied to oxygen at densities up to $60 \cdot 10^{17}$ cm^{-3} and with E/N near the critical value (108 to 120 Td). Comparisons of the obtained optogalvanic signal with simulations* underline the need for critical assessment of reaction data in the literature.

* collaboration with I. Gallimberti, E. Poli and S. Stangherlin, University of Padova.

GB-2 Photodetachment Measurement of H^- Density Profile in a Planar Diode Glow Discharge, B. N. Ganguly and Alan Garscadden, APL, Wright-Patterson Air Force Base. -- The axial and radial variations of H^- density profiles in a planar diode, hydrogen glow discharge, 1 torr pressure and current density less than one mA/cm^2, has been measured. The experiment employed photodetachment techniques using 1.06 micron laser excitation. The H^- photodetachment signal has been measured by the optogalvanic effect. A distinct H^- density maximum in the axial profile was found in the negative glow region. The radial distribution of H^- density profile was found to be almost uniform indicating that under the measured discharge conditions, the H^- loss processes are dominated by collisional processes and that H^- diffusion loss is not significant.

GB-3 Radial Dependent Density Measurements of Hg ($^3P_{0,1,2}$) in a Hg-Ar Discharge, L. BIGIO, General Electric R&D Center - Two techniques are used to derive absolute and radial density distributions for three excited states of mercury in the positive column of a low-pressure Hg-Ar DC discharge. A dye laser, traversing the discharge axially, is scanned through the $6(^3P_{0,1,2}) \rightarrow 7(^3S_1)$ transition. At high laser powers the power loss on resonance approaches a constant saturated value directly proportional to the number density of Hg atoms in the ^3P state being investigated.[1] Radial distribution results are presented for the three states at several discharge conditions. The hook method[2] establishes the absolute density on axis while several off-axis measurments are compared with the above saturated absorption results.

[1]A. Yariv, "Quantum Electronics", John Wiley & Sons, New York, 1975, pp. 149-162.
[2]W.C. Marlow, Appl. Opt. 6, 1715 (1967).

GB-4 BARIUM DENSITY MEASUREMENT IN THE VICINITY OF OXIDE COATED ELECTRODES - A. K. BHATTACHARYA AND A. AWADALLAH, LIGHTING BUSINESS GROUP, GENERAL ELECTRIC, NELA PARK, CLEVELAND, OH., 44112
The tungsten electrodes of low pressure discharge devices, e.g., fluorescent lamps, are usually coated with oxides of Ba-Sr-Ca to enhance electron emission at low electrode temperatures. The useful lives of such devices are mainly controlled by the loss of the emission mix by evaporation. Absorption of Ba resonance radiation, 553.5nm, was used to determine the number density of Ba in the vicinity of fluorescent electrodes coated with a mixture of triple oxides. A barium atom density of 1.5E9/cc was measured at a distance of 2mm from electrodes heated to a temperature of 1460K. Addition of Zr to such an oxide mixture significantly reduces the evaporation rate of Ba from such electrodes heated to temperatures of 1300-1400K. Laser induced fluorescence was used to measure the spatial distribution of Ba atoms in the vicinity of an electrode. The results are compared with a simple diffusion model calculation.

GB-5 Direct Observation of Ba^+ Velocity Distributions in a Drift Tube using Single-Frequency Laser-Induced Fluorescence,* R. A. Dressler, H. Meyer, A. O. Langford, V. M. Bierbaum, and S. R. Leone, JILA, NBS and Dept. of Chem., University of Colorado - Ion velocity distributions of Ba^+ drifted in helium are measured both parallel and perpendicular to the electric field using single-frequency laser-induced fluorescence detection. The observed Doppler profiles yield the average ion energies parallel and perpendicular to the drift field for the first time, as well as the mobilities of the ions. The velocity distributions parallel to the electric field fit a Maxwell-Boltzmann distribution for fields up to 23 Td. The widths of the distributions perpendicular to the field appear to correlate with the random energy defined by Wannier,[1] however the parallel widths are only observed to increase above 18 Td, in disagreement with previous theoretical work.

*Research supported by AFOSR.

[1] G. H. Wannier, Bell Syst. Tech. J. 32, 170 (1953).

GB-6 Optogalvanic Spectrum of OH in a Water-Neon Hollow Cathode Discharge*, S. P. LEE, S. DESHMUKH, G. P. RECK, AND E. W. ROTHE, Wayne State University - Tunable ultraviolet laser light in the wavelength range 307.4 to 309.7nm is directed into a hollow cathode discharge of neon that contains ≤½% of water vapor. Typical discharges have 3-5 mA current and 3-5 Torr pressure. The laser beam has a 4 mm diam, ≈0.6 cm^{-1} resolution, and ≈1 mJ energy per pulse. The frequency-doubled light from an excimer-pumped dye laser is used. The resulting optogalvanic spectrum (about twenty lines) is part of the well-known A - X band. It is the first time it has been reported as an optogalvanic signal. Greater partial pressures of water suppress the spectrum. Simulations indicate that the OH is near room-temperature.

*Research supported by PRF, NSF, AFOSR, and the WSU Institute for Manufacturing Research.

SESSION H

3:15 - 6:00 PM, Wednesday, October 14

Space Science and Technology Center, Room 3

POSTERS

Chairman: M. Menendez (*University of Georgia*)

SESSION HA

3:15 PM - 6:00 PM. Wednesday, October 14

Space Science and Technology Center, Room 3

ELECTRON-IMPACT EXCITATION: EXPERIMENT

Chairman: M. Menendez (University of Georgia)

HA-1 Quantitative V.U.V. Polarization Data Using an Electron-Impact Source.* W. KARRAS, P. HAMMOND† and J.W. McCONKEY††, University of Windsor--Accurate polarization data for the resonance radiation of a variety of gaseous targets have been obtained as a function of incident electron energy from threshold to 500 eV. A crossed electron-gas beam system has been used in conjunction with a single reflection, gold-surfaced, polarization analyser. Previous measurements of the polarization of He resonance radiation have been confirmed and extended. Threshold polarizations have been compared with values deduced from angular momentum arguments and particular attention has been paid to the region where P reverses sign.

* Research Supported by the Natural Sciences and Engineering Research Council of Canada.

† U.K. SERC/NATO Fellow.

†† Canada Council Killam Fellow.

HA-2 Laser-Induced-Fluorescence Studies of Electron-Molecule Collisions.* M. DARRACH, P. HAMMOND† and J.W. McCONKEY††, University of Windsor--L.I.F. techniques are used to probe the products of electron collisions with cold target molecules from a pulsed supersonic jet. By introducing the laser pulse at varying distances down-stream from the point of intersection of the electron and gas beams, and by using coincidence techniques both the rotational and translational temperatures of the target N_2^+ molecules were directly probed. Data will be presented for a full range of incident electron energies.

* Supported by the Natural Sciences and Engineering Research Council of Canada.

† U.K. SERC/NATO Fellow.

†† Canada Council Killam Fellow.

HA-3 Excitation of Metastable Fragments Following Electron-Impact on O_2.* J. J. CORR, M.A. KHAKOO, A.G. McCONKEY and J.W. McCONKEY†, University of Windsor--A pulsed electron-gas beam system combined with time-of-flight techniques has been used to study the excitation of metastable fragments following dissociation of O_2. A special detector consisting of a freshly deposited Xe layer on a surface cooled to 70K is used. Excited XeO dimers are formed on the surface and immediately de-excite. A cooled photomultiplier detects the resultant radiation. Full details of the detection system and data taken over a range of electron energies will be presented at the Conference.

* Supported by the Natural Sciences and Engineering Research Council of Canada.

† Canada Counil Killam Fellow.

HA-4 Dissociative Excitation of CF_4 Following Electron Impact.* S. WANG, J.L. FORAND, and J.W. McCONKEY†, University of Windsor--A crossed electron-gas beam arrangement has been used together with a 0.5 m Seya-Namioka vacuum monochromator to study the dissociative excitation of CF_4 in the wavelength range, 45-130 nm, to 600 eV. Cross-sections were made absolute by comparison with emissions from a variety of target gases whose cross-sections had been established previously. Excitation functions and appearance potentials have been determined for selected spectral features. Full details of the techniques used, errors involved and data obtained will be presented at the Conference.

* Supported by the Natural Sciences and Engineering Research Council of Canada.

† Canada Council Killam Fellow.

HA-5 Polarization Correlations in the Rare Gases Following Controlled Electron Impact.* P. PLESSIS, P. HAMMOND**, M.A. KHAKOO†, J.J. CORR and J.W. McCONKEY††, University of Windsor--Measurements are presented of the four normalized Stokes parameters resulting from electron impact excitation of the heavy rare gases and the subsequent coincidence detection of the inelastically scattered electrons and resonance photons. Data will be presented for a range of incident electron energies and electron scattering angles. Of particular interest are the so-called P_4 measurements which reveal significant breakdown of positive reflection symmetry in the scattering plane even for Ne.

* Supported by the Natural Sciences and Engineering Research Council of Canada

** U.K. SERC/NATO Fellow.

† Present Address: University of Missouri-Rolla.

†† Canada Council Killam Fellow.

HA-6 Collision Cross Sections and Excitation Rate Coefficients in Neon. L. TORCHIN, S. MIZZI, Laboratoires de Marcoussis, and V. PUECH, U. Paris-Sud, France – Excitation rate coefficients of about 20 electronic levels have been calculated for neon by solving the Boltzmann equation for $10^{-19} \leq E/N \leq 10^{-15}$ V.cm². As for Argon[1], a detailed set of collision cross sections adapted both to relativistic-electron-beam-produced and discharge-produced plasma has been derived. A comparison of the calculated and measured values of the various transport parameters will be shown, together with the excitation rate coefficients both for direct excitation from the ground state and originating from the upper levels cascades. Our predicted rates agree well with the available experimental results.[2]

[1]V. PUECH, L. TORCHIN, 39th GEC, 7-10 October 1986, Madison (USA).

[2]K. TACHIBANA, H. HARIMA, Y. URANO, J. Phys. B : At. Mol. Phys., 17, 879 (1984).

HA-7 Coherence in Electron-Heavy Rare Gas Collisions*. K.E. MARTUS and K. BECKER, Lehigh University. The electron-polarized-photon coincidence technique is used to study the electron impact excitation of the spin-orbit-coupled $(n+1)s'\ [1/2]_1^0$ and $(n+1)s\ [3/2]_1^0$ states from the $np^6\ ^1S$ ground state in Ne, Ar and Kr (n=2,3,4). The excited states can be pictured as linear combinations of LS-coupled ^1P and ^3P states. Linear polarization correlations have been measured for forward scattering to elucidate the role of the singlet and triplet scattering channels at various impact energies. Previous measurements in Ar at 50 eV[1] disagree with recent calculations[2].

*Supported by the Research Corporation through a Cottrell Research Grant and by NSF through grant PHY-8517629.

[1]Malcolm and McConkey, J. Phys. B 12, 511 (1979)

[2]Madison and Bartschat, Bull. APS 32, 1232 (1987)

HA-8 Accurate Absolute Photoemission Cross Sections in the VUV, R. C. G. LIGTENBERG, P. J. M. VAN DER BURGT, W. B. WESTERVELD and J. S. RISLEY, North Carolina State University. -- The measurement of absolute photoemission cross sections in the VUV requires accurate determination of the efficiency of the detector system used, the photon emission rate from electron - atom (molecule) collisions, and the target gas density. Our previous measurements of the H_2(H I Ly-α) and Ar II (92.0, 93.2 nm) emission cross sections have established the reproducibility of our method[1,2], which employs synchrotron radiation for the determination of the efficiency. Our recent measurements (taken at low pressure to eliminate self-absorption of resonance radiation) have reproduced the He I (58.4 nm) emission cross section, which is the most accurately determined cross section in the VUV.[3] The accuracy of our method is presently limited to ≈10% because of uncertainties in the temperature of the target gas, which was determined by measuring the transmission of the 58.4 nm resonance radiation as a function of pressure. Work is in progress to mount an electron gun outside the interaction region to eliminate any thermal gradients within the apparatus.

[1]A. McPherson et al., Appl. Opt. 25, 298-310 (1986).
[2]R. L. Kendrick et al., Appl. Opt. 26, 2029-2041 (1987).
[3]W. B. Westerveld et al., J. Phys. B 12, 115-135 (1979).

HA-9 Positron and Electron Differential Elastic Scattering by Atoms*, W.E. KAUPPILA, STEVEN J. SMITH, G.M.A. HYDER, M. MAHDAVI-HEZAVEH, C.K. KWAN, and T.S. STEIN, Wayne State U. - Relative elastic differential cross sections (DCS's) are being measured for 10 - 300 eV positrons and electrons scattering at angles from 30 - 135° by various atoms (e.g., argon and neon) in a crossed-beam experiment.[1] Comparisons of these DCS measurements for positrons and electrons (which are showing some similarities at 300 eV for argon), as well as with available theoretical calculations,[1,2] are providing new insights that may help lead to a better understanding of the static and polarization interactions as they contribute to positron and electron scattering by atoms. At low to intermediate energies the DCS's for electrons exhibit more structure, related to diffraction effects, than for positrons. Searches are being made for cusps in the elastic DCS's for positrons at the positronium formation thresholds.

*Research supported by NSF.

[1]G.M.A. Hyder et al., Phys. Rev. Lett. 57, 2252 (1986).
[2]W.E. Kauppila and T.S. Stein, to appear in Atomic Physics with Positrons, edited by J.W. Humberston (Plenum, New York and London, 1987-8).

HA-10 Electron Beam Growth in N_2, W.A.M. BLUMBERG and P.C.F. IP, Air Force Geophysics Laboratory, Hanscom AFB, MA 01731, B.D. GREEN, W.J. MARINELLI, and J. PERSON, Physical Sciences, Inc., Research Park, Andover, MA 01810* -- Spatial distributions of electrons scattered out of a collimated electron beam incident on low pressure N_2 targets have been measured using the AFGL LABCEDE facility. Radial density distributions of energetic electrons were obtained from N_2^+ fluorescence profiles using Abel inversion techniques for 2-6 keV electron beams propagating through 0.05-3.5 Torr-cm target thicknesses. Monte Carlo calculations of the contributions of elastic and inelastic scattering processes to the spatial growth of the electron beam were performed. The dependence of predicted radial electron density profiles on uncertainties in the inelastic cross sections was determined. Good agreement between the observed and predicted electron density profiles was obtained. The present results will be compared with prior measurements and calculations.

*Supported by the Air Force Office of Scientific Research and the Defense Nuclear Agency.

HA-11 Low Energy Cross Section Measurements for Inelastic Scattering of Electrons from Disilane*, HIROSHI TANAKA and LUDWIG BOESTEN Sophia University, Tokyo, MICHAEL DILLON and DAVID SPENCE, Argonne National Laboratory, — Cross sections for elastic scattering of electrons from disilane were determined using the relative flow technique[1] with helium as the comparison gas. The measurements were carried out employing incident electron energies of 15 to 100 eV over an angular range of 3-130°. These results were then used to normalize relative cross sections for both vibrational and electronic excitation obtained at the same conditions of incident energy and angular range over an energy loss regime of 0 to 15 eV.

*Work supported in part by the U.S. Dept. of Energy, Office of Health & Environmental Research, under Contract W-31-109-Eng-38.

[1]S. K. Srivastava, A. Chutjian, and S. Trajmar, J. Chem. Phys. 63, 2659 (1975).

HA-12 Plasma Double Layers in Electron Impact Spectroscopy of Hg, P. NICOLETOPOULOS, University of Brussels Belgium - A classic but poor method for showing critical potentials of Hg with a two-grid Franck-Hertz tube[1] is upgraded thanks to a novel experimental arrangement capable of creating monochromating apparatus dynamically. This is achieved by a double discharge initiated at low voltage between the hot cathode and grids whose key feature is a double layer (DL) joining two plasmas at different potentials. The electron beam is abruptly decelerated by the DL before entering the low potential plasma which constitutes the useful field free drift space. The formation of the DL is diagnosed by analysis of the resulting excitation spectrum. Several critical potentials of Hg are measured within 0.1 eV. Also displayed is a clear dip at 0.4 eV attributed to the Burrow-Michejda shape resonance.[2]

1. F.L. Mohler et al., J. Opt. Soc. Am. 4, 364 (1920)

2. P.D. Burrow et al., J. Phys. B 9, 3225 (1976).

HA-13 Secondary Electron Energy (1eV-200eV) and Angular Distributions for Electron Impact Ionization of CO by 800eV Electrons. CE MA and R.A. BONHAM, Indiana University*-The pulsed electron beam time of flight method[1,2] was used to obtain the angular and energy dependence of ejected electrons produced by 800eV electron impact on CO. The doubly differential cross sections were obtained at 15° intervals in scattering angle from 30° to 150° and for electron kinetic energies from 1eV to 200eV. Results have been summarized in terms of analytical expressions obtained by least squares fit of the experimental data by a linear combination of a few (3-6) Legendre polynomials. The singly differential cross section in terms of the ejected electron kinetic energy will be presented in terms of a Platzman plot. The plot is dominated by numerous autoionizing lines and assignments of many of these lines in the low energy range (<2eV) are made.[3] The total ionization cross section obtained from this data is in excellent agreement with the earlier results of Rapp and Englander-Golden.[4]

*Supported by NSF Grant CHE86-00746

1.) R.R. Goruganthu and R.A. Bonham, Phys. Rev. A 34, 103 (1986).
2.) R.R. Goruganthu, W.G. Wilson and R.A. Bonham, Phy. Rev. A 35,540 (1987).
3.) M. Ogawa and S. Ogawa, J. Mol. Spec. 41, 393 (1972).
4.) D. Rapp and P. Englander-Golden, J. Chem. Phys. 43, 1464 (1965).

SESSION HB

3:15 PM - 6:00 PM, Wednesday, October 14

Space Science and Technology Center, Room 3

ELECTRON-IMPACT EXCITATION: THEORY

Chairman: M. Menendez (University of Georgia)

HB-1 Electron Impact Ionization Cross Section of Atoms.* H. DEUTSCH, Universität Greifswald, GDR, P. SCHEIER, T.D. MÄRK, Universität Innsbruck, Austria - We report the development of a new formula which allows calculation of electron impact ionization cross section functions of atoms. The formula consists of the energy dependent part of the classical binary encounter approximation and a part taking into account the radii of the charge densities of the contributing electron subshells. Results obtained for the rare gases, N, F and Ba lead to a better agreement with experimental results than previous formulae.

* Work partially supported by the Österr. FWF, grant Nr. 5692.

HB-2 Electron Scattering By Na*, A.Z. MSEZANE, Atlanta U. - Cross sections for elastic scattering and excitation of Na by electron impact are calculated for the energy range $3.5 \leq E \leq 200$ eV in four-state and six-state close-coupling(CC) approximations. Accurate CI target wave functions are used to represent the ground state 3s ^{2}S and the excited states 3p ^{2}P^o, 3d ^{2}D, 4s ^{2}S, 4p ^{2}P^o and 4d ^{2}D. The resulting energy splittings and oscillator strengths in the length and velocity formulations are almost the same and are consistent with accepted values. Up to 10eV our 4CC and 6CC total cross sections agree very well with measurement[1], while above 10eV excellent accord is achieved with theoretical estimates.[2] For E>10eV our 6CC total cross sections favor the measurement of reference 3 over those of Kasdan et al[1]. Further, the 6CC resonance cross sections agree very well with measurement.[4]

*Supported in part by NSF

1. A. Kasdan, et. al., Phys. Rev. A8, 1562 (1972).
2. B.H. Bransden and M.R.C. McDowell, Phys. Rev. 46, 250 (1978).
3. S.K. Srivastava and L. Vuskovic, J. Phys. B. 13, 2633 (1980).
4. E.A. Enemark and A. Gallagher, Phys. Rev. A6, 192 (1972).

HB-3 Orientation and Alignment Parameters for e^- + He ($2^{1,3}S$, $2^{1,3}P$) → e^- + He($3^{1,3}P$, $3^{1,3}D$) Collisions†, E. J. MANSKY II and M. R. FLANNERY, Georgia Institute of Technology - The multichannel eikonal theory results for the coherence and alignment parameters characterizing the decay of the metastable $3^{1,3}P$ and $3^{1,3}D$ states of helium, excited in the $2^{1,3}S \rightarrow 3^{1,3}P$ and $2^{1,3}P \rightarrow 3^{1,3}D$ transitions respectively, are examined. A detailed examination of the resulting λ, χ parameters (for the $3^{1,3}P$ states) and the λ, μ, χ, ψ parameters (for the $3^{1,3}D$ states) provides a clear picture of the effect interchannel couplings within the target basis set have upon the final state probabilities. The pattern of the coherence and alignment parameters for these transitions also provides a direct, physical explanation of the qualitative behavior of the integral cross sections for the $2^{1,3}S \rightarrow 3^{1,3}P$ and $2^{1,3}P \rightarrow 3^{1,3}D$ transitions.

†Research supported by U.S. Air Force Office of Scientific Research under Grant No. AFOSR-84-0233.

HB-4 A Theoretical Investigation of ^2P Shape Resonances in Group II Atoms Using an Approximate Version of Fano's Theory, D. CHEN & G. A. GALLUP, University of Nebraska-Lincoln - The ^2P shape resonances for atoms Be, Mg, Ca, Zn and Cd have been calculated by putting an extra np orbital in an SCF calculation to get a better virtual orbital, then using Fano's method[1] to find the resonance for each atom. By optimizing the np orbital, the minimum of the resonance energy has been found, with very good agreement with the experimental results[2] for all but Ca. Our calculation shows that the negative Ca ion is stable, which agrees with Fischer's[3] MCHF result. The resonance energies for Be, Mg, Zn and Cd are 0.23, 0.19, 0.60 and 0.54 eV. This method has also been successfully used in small molecules such as ethylene which like the group II atoms, have negative electron affinities.

1. U. Fano, Phys. Rev. 124, 1866 (1961).
2. L T S F Lam, J. Phys. B: At Mol. Phys. 14 1437 (1981)
P. Burrow et al; J. Phys. B: At Mol. Phys. 9 3225 (1976)
3. C. F. Fischer et al; pvt. Communication. (1987)

HB-5 *Electron-Impact Excitation of O-Like Ions**, *A.Z. MSEZANE, Atlanta U., K.J. Reed, LLNL, and R.J.W. HENRY, LSU - We report continuing theoretical studies of electron-impact excitation from the ground state* $2s^2 2p^4\ ^3P$ *to the n=2 levels of O-like ions: Ar, Fe and Kr for electron impact energy, E from near threshold to about 200 Ry. Coupling effects among the channels for collisional excitation of the* $2s^2 2p^4$, $2s2p^5$ *and* $2p^6$ *configurations have been investigated using CI type wave functions by comparing 3CC, 4CC, 5CC and 6CC cross sections. For the transitions of interest in* Ar^{+10}, Fe^{+18} *and* Kr^{+28} $(Z-8)^2\Omega$ *versus X behaves as expected of spin-forbidden transitions for large X. Unexpected results for the* $2p^6\ ^1S$ *and* $2s2p^5\ ^1p^0$ *levels of* Kr^{+28} *are found near threshold due to influence of coupling. For both* $2p^6\ ^1S$ *and* $2s2p^5\ ^1p^0$ *states of* Kr^{+28} *the removal of* $2s^2 2p^4\ ^1D$ *results in a dramatic reduction in the near threshold cross sections. Results will be presented and discussed, including coupling effects.*

**Performed under the auspices of the U.S. DOE by LLNL. A.Z.M and RJWH are supported in part by the U.S. DOE, Division of Chemical Sciences.*

HB-6 Electronic Excitation of $H_2(X\ ^1\Sigma_g^+, v")$ Molecules to Yield $H_2(X\ ^1\Sigma_g^+, v")$ Molecules Via Excitations of the Electronic Singlet Spectrum.* J. R. HISKES, Lawrence Livermore National Laboratory--The cross sections are evaluated for excitation of the vibrational spectrum of the ground electronic state of H_2 via initial electronic excitations through the excited singlet spectrum. The population of a particular vibrational level v' belonging to an excited singlet state is taken to be proportional to the dipole transition moment. Specific calculations are reported for excitations to the $B'^1\Sigma_u^+$, $C'^1\Pi_u$ states together with a sum over higher states. Radiative transitions to final levels v" include contributions to discrete and continuum levels. For the special case v" = $\bar{v}$", these cross sections show large enhancements toward the higher $\bar{v}$" levels. The dependences on other combinations of $\bar{v}$", v" appropriate to hydrogen discharge analysis will be reported.

*Performed by LLNL for USDOE under Cont. W-7405-ENG-48.

HB-7 Molecular Structure Effect on Momentum Transfer Cross Sections in Electron-Polyatomic Molecule Collisions*, M. KIMURA, Argonne National Laboratory and Rice University, H. SATO, Ochanomizu University, AND K. FUJIMA, Institute of Physical and Chemical Research - Theoretical study of momentum transfer cross sections in electron impact on C_2H_2 (triple bond), C_2H_4(double bond) and C_2H_6 (single bond) molecules has been conducted using the continuum-multiple-scattering method in the energy region from 1-150 eV. Molecular structure effect on shape resonances was studied systematically for the first time in electron-polyatomic molecules. For unsaturated hydrocarbons, pronounced shape resonances around E = 1 ~ 3 eV due to the π^* molecular orbital were clearly observed in addition to weaker broad resonances at higher energy side, while this strong shape resonance was completely missing in saturated hydrocarbon due to unavailability of vacant molecular orbitals in this case. Also, enhancement effect in vibrational excitation due to the shape resonances were also studied.

*Supported in part by the U.S. Dept. of Energy, Office of Health & Environmental Research, under Contract W-31-109-Eng-38, and by Office of Basic Energy Science.

HB-8 Theoretical Study on the Total (Elastic + Inelastic) Cross Sections for e-H_2O and NH_3 Collisions at 10-3000 eV, by ASHOK JAIN, Physics Dept., Kansas State University, Manhattan, KS 66506. By employing a parameter-free ab initio complex-optical-potential[1] for the e-H_2O (NH_3) systems, we present total (sum of elastic and all inelastic channels) cross sections in the range 10-3000 eV. The computed values for the inelastic cross sections are compared with experimental total ionization (including dissociation) cross sections for both the H_2O and NH_3 targets: we found a very good accord between present theory and the measurements from threshold to up to higher energies. For the total cross sections our results are again in very good agreement with several recent measured values at all energies considered here. Below 100 eV, the non-spherical interaction term (mainly dipole) is important and included incoherently via the first-Born-approximation in a rotating dipole model. The theoretical results on the reduced differential and corresponding integral and momentum transfer cross sections are also reported along with measured data. We notice that the absorption effects are important in deducing the DCS qualitatively. No previous calculation exists on these systems in the present energy range.

1. A. Jain, Phys. Rev. A34, 3707 (1986).

HB-9 Swarm-Derived Scattering Cross Sections of cyclo-C_4F_8, M.F. FRECHETTE AND J.P. NOVAK, IREQ.Varennes, Canada-A set of cross sections representing the electron-molecule collisional interactions in perfluorocyclobutane (c-C_4F_8) has been obtained following the theoretical study of the transport properties of electron swarms in this gas via the two-term approximation of the Boltzmann equation. The final set which comprises five cross sections: ionization, attachment, vibration, excitation and momentum transfer, is self-consistent with respect to the transport coefficients published by Naidu et al.[1] Calculations for the mixtures with N_2 were also performed. While most theoretical coefficients for the mixtures await experimental check, calculated limit field compares reasonably with published breakdown-potential measurements.

[1]M.S. Naidu, A.N. Prasad, and J.D. Craggs, J. Phys. D 5, 741 (1972).

HB-10 Resonance Overlap Structure in the Microwave Ionization of the Hydrogen Atom*, T. Uzer, Georgia Tech, and D. Farrelly, UCLA - The multiphoton ionization of the hydrogen atom in a microwave field [1-3] involves most of the open issues about quantal and classical stochasticity. Current research considers elongated, quasi one-dimensional hydrogen atoms. The ionization thresholds are in harmony with predictions of a classical picture where ionization proceeds through the overlap of an infinity of nonlinear resonances [2,3]. We present a new canonical transformation which makes the two-dimensional nature of the problem explicit, and which, in the one-dimensional limit, yields an accurate and improved ionization threshold through the overlap of only two resonances. We believe this particular form to be potentially very useful for treating realistic hydrogen atoms.

*Research supported by AFOSR and NSF.
1.J.E.Bayfield and P.M.Koch, Phys.Rev.Lett.33,158 (1974).
2.B.I. Meerson et al., JETP Lett. 29, 72 (1979).
3.N.B. Delone et al., Sov. Phys. Usp. 26, 551 (1983).

HB-11 Study of Dependence of Scattering Phase Shifts on Atomic Charge and Mass Number, by W. J. ROMO and S. R. VALLURI, University of Western Ontario, London, ON, CANADA N6A 5B9—Analytic expressions are derived for the partial derivatives of the phase shifts and S-matrix elements, obtained from an optical model potential, with respect to the charge Z and mass number A of the target atom. In the case of the scattering of two nuclei, detailed calculations are performed to yield linear approximations to phase shifts and S-matrix elements in which the charge or mass number has been changed by plus or minus one unit. The present treatment may provide interesting connections with the scattering of electrons or atoms by atoms.

SESSION HC

3:15 PM - 6:00 PM, Wednesday, October 14

Space Science and Technology Center, Room 4

RF PLASMAS

Chairman: M. Menendez (University of Georgia)

HC-1

A Particle Model of a Plasma-Etching Discharge, W.N.G. Hitchon and G.J. Hofmann, Electrical and Computer Engineering, University of Wisconsin-Madison -- A particle model will be described which calculates the electron and ion energy distributions as functions of space in an etching discharge. The electron and ion motions are integrated separately, on different time-scales. The time-averaged electron positions are used to solve Poisson's equation, during the ion integration, which is allowed to converge. The ion positions are then used in Poisson's equation during the electron integration, which may be accelerated in some circumstances;[1] when this converges the process is repeated until the overall solution converges. The results of the calculations allow the production rates of the chemical species to be found. Comparisons of the distributions with experiments will be presented.

[1] "A Plasma-Optical System Modeled Using Particles," University of Wisconsin Report ISL-87-2 (1987). (To be published in J. Plas. Physics).

HC-2 Modeling Species Transport and Etching Kinetics in SF_6 Discharges for Plasma Etching, H. M. ANDERSON and J.A. MERSON, University of New Mexico, Albuquerque, NM 87131 - A discharge and rate equation model are combined to study the flux of incident ion and neutral reactive species on Si substrates during plasma etching with SF_6. Recently reported experiments (1) suggest that previous models for SF_6 rf discharges have largely overestimated the extent of dissociation occurring in the plasma. In this study, electron impact dissociation, ionization, and dissociative attachment reactions are reexamined in light of these reports, and an attempt is made to reconcile these findings consistent with large experimentally observed etch rates. Assuming charged and neutral fluxes are well represented by ambipolar and free diffusion rates, the critical flux of reactive species is shown to be the ion flux. General agreement with experimentally observed etch rates and dissociation is shown.

1) P.J. Hargis, paper EG-5, 39th GEC, Madison, WI (1986).

HC-3 Self-Consistent Stochastic Electron Heating in High Frequency R. F. Discharges*, C. G. GOEDDE, A. J. LICHTENBERG, AND M. A. LIEBERMAN, U. C. Berkeley—We consider Fermi acceleration as an underlying mechanism for electron heating in r. f. discharges, in which the heating arises from the reflection of electrons from moving sheaths. By examining the dynamics of the electron collisions with the sheaths, we derive the map that describes the electron motion. We show that for high frequency, low pressure discharges ($\omega/2\pi > 50$ MHz, p $\sim$ 1 mTorr), the electron motion will be stochastic. By combining these dynamics with collisional effects in the bulk plasma and incorporating self-consistent physical constraints, we develop a self-consistent simulation model of the discharge. The model is used to calculate physically interesting quantities, such as the electron temperature and average lifetime, and to predict the minimum pressure necessary to sustain the plasma. The distribution of electron energies is calculated and shown to be non-Maxwellian. These results can be applied to experimentally interesting parallel plate r. f. plasma discharges to predict the operating conditions necessary for stochastic heating to occur.

*Research supported by NSF Grant ECS-8517363.

HC-4 Measurements and Modelling of Plasma Properties in Planar Magnetron Discharges*, A. E. WENDT, L. GU, AND M. A. LIEBERMAN, U. C. Berkeley—Results will be presented from an ongoing investigation of a DC planar magnetron. The cylindrically symmetric system consists of a 12" D aluminum vacuum chamber with 9" D copper parallel plate electrodes which may be moved axially. The discharge is operated in argon, and a variable magnetic field is provided by an iron core electromagnet. Our studies have focused on the spatial structure of the discharge and the dependence of the structure on external parameters. The radial distribution of current at the cathode has been measured with a radially separated array of 1 mm current probes imbedded in the cathode plate. We have developed a simple model of the distribution of ions at the cathode, in the form of an integral equation. A comparison of the model with experiment will be presented, showing agreement in the range of validity of the model, and showing the dependence on magnetic field strength. Optical measurements of dark space thickness will be presented and compared with Child-Langmuir theory and spatially resolved emissive probe measurements of plasma potential.

*Research supported by a gift from Varian Associates.

HC-5 Optical Diagnostics of a High Power, RF Driven, Inductively Coupled Plasma*, M. Trkula, N. S. Nogar, G. L. Keaton, and J. E. Anderson, Los Alamos National Laboratory - Emission spectroscopy and laser-induced fluorescence have been used to study the field and tail flame regions of a Hull design+ inductively coupled plasma. Spectra of pure Ar and Ar/N_2 mixture plasma gasses, far down stream of the plasma field region, indicates that the system is far from thermal equilibrium. Time resolved spectra from the field region of the plasma exhibits some unusual sub-harmonic generation. This sub-harmonic generation, indicative of a nonlinear coupling mechanism, depends on rf power and pressure but is independent of axial position.

*This work performed under the auspices of the U. S. Department of Energy.
+U. S. Patent 4,431,901 (February 14, 1984).

HC-6 Plasma and free radical parameters in an Ar-NH_3 RF positive column, S. ONO, J.S. CHANG, McMaster Univ. Canada, M.YAMADA, S. TEII, Musashi Inst. Tech., Japan -- The influence of gas pressure, NH_3 % mixture and plasma density on the plasma and free radical parameters in an Ar-NH_3 RF positive colum have been studied both experimentally and numerically. 12 ϕ I.D. discharge tube with the ring type 13.65 MHz RF discharge was used in the present investigation. The side light emission, mass spectrometer and electrostatic probe measurements were conducted and compared with numerical modelling (Chang et al.[1]) The results show that : 1) NH and H free radicals increase with increasing gas pressure, plasma density and NH_3 percent mixture; 2) Plasma density observed to be less influenced by gas pressure and NH_3 percent mixture for a fixed power while electron temperature decreases with increasing gas pressure and increases with increasing NH_3 percent mixture; 3) NH_3^+ and Ar^+ observed to be dominant ion species and these results agree well with theoretical predictions; 4) No significant RF power dependence of electron temperature has been observed; 5) Ar^+ decreases with increasing NH_3 mixture and gas pressure while NH_3^+ increases with these parameters.

1. J.S. Chang et al, Proc. Inst. Conf., Plasma Sci. and Tech., Science Press, Beijing, 351 (1986)

HC-7 Tunable Diode Laser Diagnostics of Molecules in Plasma Etching Systems.* J. WORMHOUDT, Aerodyne Research, Inc.--Tunable diode lasers can detect both radicals and stable molecules important in plasma etching systems. The CF_2 radical is of particular interest but only theoretical predictions exist of the band strengths needed to obtain absolute concentrations. We report band strength measurements in fast flow systems, using both a self-calibrating method involving the thermal decomposition of CH_2HCl, and CF_4 discharge production quantified by laser absorption of a CH_2 electronic band. Band strength investigations into CF_3 and SiF_2 will also be reported, and implications for diagnostic experiments in plasma etching systems will be presented.

*Supported by AFOSR Contract No. F49620-84-C-0036.

HC-8 Laser-Induced Fluorescence of SiCL: Spectroscopy and Collision Dynamics for Quantitative Measurements*, JAY B. JEFFRIES, Chemical Physics Laboratory, SRI International - Laser-Induced fluorescence (LIF) is an ideal technique for measurements of the concentration of chemically reactive radical species in discharges. Quantitative species concentration measurements require spectroscopic and collision dynamic data. We describe such experiments on the $B^2\Sigma^+$ and $B'^2\Delta$ states of SiCL. For these measurements to provide quantitative species concentration, both spectroscopic and collision dynamics data is required. Such data for the SiCL radical has been obtained for the $B^2\Sigma^+$ and $B'^2\Delta$ states. SiCL is produced in the afterglow of a microwave discharge in rare gas (He, Ne, Ar), and detected via LIF. Transistion strengths, radiative lifetimes, and collisional removal rates are determined. Electronic transfer $B' \rightarrow B$ shows a very unusual specificity in both initial and final vibrational levels, which is quite different among the three rare gas collision partners.

*Supported by internal research and development funds of SRI International.

HC-9 Characterization of a Low Pressure Oxygen Surface-Wave Discharge A. GRANIER, J. MAREC, P. SUPIOT, C. BOISSE-LAPORTE, R. DARCHICOURT, S. PASQUIERS and P. LEPRINCE, University of Orsay-FRANCE- Low pressure Oxygen microwave discharges created by surface wave have been studied under various operating conditions. A complete characterization is presented for a discharge created at 390 MHz in a tube of inner diameter 16 mm.

First of all, the power balance of the discharge yields the longitudinal electron density profile, the effective maintaining electric field, the effective collision frequency, from 30 mT to 3T.

Afterwards the concentration of singlet oxygen $O_2(^1\Delta)$ is determined from U-V absorption experiments (120-150nm). It is about 10% of the fundamental oxygen concentration $O_2(^3\Sigma)$, whatever the microwave power and the pressure (200mT-3T). The measure of fundamental atomic oxygen and ozone concentrations are in progress.

At last the results are compared with the characteristics of an Oxygen positive column obtained by G Gousset et al[1]

[1]G. GOUSSET et al., Plasma Chem. and Plasma Process. (to be published in 1987).

HC-10 RF Plasma Generation using Inductively Coupled Loop Antenna,* M.H. CHO, G.H. KIM, N. HERSHKOWITZ, P. NONN, University of Wisconsin-Madison--We have performed experimental studies on an electrodeless rf induction plasma generator using a multidipole device. This source uses a single turn loop antenna made out of insulated copper strip, and operates at a tuned resonance frequency of several MHz and at neutral pressure (argon) as low as 5×10^{-5} torr. The preliminary results showed that the plasma density was strongly dependent on rf power level and the electron temperature was strongly dependent on neutral gas pressure. It was also observed that the ionization ratio was ~ 1 percent and electron temperature could be as high as ~ 15 eV with the modest power level of ~ 100 watts. The detailed antenna structure and the rf circuit will be presented together with the characteristics of plasmas, i.e. rf frequency, rf power, and neutral pressure dependences, in the newly developed rf induction plasma generator.

*Supported by NSF Grant ECS-8314488 and NASA Grant NAGW-275.

HC-11 Short-Pulse Microwave Breakdown in Air, T. ARMSTRONG, M. I. BUCHWALD, R. KARL, AND R. A. ROUSSEL-DUPRE', Los Alamos National Lab., T. TUNNELL, EG&G/EM, Los Alamos- Optical emissions of N_2 and N_2^+ were used to analyze microwave-induced breakdown in air at pressures below 150 Torr. Microwave pulses were between 6 and 250 ns in duration and focused away from surfaces. Time-integrated spectra and images as well as time-resolved filtered photometry were collected. The images are compared with a 1-D fluid model[1] and qualitative agreement is found for the variation in the spatial luminosity as a function of pressure. The observation of a delayed maximum in the time history of the 337.1 nm N_2 emission is discussed within this model. Experimental studies were performed varying air pressure and pre-ionization while maintaining isolation of the breakdown volume.

[1] R. A. Roussel-Dupre' et al., ICPIG XVIII, July 1987.

SESSION I

7:30 PM - 10:00 PM, Wednesday, October 14

Space Science and Technology Center, Room 5

ELECTRON COLLISIONS: THEORY PANEL

Chairmen: J. N. Bardsley (Lawrence Livermore Laboratory)

and M. R. Flannery (Georgia Tech)

I-1 Differential and Integral Cross Sections for Electron Impact Excitation Determined By FOMBT/DW-Type Theories*, D. C. CARTWRIGHT AND G. CSANAK, Los Alamos National Laboratory - Differential and integral cross sections obtained from FOMBT/DW-type theories are compared with experimental data for electron-impact excitation of the inert gases He, Ne, Ar and Kr. Comparisons of the experimental data with results from the Born and Eikonal approximations show that these theories fail for scattering angles greater than about 40° and at low and intermediate energies because of the lack of exchange in the models. Detailed comparisons with results from R-matrix theory will also be made whenever possible. The fact that certain coherence and correlation parameters are essentially independent of the principal quantum number (n), predicted by FOMBT[1] and partially verified by recent experiments, indicates that cross sections to large (n) can be accurately obtained by straightforward extrapolation of theory or experimental data.

*Research supported by the NSF/IP and the DOE.
[1]G. Csanak and D. C. Cartwright, Phys. Rev. A34, 93 (1986).

I-2 Multichannel Eikonal Theory of Electron-Metastable Atom Collisions†, E. J. MANSKY II, Georgia Institute of Technology - An overview of recent[1] multichannel eikonal theory[2] cross section results for electron-impact excitation of hydrogen (e^- + H(2s,2p) → e^- + H(1s,2s,3s,3p,3d)) and helium (e^- + He(2^1S,2^1P) → e^- + He(1^1S,2^1S,2^1P,3^1S,3^1P,3^1D) and e^- + He(2^3S,2^3P) → e^- He(2^3S,2^3P,3^3S,3^3P,3^3D)) will be given. Comparison of the present theoretical results with the available experimental data clearly shows the necessity of using an extensive basis set in order to obtain accurate cross sections for excitation of initially metastable targets. Attention will be focused upon highlighting the systematic trends observed in the excitation cross sections of H* and He*, and contrasting them with the corresponding results for excitation of H(1s), He(1^1S).

†Research supported by U.S. Air Force Office of Scientific Research under Grant No. AFOSR-84-0233.
[1]E. J. Mansky II and M. R. Flannery in preparation.
[2]M. P. Flannery and K. J. McCann J. Phys. B 7 2518 (1974), Phys. Rev. A 12 B46 (1975).

I-3 Effective Collision Strengths for Excitation of Hydrogen by Electrons*, J. CALLAWAY and K. UNNIKRISHNAN, Louisiana State University, Baton Rouge, LA, and D.H. OZA, National Bureau of Standards, Gaithersburg, MD - Rate coefficients for transitions in electron-atom collisions are conveniently represented in terms of the dimensionless effective collision strength. These quantities are computed for all n = 1 to n = 2 or n = 3 and n = 2 to n = 3 transitions in electron hydrogen scattering. The results are based on six state close coupling calculations including an optical potential. The optical potential is evaluated using a pseudo-state expansion. Incident energies are in the range 10 - 100 ev. Analytic fits are made to the cross sections from which the effective collision strengths are determined by averaging over a Maxwellian distribution of electron velocities.

*Supported in part by the National Science Foundation.

I-4 Oscillator Strengths and Collision Strenghts for Complex Atoms and Ions. RONALD J. W. HENRY *, Louisiana State University - Accurate atomic data for complex atoms and ions results after setting up large non-sparse matrices and obtaining the eigenvalues and eigenvectors. The resultant wave functions obtained from CIV3[1] can be used to calculate oscillator strengths or as input to a scattering calculation. Eigenvalue solutions are needed if the RMATRIX[2] program is used in the collision problem or, alternatively, very large sets of linear algebraic equations have to be inverted if the NIEM[3] method is used. Such techniques are at the core of a close coupling expansion method which includes the important physical effects of electron exchange, correlation and resonances. Many channels are needed to achieve convergence of the close coupling expansion.

*Research supported in part by the U.S. Department of Energy, Office of Basic Energy Sciences, Division of Chemical Sciences.

1. A. Hibbert, Comp. Phys. Commun. 9, 141 (1975).
2. K. A. Berrington et al., Comp. Phys. Commun. 14 367 (1978).
3. R. J. W. Henry, S. P. Rountree, and E. R. Smith Comp. Phys. Commun. 23, 233 (1981).

I-5 Ionization in Collisions between Electrons and Complex Ions. C. BOTTCHER, D. C. GRIFFIN*, and M. S. PINDZOLA†, Oak Ridge National Laboratory‡, Oak Ridge, TN--Most models of hot plasmas containing complex ions still rely on simple, semi-empirical formulae for electron-impact ionization rates. These formulae often fail when applied to complex ions, through neglect of two factors: (1) indirect ionization mechanisms involving autoionizing states, and (2) long-lived metastable states of the target ion. Extensive calculations and measurements on the iron isonuclear sequence, carried out by groups at Oak Ridge,[1] provide an instructive case study. While the distorted-wave approximation is often adequate, some progress has been made toward more precise calculations. Even approximate calculations on complex systems require extensive computer resources.

*Dept. of Physics, Rollins College, Winter Park, FL 32789.

†Dept. of Physics, Auburn Univ., Auburn, AL 36849.

‡Operated by Martin Marietta Energy Systems, Inc. under Contract DE-AC05-84OR21400 with the U.S.D.O.E.

[1]M. S. Pindzola, D. C. Griffin, and C. Bottcher, Phys. Rev. A 34, 3668 (1986).

I-6 Theory of Resonant Electron-Molecule Collisions* A. HAZI, Lawrence Livermore National Laboratory--Autoionizing states of molecules play an important role, as intermediate states, in many low-energy, electron-molecule collision processes, e.g., vibrational excitation, dissociative electron attachment and recombination. Significant progress has been made recently in developing computationally feasible theoretical methods for describing resonant electron scattering from simple molecules. This presentation will review the methods available for treating both the electronic properties of molecular autodetaching states and the dynamics of nuclear motions. Recent calculations of cross sections for diatomic molecules will be given as examples. Some discrepancies between theory and experiment will also be discussed to illustrate possible shortcomings of current theories and to stimulate additional experimental studies.

*Supported by DOE Contract No. W-7405-Eng-48.

I-7 Rotational and vibrational excitation of simple molecules. D. W. Norcross and S. Alston, JILA, Univ. of Colo. & NBS.--Our use of the integral-equations approach to calculations will be outlined. The technique is one of many forms of the close-coupling approximation, which permits a rigorous and complete treatment of the nuclear dynamics for vibrational excitation, but an adiabatic (a.k.a. fixed-nuclei) approximation for rotational excitation. The former is, in principle, as accurate as the representation of the interaction potential and the extent of the expansion will permit, while the latter is a high-energy (relative to dE_j) approximation. We can achieve an essentially exact treatment of the tricky exchange interaction, and employ a parameter-free, but local, representation of correlation/polarization forces. Today's software restricts us to linear molecules (we have worked on H_2, N_2, HF, HCl, CO, and HCN), but this is not an essential limitation. We are working to develop, as well as an expanded capability to treat non-linear polyatomics, a facility for obtaining both anion and neutral Rydberg potential energy surfaces, and to study processes like photodetachment, and attachment/detachment reactions.

I-8 An Algebraic Variational Approach to Electron-Molecule Scattering*. T. N. RESCIGNO, Lawrence Livermore National Laboratory, and B. I. SCHNEIDER, Los Alamos National Laboratory - Algebraic variational methods (such as the Kohn method and related techniques) have been used to calculate electron-atom scattering cross sections for many years. Two principal diffuculties have hitherto hindered their application to molecular problems: the troublesome occurance of singularities (pseudo-resonances) and the diffucult evaluation of the required matrix elements. Both of these obstacles have been overcome. The problem of pseudo-resonances can be avoided by formulating the variational principle with outgoing- rather than standing-wave boundary conditions.[1] A judicious mixture of numerical and analytic techniques can be used to evaluate all the requisite matrix elements. These techniques will be explained and the methods demonstrated by a number of illustrative calculations.

*Work performed under the auspices of the U. S. Department of Energy by the Lawrence Livermore and Los Alamos National Laboratories under contracts W-7405-ENG-48 and W-7405-ENG-36.

C. W. McCurdy, T. N. Rescigno and B. I. Schneider, Phys. Rev. A 36, XXXX (1987).

I-9 Studies of Low-Energy Electron-Molecule Collisions. W. M. HUO, NASA-Ames Research Center, H. PRITCHARD, K. WATARI*, M. A. P. LIMA*, AND V. McKOY**, California Institute of Technology - We will present the results of several applications of the Schwinger multichannel method to the scattering of low-energy electrons by diatomic and small polyatomic molecules. Cross sections for excitation of various electronic states of H_2, N_2, CO, CO_2, and H_2O by electrons with near-threshold energies and higher will be reported. Elastic scattering and momentum transfer cross sections for low-energy collisions with the small polyatomic molecules H_2O, NH_3, CH_4, and C_2H_4 will also be discussed. These results will be compared with available theoretical and experimental data.

*Supported by CNPq (Brazil)

**Work supported by NSF Grant PHY-8604242, NASA-Ames Cooperative Agreement NCC 2-319, and by the Innovative Science and Technology Program of the Strategic Defense Initiative Organization under Contract No. DAAL03-86-K-0140.

SESSION J

7:30 PM - 10:00 PM, Wednesday, October 14

Space Science and Technology Center, Room 3

POSTERS

Chairman: T. Eddy (Georgia Tech)

SESSION JA

7:30 PM - 10:00 PM, Wednesday, October 14

Space Science and Technology Center, Room 3

SWARMS AND BREAKDOWN

Chairman: T. Eddy (Georgia Tech)

JA-1 Electron Degradation Spectra and Initial Yields of Ions in Binary Mixtures*, M. KIMURA, Argonne National Laboratory and Rice University, MITIO INOKUTI, and M. A. DILLON, Argonne National Laboratory - The electron degradation spectrum (EDS) is a key element in the description of the elementary processes induced by ionization radiation. It represents the energy distribution of all incident and subsequently generated electrons. The original study by Spencer and Fano[1] defines the degradation spectrum in time-independent representation which is applicable to stationary irradiation, although the notion can be extended to transient aspects of electron degradation that occur immediately after pulse irradiation. We have calculated the electron degradation spectra in gaseous binary mixtures of H_2, CO_2, and H_2O molecules irradiated by 1, 5, and 10 keV incident electrons. Details of results will be presented at the meeting.

*Supported in part by the U.S. Dept. of Energy, Office of Health & Environmental Research, under Contract W-31-109-Eng-38, and by Office of Basic Energy Science.

[1]L. V. Spencer and U. Fano, Phys. Rev. 93, 1172 (1954).

JA-2 Simulation of Electron Swarm Motion in CCl_2F_2 using Monte Carlo Technique, V. K. LAKDAWALA, S.T. KO, AND S. ALBIN, Old Dominion University - Dichloro-difluoro-methane (CCl_2F_2) is an important gas for plasma etching (1) and a likely candidate for use as a constituent of insulating gas mixtures such as SF_6 + CCl_2F_2. We have simulated the electron swarm motion in CCl_2F_2 using a Monte Carlo Technique and swarm parameters have been evaluated for electrons in CCl_2F_2 over the E/p range 80 to 200 V cm^{-1} $torr^{-1}$. Comparison has been made with the published experimental results for the ionization coefficient, attachment coefficient and the electron drift velocity. A set of electron/molecule collision cross-sections has been assembled for CCl_2F_2 which gave a good fit between the simulated and the experimental values over the entire E/p range.

[1]G. Smolinsky et. al., J. Vac. Sci. Tech., 18, 12, 1981

JA-3 Time Evolution of Electron and Positron Swarms in Neon*. P.J. Drallos and J.M. Wadehra, Wayne State University - The time evolution of swarm parameters in gaseous neon are calculated using a finite difference solution of the Boltzmann Equation. The finite difference method provides a more accurate representation of the distribution function[1] than does the more commonly used two-term expansion method. However, this method normally leads to strong instabilities due to derivatives which must be evaluated numerically. In the present work we use a novel algorithm for evaluation of the derivatives in which they can be obtained simply and exactly, thus eliminating the instability problems normally associated with this method. Swarm parameters for electrons and positrons in neon are calculated for various values of E/N.

* Research supported by the U.S. Air Force Office of Scientific Research through Grant No. AFOSR 84-0143.

1 H. Tagashira et al., J. Phys. D 11, 283 (1978).

JA-4 Low Energy Electrons in Deuterium

W.Roznerski, K.Leja, Technical University of Gdansk, and Z.Lj. Petrović, Institute of Physics, University of Belgrade

In this paper we present the data for the transport coefficients of electrons in deuterium at moderate values of E/N. Characteristic energies were taken between 20 and 1000 Td using a Townsend-Huxley type apparatus. Drift velocities were measured using a double grid Bradbury-Nielsen time of flight method in the E/N range between 3 and 125 Td. Present results are in good agreement in the range of overlap with the data of Petrović and Crompton that were obtained with a more accurate equipment. Present data will enable us to check the existing cross section data for deuterium, especially the data for the vibrational excitation.

JA-5 A New Swarm Determination of Electron Molecule Cross Sections in Tetrafluoromethane. P. SÉGUR, M. BREZNOTITS and J.P. ZURRU, University Paul Sabatier, Toulouse, France. - It is now well known that in some molecular gases where very important inelastic (rotational or vibrational) processes occur at low energy the electron energy distribution function is very anisotropic. The calculation of swarm parameters is then made difficult and a very sophisticated numerical method of solution of the Boltzmann equation is necessary. In this work, it is shown that errors in the calculation of transversal or longitudinal diffusion coefficient (compared to the calculations made by using the usual two term approximation) may reach 500%. Obviously, the cross sections we have obtained by using our numerical method of solution of the Boltzmann equation are then very different from the cross sections previously determined by other authors[2] and agreement between measured and calculated swarm parameters are much better. By using this new set of cross sections, calculations of the drift velocity are made in argon-CF_4 and methane-CF_4 mixtures giving very good agreement with available experimental data[2].

[1]M. Hayashi, 5th. International Symposium on Gaseous Dielectric, Knoxville, U.S.A.,-May 3-7, 1987.
[2]S.R. Hunter, J.G. Carter, L.G. Christophorou, J. Appl. Phys. 58, 3001 (1985).

JA-6 Effect of Pulse Rising Rate on Current Emission and Ozone Generation in a Pulsed Streamer Corona Discharge in Air, AKIRA MIZUNO, AND YUKIHIRO KAMASE, Toyohashi University of Technology, Toyohashi, Japan 440, - Streamer corona discharge energized by a fast rising pulse voltage can produce an intense plasma, which effectively promotes gas phase chemical reactions such as ozone generation, oxidation or decomposition of nitrogen mono-oxide and sulfur dioxide in exhaust gas, etc. The authors carried out an experiment to study the effect of pulse rising rate on current wave form, mode of discharge, and ozone generation of positive and negative pulsed streamer corona discharges in air. Large pulse current is emitted at the rising period of the applied pulse voltage, and peak value of the current decreased with the decrease in the pulse rising rate. In this case, development of the streamers is quenched and reaction of ozone generation is suppressed. When the pulse rising rate was decreased from 1.0 to 0.3 kV/nsec, ozone concentration decreased to 80 % in positive polarity, and to 44 % in negative polarity.

JA-7 Short-Gap Breakdown at Low Overvoltage* J.P. NOVAK and R. BARTNIKAS, IREQ, Varennes, Québec, Canada. Quantitative model described earlier (Ref. 1) has been applied to a short plane-parallel gap under conditions of a low overvoltage. Model consists of conservation eqs. for electrons, atoms, and excited particles and Poisson eq., including feed-back via ion and metastable atom stimulated cathode emission and photoemission. The electrode separation is 0.48 mm at an applied voltage 192 V. Densities of the particles have been calculated in two dimensions as functions of time. As compared to the formerly reported case of a high overvoltage, diffusion phenomena in juxtaposition to the effect of space charge field exert much a stronger influence on breakdown development. Characteristic features of the discharge, i.e. spreading of the ionized zone over a large diameter (compared to electrode separation) and slow current rise, are typical for glow or pseudo-glow discharges, which are experimentally observed under similar conditions.

*This work was supported by CEA (Canada).

[2] J.P. Novak and R. Bartnikas, J. Appl. Phys., to be published.

JA-8 The Studies of Gas Breakdown Processes in a Capillary Glow Discharge, Z. M YANG, Z. N. LUO, J. R. YU, and G. J. COLLINS, Nanjing Institute of Technology and Colorado State University - The gas breakdown processes in a capillary glow discharge have been examined. The summary breakdown equation closely follows Paschen's formula and is as follows:

$$V = Bpd/f(\frac{D}{d})\ln\{1+\exp[-(\frac{eVw}{kT} + \frac{APD}{2})]\}$$
$$\{\ln(1+\frac{1}{\gamma})/APd+\exp[-(\frac{eVw}{kT} + \frac{APD}{2})]\}$$

This theoretical expression agrees with the experimental results which we obtained for mixtures of Helium and Neon very well. If the capillary diameter D is increased, the expression tends towards Paschen's empirical formula:

$$V_p = BPd/\ln[APd/\ln(1 + \frac{1}{\gamma})]$$

SESSION JB

7:30 PM - 10:00 PM, Wednesday, October 14

Space Science and Technology Center, Room 3

D. C. GLOWS

Chairman: T. Eddy (Georgia Tech)

JB-1 Photoabsorption Cross Section of XeF_2 from 150 to 275 nm by Forward Scattering EELS*, DAVID SPENCE, HIROSHI TANAKA,† and M. A. DILLON, Argonne National Laboratory - Using the technique of high incident energy, forward scattering, electron energy-loss-spectroscopy, we have derived the relative photo-absorption cross section of xenon difluoride from 150 to 275 nm. Normalization of our data to two previously measurements which used conventional photoabsorption techniques shows good agreement with an early measurement[1] over the entire spectral range, but significant disagreement with more recent data[2] for wavelengths greater than 175 nm.

*Work supported in part by the U.S. Dept. of Energy, Office of Health & Environmental Research, under Contract W-31-109-Eng-38.

†Sophia University, Dept. of General Science, Chiyoda-ku, Tokyo 102, Japan.

[1]J. Jortner, E. G. Wilson, and S. A. Rice, in Noble-Gas Compounds, edited by H. H. Hyman (University of Chicago Press, Chicago, IL, 1963).

[2]G. Black, R. L. Sharpless, D. C. Lorents, D. L. Huestis, R. A. Gutcheck, T. D. Bonifield, D. A. Helms, and G. K. Walters, J. Chem. Phys. 75, 4840 (1981).

JB-2 Buffer Gas Effects on the Performance of a Self-Sustained Discharge ArF laser, M.OHWA AND M.OBARA, Keio University, - In self-sustained discharge pumping of rare-gas halide lasers, either neon or helium has widely been used as a beffer gas. Because the recombination rates for rare-gas halide excimers in Ne-diluted mixtures are faster than those in He-diluted mixtures, the use of neon rather than helium can improve the electrical efficiency of KrF and XeCl lasers, although the He-diluted mixtures is found to excite the laser efficiently due not to low discharge resistance[1]. However, there is appreciable difference in the electrical efficiency of ArF lasers between the Ne-diluted and He-diluted mixtures. We have developed a comprehensive computer code for self-sustained discharge ArF lasers to clarify the effects of Ne and He diluents on the performance of ArF lasers. Intense pumping of He-diluted mixtures rather than Ne-diluted mixtures is found to improve the output performance of ArF lasers. For a 4-atm mixture of 94.9% He/5% Ar/0.1% F_2 a pump rate of 8-10 MW/cm^3 leads theoretically to high-efficiency operation.

[1]H.Hokazono et al., J.Appl.Phys. 56, 680 (1984).

JB-3 Two Dimensinal Model of dc Glow Discharges. J.-P. BOEUF and P. SEGUR, CNRS, Université Paul Sabatier, Toulouse, France. - A two dimensional cylindrical model of dc glow discharges has been developed. This model is based on numerical solutions of the continuity and momentum for electrons and ions, coupled with Poisson's equation, assuming local equilibrium between charged particle kinetics and electric field (the model is therefore not valid for strongly abnormal glow discharges). Continuity and Poisson equations are solved alternately until steady state is reached; a very efficient and stable implicit exponentially fitted discretization scheme is used for the continuity equations, while Poisson's equation is solved using FFT or ADI methods (with Dirichlet or Von Neuman boundary conditions). The transition between the normal and abnormal regime is described self-consistently for the first time: the 2D spatial variations of the charged particle densities, potential and electric field in dc discharges in Helium are presented for normal and moderately abnormal discharge regimes. The calculations show the important role of the radial electric field which confines the electrons in the core of the negative glow and is responsible for the stabilization of the discharge in the normal regime.

JB-4 Operating E/n and metastable production in the positive column of an H_2-Ar discharge. M.A. ISLAM* and A.V. PHELPS. JILA, Univ. of Colorado and NBS — The H_2-Ar discharges were operated at 0.1-0.3 mA and 5-20 torr with 2% H_2 in Ar. The electric field strength was determined using floating probes close to the tube wall. The density of Ar metastables was obtained from absorption measurements at 763.5 nm for the $^3P_2$ state and at 794.8 nm for the the $^3P_0$ state using a capillary discharge in Ar as a source. The widths of the lines from the source were measured with a confocal Fabry-Perot interferometer which was calibrated with a narrow line diode laser. The discharge operating conditions will be compared with those calculated from the transitional ambipolar diffusion model of Muller and Phelps[1]. The Ar metastable densities will be compared with the results of Boltzmann calculations at the measured E/n values.

* Present Address: Phys. Dept., State University of New York College at Potsdam.

1. C.H. Muller, III and A.V. Phelps, J. Appl. Phys. 51, 6141 (1980).

JB-5 Numerical Analysis of Self-sustaining Bulk Pulsed Discharge in Nitrogen*, S.K. DHALI, L.H. LOW, Southern Illinois University - The growth of the current, ionization and the excited molecules in a pulsed nitrogen discharge is simulated using a self-consistent calculation of the electron distribution function, the vibrational population, and densities of some electronically excited states. We find a strong coupling between the electron energy distribution and the ground state vibrational population. We have carried out these calculations for a wide range of voltages (70-150 Td), pressures (1-100 Torr) and pulse lengths (1-700 μsec). The time evolution of the discharge current, and the densities of the excited states and electrons will be presented. The afterglow region of the discharge will also be discussed.

*Research supported by AFOSS, Bolling AFB, DC.

JB-6 Spatially Resolved Temperature Measurements in a Positive-Column Nitrogen Discharge Using Planar BOXCARS, D. D. HODSON, C. J. EMMERICH, and P. P. YANEY, U. of Dayton,* and S. W. KIZIRNIS, USAF Aero Propulsion Lab. -- Rotational and vibrational temperatures were determined along the axis of a dc parallel-plate discharge having a 20-mm plate spacing and operated at 15 Torr and $E/N = 8 \times 10^{-16}$ V-cm^{-2}. Measurements were taken in 2 mm steps starting 1 mm from the cathode. A crossed-beam geometry of the CARS beams was used to obtain a spatial resolution of about 1.2 mm long by 40 μm in diameter. An 800 K temperature observed near the cathode was the highest rotational temperature, while a vibrational temperature of 1650 K near the anode was the highest vibrational value obtained. Sufficient signal was available at the anode end to show that the first hot band was rotationally in equilibrium with the ground state band. The estimated uncertainties in these results are about ±50 K.

* Supported by USAF Cntrt No. F33615-81-C-2012.

JB-7 Continuum Model of DC Negative Glow Discharges: Argon and Nitrogen , M. SURENDRA AND D. B. GRAVES, University of California,Berkeley - Continuum models of argon and nitrogen DC negative glow discharges are presented. The model (conservation equations for electrons and ions, Poisson's equation for a self consistent electric field, equations for electron energy and momentum) employed here is an extension of the model presented by Graves and Jensen[1]. Rate and transport coefficients are fitted using approximate analytical formulae based on either electron temperature or E/n (ratio of electric field to gas density). The governing equations were solved numerically with the Galerkin finite element method. Predicted profiles for ion concentration, electron temperature, plasma potential and optical emission are compared to experimental results reported in a companion paper.

[1]D. B. Graves and K. F. Jensen, IEEE Trans. Plasma Sci. PS-14, 78 (1986).

JB-8 Experimental Study of a DC Nitrogen Discharge, K. E. HUFFSTATER, G. M. JELLUM, D. B. GRAVES, University of California,Berkeley - There exist a number of diagnostic techniques which may be used to study discharge properties. It is desirable to understand how the results obtained from one technique compare to those obtained from another. With this goal in mind, a parametric study of a negative glow DC nitrogen discharge was carried out using a number of diagnostic techniques including laser-induced fluorescence (LIF), laser optogalvanic spectroscopy (LOGS), optical emission spectroscopy and Langmuir probes. Spatially resolved measurements have been made of ground state ion (N_2^+) and metastable ($A^3\Sigma^+_u$) densities, electron temperature, plasma potential, optical emission, and vibrational and rotational temperatures. The discharge pressure and power were varied from 0.2 to 2.0 torr and .08 to .8 watts/cm^2, respectively. The diagnostic techniques which measure the same quantity were compared to each other whenever possible. For example, ion density profiles obtained with the Langmuir probe were compared to those measured with LIF. Another goal of this study is to compare the results with continuum modelling predictions of a nitrogen discharge which are presented in a companion paper.

JB-9 Mass Spectrometer Measurements of Disilane Glow Discharges.* G. H. LIN, J. R. DOYLE, M. Z. HE, and A. GALLAGHER,† JILA, Univ. of Colorado and NBS.--Mass spectrometric measurements of stable molecule production in disilane and disilane-hydrogen glow discharges are reported. Silane and trisilane production and disilane depletion were studied as a function of substrate temperature, gas pressure, dc discharge current and rf power. Disilane depletion is found to be independent of gas flow and substrate temperature. Hydrogen production is very low compared to pure silane discharges for all conditions. The relative roles of surface and gas phase reactions in the production of these stable molecules are discussed. Based on simple models, the mechanisms of a-Si:H film growth from silane and disilane glow discharges are compared.

*Work supported in part by the Solar Energy Research Institute.

†Staff member, National Bureau of Standards.

JB-10 Spectroscopic Study of Resist Stripping by a Glow Discharge Electron Gun, LUMIN LI, YI HANWEI, J. KRISHNASWAMY, and G. J. COLLINS, Colorado State University - An electron beam created by a glow discharge electron gun in soft vacuum (50-500mTorr) is used to strip resists such as PMMA, HPR, CMS Polyamic acid and Polyimide in an oxygen ambient. Oxygen appears to play an important role since stripping in Helium ambient was negligible. Resists removal rate were 1.5 um/min compariable to those recently published[1]. The etch rate electron beam achieved for Polyimide is larger than the etch rate in a microwave oxygen plasma. A preliminary spectroscopic emission study shows that the violet band originating from CN ($B\,^2\Sigma$-$X\,^2\Sigma$) appears strong in Polyamic acid etching but is absent in PMMA. The blue C_2 band was also observed[2] and the CH and CO bands were prominent in PMMA electron beam etch plasma.

[1]D.C.Sun,etal.,J.Appl.Phys., 61, 5180 (1987)
[2]G.Koren and J.T.C.Yeh, Appl.Phys. Lett., 44, 1112 (1984)

SESSION JC

7:30 PM - 10:00 PM, Wednesday, October 14

Space Science and Technology Center, Room 3

SHEATHS

Chairman: T. Eddy (Georgia Tech)

JC-1 Spectroscopic Diagnostics in the Cathode Region of a Nitrogen Discharge* A. MARGULIS and J. JOLLY, Lab. Phys. Plasmas, Univ. Paris-Sud, Orsay, France -Spatially resolved laser-induced fluorescence (LIF), optogalvanic effect (LOG) and plasma induced emission spectroscopy (PIE) were used to study the cathode region of a DC discharge in N_2. The rotational temperatures of the states $N_2^*(X)$, $N_2^*(B)$ and $N_2(C)$ were analysed along the discharge axis using LIF, LOG and PIE spectroscopy. Laser-induced fluorescence intensities of $N_2^*(B \leftarrow X)$ were corrected from the spatial variations of the partition function with temperature to determine the relative distribution of the ionic concentration. N_2^* density is observed to be $\sim$ 20 times smaller in the cathode fall than in the negative glow. PIE of the $N_2(C)$ level exhibited an axial profile similar to the ion profile. The LOG signal on the ions is interpreted as a laser induced change in ion mobility; and a model, based on a difference in the ion velocities, fits correctly the experimental data points.
*Research supported by DRET and CNRS.

JC-2 Analysis of the Cathode Fall of Abnormal Glow Discharges in an Electronegative Gas*, K. H. Schoenbach and Hao Chen, Old Dominion University, Norfolk, VA, - The cathode fall and the positive column of a glow discharge in a SF_6/He gas mixture was modeled for current densities in the range of 1 A/cm^2. A one dimensional Monte-Carlo code was used to calculate the electron energy distributions and the transport and rate coefficients as a function of position in the discharge, assuming a linearly varying electric field in the cathode fall region. Subsequently the charge carrier densities and electron and ion current densities were computed by means of a continuum model. The results were used to correct the assumed electric field distribution and through an iterative procedure to approach a self consistent solution for the cathode fall. The influence of a transverse magnetic field on the glow discharge was studied with the same technique. The calculated discharge voltages were compared with experimentally obtained values.
*Research sponsored by the Physical Electronics Research Institute at ODU and by the SDIO/IST under the management of ONR.

JC-3 On the Effect of Charge Exchange Collisions in the Space Charge Sheath - K.U. RIEMANN, Ruhr-Universität Bochum, FRG.

In most discharges the plasma sheath transition presents itself as a two-scale-problem with a quasi-neutral presheath (extension some mean-free-paths λ) and a collision-free space charge sheath (extension some Debye-lengths λ_D) with $\lambda \gg \lambda_D$. Since the sheath is collision-free the main difficulty of a theoretical analysis arises from the self-consistent calculation of the ion distribution and field in the presheath. For large negative sheath voltages, however, the sheath thickness is no longer characterized by the Debye length but results from the $U^{3/2}$ -law. In this case elementary processes within the sheath can again be important. This influences the potential variation in front of a surface as well as the energy distribution of the ions striking the wall. We analyze this influence by a kinetic investigation, which is based on the charge exchange model for the ions. The problem of the selfconsistent potential variation is tackled at present by a parameter-ansatz interpolating between the limiting cases of an inertia resp. mobility controlled sheath.

JC-4 The Boundary Layer of a Weakly Ionized Plasma with Hot Neutrals - S. BIEHLER and K.U. RIEMANN, Ruhr-Universität Bochum, FRG.

The key problem for the solution of the plasma sheath transition is the selfconsistent calculation of the ion distribution function and potential variation in the quasi-neutral presheath. A closed analytic solution exists for the collision-free Tonks-Langmuir-plasma and for the charge exchange model with cold neutrals. In both models the energy of the ions emerging from an elementary process is neglected against the thermal energy of the electrons. Emmert et al. could account for the effect of hot neutrals in the Tonks-Langmuir-model. The result was an essential modification of the sheath edge structure. Therefore it is of interest to investigate the influence of hot neutrals on the charge exchange model of the boundary layer. We have investigated this problem starting from a suitable parameter-ansatz for the selfconsistent potential. The results show that the modification of the sheath edge structure is restricted to the collision-free case. Nevertheless, the hot neutrals have a surprisingly high influence on the energy distribution of the ions, which can not be explained by the thermal energy of the charge exchange partners.

JC-5 Effect of Electrode Area Ratio on Radio Frequency Glow Discharge Sheath Fields*, T. INTRATOR*+, G.R. SCHELLER, R.A. GOTTSCHO, AT&T Bell Laboratories--In many radio frequency plasma applications, use of unequal area electrodes leads to a dc self-bias voltage. Since this bias voltage can be large, it often affects sputtering, etching, and deposition rates. Using the technique of Stark-mixed laser-induced fluorescence[1,2] we measured fields as a function of electrode area ratio (from 1:1 to 9:1) in discharges through BCl_3 and five percent BCl_3 in Ar. Not only the magnitudes but also the shapes of the fields differ for different electrode area ratios. Along the electrode axis, double layers are observed throughout most of the rf cycle at both the large and small area electrodes. In the radial direction, large double layers are observed near the large electrode.
*Support provided by Wisc. Plasma Processing & Technology Center.
+Permanent address - Dept. Nuclear Engr. & Engr. Physics, Univ. of Wisconsin-Madison, WI.
[1]M.L. Mandich, C.E. Gaebe, and R.A. Gottscho, J. Chem. Phys. 83, 3349 (1985).
[2]J. Derouard and N. Sadeghi, Opt. Comm. 57, 239 (1986).

JC-6 Plasma-Sheath Structure for an Electrode Contacting a Thermal Plasma, Including Electron Energy Effects*, L. D. ESKIN AND S. A. SELF, Mech. Engr. Dept., Stanford University - The electron and ion continuity and momentum equations are solved with Poisson's equation and the electron energy equation for the cathode electrical boundary layer of a collision dominated plasma. The results are compared with previous computations which did not include electron energy effects. Electron impact ionization and three-body (electron) recombination are considered, and are shown to play an important role in the current saturation process. As the current to the cathode increases, Joule heating is observed to increase the net generation rate in the ionization non-equilibrium layer. This in turn increases the saturation current above the value found when neglecting electron energy effects. The conditions are being investigated whereby the increase in total net ionization rate leads to the transition from a diffuse to a constricted current transfer mode.

* Work supported by the Air Force Office of Scientific Research, Grant No. 83-0108.

JC-7 Collisions of Atoms With a Liquid Metal Surface in a Sputtering Environment, W. L. MORGAN, Lawrence Livermore National Lab*- Recent research into the distribution of atoms near a liquid metal surface[1,2] has shown that the liquid/vapor interface is stratified for several atomic diameters into the bulk liquid. This will have consequences for collisions of ions and atoms with possible liquid metal surfaces in some sputtering and discharge environments. I have performed dynamical calculations of low energy Hg atoms (ions are neutralized quite far from the surface) colliding with a liquid Hg surface. I used potentials and statistical surface profiles from Ref. 2. Compared to scattering from a crystalline solid surface, atomic scattering from a liquid metal surface is characterized by enhanced energy loss and diffuse reflection.

*Work performed under the auspices of the U.S. Department of Energy by the Lawrence Livermore National Laboratory under contract number W-7405-ENG-48.

[1]S.W. Barton, et al., Nature 321, 685 (1986).
[2]M.P. D'Evelyn and S.A. Rice, J. Chem. Phys. 78, 5081 (1983).

SESSION KA

8:00 AM - 9:45 AM, Thursday, October 15

Space Science and Technology Center, Room 5

RECOMBINATION AND ION-MOLECULE COLLISIONS

Chairwoman: M. Mandich (AT&T Bell Laboratories)

KA-1 Dissociative Recombination of Electrons with H_2^{+**}, A. P. HICKMAN, SRI International - Direct and indirect mechanisms contribute to the dissociative recombination of electrons with H_2^+. The direct is well understood; the indirect is a two-step process involving intermediate Rydberg state resonances of H_2^{**}. We have calculated the real and imaginary parts of the Greens function matrix elements describing the indirect process, including the nonlocal terms in the interaction.[1] Previous calculations neglected the real part of the amplitude for the indirect process, and observed predominantly destructive interference between the direct and indirect processes. We find that the interference is sensitive to the phase of the indirect amplitude, and cancellation does not occur when the full complex amplitude is used. For electrons energies 0.01-0.5 eV, we find that including the indirect process leads to a larger cross section for recombination when v_0 (of H_2^+) = 0.

* Research Supported by NSF Physics

[1] A. P. Hickman, J. Phys. B 20, 2091 (1987)

KA-2 Density Dependence of Ion-Ion Recombination in Helium and Argon at Atmospheric Pressures, H.S. Lee and R. Johnsen, University of Pittsburgh- We have measured the density dependence of the recombination coefficients for

$$H_3O^+(H_2O)_2 + NO_3^- + M \longrightarrow \text{Neutrals}$$

for M= He or Ar and $0.25N_L < [M] < 1.25\ N_L$ by observing the decay of the ionic conductivity in photoionized afterglow plasmas. Ions were identified by mass-spectrometric sampling. The increase of the recombination coefficients with gas density indicates three-body recombination coefficients

$\alpha(He)=1.4\times10^{-26}cm^6/s$ and $\alpha(Ar)=7.8\times10^{-26}cm^6/s$, in acceptable agreement with calculations based on the theories of Bates and Mendas and of Bates and Flannery.

*Research supported, in part, by ARO

KA-3 Measurement of Ion-Ion Recombination in High-Pressure Gases using a Two-Slit Method.* C. R. TENNEY, F. A. DIBIANCA, D. J. WAGENAAR, J. E. FETTER, J. E. VANCE, J. J. BROPHY, UNC-CH, D. L. MCDANIEL, and P. GRANFORS, GE Med. Sys. Group --Ion-ion recombination coefficients have been determined for noble gases doped with electron-attaching agents. Pressures up to 35 atm were studied in a gridded drift chamber. X-rays flashed through a slit in front of the chamber produce positive ions which drift past the grid and produce a signal. The process is repeated with another slit open between the original slit and the grid. As far-slit positive ions drift toward the grid, they recombine with near-slit negative ions. The far-slit signal is reduced, and comparison of the two far-slit signals gives the loss of far-slit ions from recombination with near-slit ions. Initial recombination does not affect the measurement.

*Work supported by GE Med. Sys. Group

KA-4 The Reaction of N_2^+ with H_2O, D_2O, and D_2O^{18}, F. J. WODARCZYK, Air Force Office of Scientific Research, R. H. SALTER & E. MURAD, Air Force Geophysics Laboratory - The reactions of N_2^+ with D_2O^{18}, D_2O, and H_2O were studied using a double mass spectrometer which has been described previously.[1] The primary ion kinetic energy was varied between E_{CM} = 0.1 and 16 eV. There are two reaction channels:

$$N_2^+ + H_2O \rightarrow H_2O^+ + N_2 \quad (1)$$
$$\rightarrow N_2H^+ + OH \quad (2)$$

Both channels are exothermic and show dependence on kinetic energy which is typical of exothermic reactions. These reactions play a role in the steady state concentration of H_2O^+ observed on the space shuttle. An analysis of this problem will be presented.

[1]W. B. Maier, II, and E. Murad, J. Chem. Phys., 55, 2308 (1971).

KA-5 Reaction Cross Sections and Thermochemistry for the Reactions of Si^+ and SiF_3^+ with SiF_4, M. E. WEBER, UC Berkeley, P. B. ARMENTROUT, University of Utah - The title reactions have been studied using guided ion beam mass spectrometry. The reaction cross sections have been measured as a function of kinetic energy from thermal to > 50 eV,CM. The reaction of Si^+ with SiF_4 results in three endothermic channels. The SiF^+ channel is only slightly endothermic and is the predominant process at all energies. Both SiF_3^+ and SiF_2^+ have apparent thresholds at 3 eV,CM. SiF_3^+ is 20 to 50% smaller than SiF^+, while SiF_2^+ is an order of magnitude smaller. A second feature appears in the SiF_2^+ cross section function and is explained by dissociation of SiF_3^+. The reaction of SiF_3^+ with SiF_4 yields two highly endothermic channels, SiF^+ and SiF_2^+, which are likely the result of collision induced dissociation. In neither system are $Si_2F_x^+$ species observed. The apparent thresholds for both the Si^+ and SiF_3^+ reactions lie within the large uncertainties in the literature thermochemistry. Analysis of the present systems provides more accurate heats of formation for both ionic and neutral silicon fluorides.

KA-6 Collisional Vibrational Quenching of $NO^+(v)$ Ions, R.A. MORRIS, A.A. VIGGIANO, F. DALE, AND J.F. PAULSON, Air Force Geophysics Lab - Vibrational quenching rate constants have been measured for $NO^+(v)$ ions with 15 neutral molecules by the SIFDT-monitor ion technique. The temperature dependence of the quenching rate constants for the reactions of the neutrals N_2, CO_2, and CH_4 has been investigated from 200 to 450K. The dependence of the CH_4 quenching rate constant on collision energy has been determined in the energy range 0.03 - 0.12 eV. Also measured are rate constants for some of the pertinent reactions involved in the monitor ion technique. Discrepancies with some previous results are discussed.

KA-7 Quenching of $N_2(A^3\Sigma)$. R.A. YOUNG, J. BLAUER, and R. BOWER, Rocketdyne Division, Rockwell International--Using a fast flow (10^3cm s^{-1}) system and Argon metastable excitation of N_2 to give N_2 (A^3), we have measured its rate of removal by collisions with XeF_2, O_2, NO, PH_3, Cl_2, GeH_4, and SiH_4 finding rate constants (in units of cm^3s^{-1}) of (1.2 $\pm$ 0.3) 10^{-12}, (2.6 $\pm$ 0.3) x 10^{-12}, (4.3 $\pm$ 0.2) x 10^{-11}, (3.7 $\pm$ 0.4) x 10^{-11}, (3.7 $\pm$ 0.4) x 10^{-11}, (1.4 $\pm$ 0.2) x 10^{-11}, (1.4 $\pm$ 0.3) x 10^{11}, and (8.9 $\pm$ 1) x 10^{12} respectively. The quenching by XeF_2, $N_2(A) + XeF_2 \rightarrow N_2(X) + XeF^* + F$, where XeF* in its B and C state has been suggested as a key step in a chemically driven excimer laser. No emmission was observed from XeF* in the quenching of $N_2(A)$ by XeF_2 and its yield is less than 3 x 10^3. The rate constant values found for NO and NO_2 agree with the measurements of others.

SESSION KB

8:00 AM - 9:05 AM, Thursday, October 15

Space Science and Technology Center, Room 4

BEAM AND RADIATION PRODUCED PLASMAS

Chairman: K. Stalder (SRI International)

KB-1 Electrode Design and Discharge Modeling in an E-Beam Sustained Discharge with a Spreading Source*, M. VON DADELSZEN, Spectra Technology Inc. - The design of electrodes in externally sustained discharges with the triple point (electrode/dielectric/gas) exposed to the source presents several problems when the electrode and dielectric surfaces must also act as flow boundaries. The approaches frequently used to solve these problems have penalties associated with complexity, size, flow pressure drop, gas density uniformity and/or cost. A Monte-Carlo e-beam deposition code has been coupled to the ELF codes to analyze and design an electrode/dielectric interface requiring none of these approaches. By careful contouring of the electrode and dielectric profiles it is possible to recess the triple point behind the electrode in a gas purged "moat" geometry while minimizing the impact on the flow boundary layer and minimizing geometric e-field enhancements. The geometry and analysis will be described, and experimental results will be presented.

*Work supported by Rockwell SSD, MIT/LL

KB-2 Kinetics of UV-Sustained Glow Discharges, W. M. Moeny, Tetra Corporation - We have studied a variety of mixtures for UV-sustained glow discharge opening switches. There are three gas families of particular interest to UV-sustained glow discharge switches: perfluoroalkanes (C_2F_6 in Ar), N_2 mixtures that use the 108 nm emission line, and CF_4 based mixtures. For this paper we show the behavior for mixtures that have been selected theoretically and tested experimentally for application to a UV-sustained glow discharge switch. Current conduction is initiated a few nanoseconds after the UV source is turned on. Once the UV source is turned off, the discharge will recover, opening the switch with a characteristic time that is a function of the attaching gas present in the mix. The opening time of the switch may be affected by changing the concentration of the attacher present in the mix and the turn-off time of the UV source. We found mixtures of N_2, CF_4 and He provide good opening switch candidates. For the $N_2/CF_4/He$ mixture, electric fields of 1 to 4 KV/cm and current densities of about 1-2 amp/cm^2 were observed. Other gas mixtures under study at Tetra Corporation yield current densities over 4 amp/cm^2. Yet other mixtures yield high discharge electric field characteristics. We have investigated over 30 different mixtures. Research supported by Air Force Weapons Laboratory, KAFB, NM.

KB-3

Modeling of Unsteady Negative Differential Conductivity Effects in UV-Sustained Radial Glow Discharges Using the Tetra ELF Computer Codes. W. M. Mooney, Tetra Corporation - Analytical scaling laws can predict general behavior such as current/voltage orders-of-magnitude and time scales, but it's hard to gain much understanding of instabilities without realistic, detailed analysis of the dynamic, often non-linear discharge process. Numerical simulations using the Tetra ELF family of computer codes have proven to be a valuable analysis tool. Primarily, we wanted to know how the switching times and the qualitative behavior of instabilities varied with different gases, geometries and external ionization sources. C_2F_6/Ar was studied because it has a region where drift velocity decreases with increasing E/N, leading to a strong negative differential conductivity. In a 1-D simulation, the portion of the discharge at the lowest E values entered the region where drift velocity Vd is insensitive to E. Thus, a small divergence in electron density quickly produced a large divergence in E. The process accelerated in the region where $\partial Vd/\partial E$ is negative, since the resulting strong negative differential conductivity makes the field suppression strongly self-aggravating. Eventually, the local field was suppressed past the maximum Vd and to that where $\partial Vd/\partial E$ is positive again. In this stable region, an equilibrium E value was quickly established which caused the current to match that in the high-field portion of the discharge. However, the transition region was never in equilibrium. The electron density varied very little. The transition was complete as soon as enough of a space charge accumulated to change the E-field. The process wound up traveling across the discharge in what can be described as a "space-charge wave."

KB-4 Electron Production and Energy Spectrum in Heavy Ion Pumped Plasmas.* Thomas J. Moratz, and Mark J. Kushner, University of Illinois--Fission fragment (FF) or heavy ion pumped plasmas are used as gas lasers. Electron production and their energy spectrum in such plasmas differs from e- beam pumped plasmas due to differences in momen- tum transfer between projectile and target. We report on calculations of electron production rates and energy spectrum in FF pumped plasmas. The flux of heavy ions (FF) coming from planar foils is calculated. Assuming continuous slowing down of the ions, their spatially averaged velo- city distribution is next obtained. Using binary Coulomb collision cross sections, the ion distri- bution is integrated to give the rate of electron production. The source spectrum of electrons pro- duced by FF's is shifted to lower energies compared to e-beam pumping. The W value for ionizations by FF's is twice that for e-beams.

*Work Supported by Sandia National Laboratory

KB-5 Electron Distributions and Excitation Rates in Heavy Ion Pumped Plasmas.* Thomas J. Moratz, and Mark J. Kushner, University of Illinois--Heavy ions, in the form of fission fragments (FF's), slowing in a gas generate an electron source spectrum shifted to lower energy compared to e-beams. Using the electron source spectrum due to direct ionization by FF's and the zero field Boltzmann equation, the electron dis- tribution function (EDF) in FF pumped plasmas has been calculated. Electron collision rates are then obtained for mixtures of $Ne/Xe/F_2$, as used in excimer lasers. Above the ionization thresh- olds the EDF is primarily determined by the source function, and at low energies by the halo- gen donor. Including direct excitation by FF's, electrons account for about the same number of excitations and ionizations as the FF's. Compar- ing to e-beam pumped plasmas, we find a higher ratio of excitation to ionization with FF's.

*Work Supported by Sandia National Laboratory

KB-6 Heavy Ion Pumping of Excimer Lasers.* Thomas J. Moratz, Todd D. Saunders, and Mark J. Kushner, University of Illinois--Fission fragment (heavy ion) generated plasmas, result in lower power deposition (1-10 kW/cm^3), longer pulse lengths (0.1-1 ms), and higher energy deposition (0.5-1 kJ/cm^3) than e-beam pumped plasmas. We report on a modeling study of fission fragment (FF) excited excimer lasers pumped by such plasmas. Excitation by FF's differs from that by e-beams. The W value for ionization is larger when pumping with heavy ions, and the fractional excitation rate is larger. The large temperature rise (100 -1000 K) reduces the rate of ion- molecule and ion-ion reactions, thereby favoring the neutral channel. Dimer and trimer ions are also reduced in relative density. The higher temperature, though, increases the rate of quenching of the exciplex.

*Work Supported by Sandia National Laboratory

SESSION LA

10:00 AM - 11:30 AM, Thursday, October 15

Space Science and Technology Center, Room 5

ELECTRON-IMPACT CROSS SECTIONS III

Chairman: J. Ajello (Jet Propulsion Laboratory)

LA-1 Electron-Impact Excitation of Molecules and Rare Gas Atoms. S. TRAJMAR, Jet Propulsion Laboratory, California Institute of Technology - Techniques commonly used to measure electron impact excitation cross sections will be briefly described. Cross section data (differential, integral and momentum transfer) concerning elastic scattering, rotational, vibrational and electronic excitations will be summarized and compared to theoretical calculations. The emphasis will be placed on recent developments and trends. Efforts and prospects for extending cross section measurements to the near threshold region will be discussed. Brief remarks on electron collision measurements involving excited atoms and molecules and on modern techniques going beyond conventional cross section measurements will be made. Cross section data for electron impact processes - with the exception of the rare gases and H_2 and N_2 - are still scarce (optical excitation functions are not considered here). The situation is especially unsatisfactory at low near-threshold energies. It seems that the accumulation of a large body of reliable cross section data requires a joint experimental and theoretical effort.

Research supported by NASA and NSF.

LA-2 Electron Collisions in the Copper Vapor Laser*, A. HAZI and K. SCHEIBNER, Lawrence Livermore Nat'l. Lab. - The population inversion in the copper vapor laser (CVL) is created by exciting the $(3d^{10}4s)^2S$ ground state of Cu to the $(3d^{10}4p)^2P$ states by electron impact. The laser lines result from transitions to the lower, metastable $(3d^94s^2)^2D$ states. No reliable cross sections exist for $E \leq 6$ eV. We have calculated ab initio electron-impact excitation cross sections[1] using a 4-state close-coupling approximation within the framework of R-matrix theory. The cross sections are found to exhibit a rich resonance structure due to Cu^- states which have been unknown previously. The elastic momentum transfer and excitation rate coefficients are shown to be markedly altered by the resonances. The calculated photodetachment cross section of $Cu^-(4s^2, {}^1S)$ reaches a maximum near the laser wavelengths. Inclusion of the new theoretical data in a time dependent kinetic model of the CVL does not completely explain the observed laser performance as a function of discharge conditions.

*Supported by DOE contract No. W-7405-Eng-48.

[1]Phys. Rev. A 35, 4869 (1987).

LA-3 The Total Electron-Molecule Scattering Cross Sections of the Methyl Halides*, A. BENITEZ, University of Maryland - The total cross sections of the methyl halides were measured for the scattering of 0.5 to 9 eV electrons. These determinations were made with an electron transmission spectrometer modified to allow precise target pressure measurements and digital data processing. The methyl halide total cross sections typically range from near 100 $Å^2$ at the lowest energies to 20 to 30 $Å^2$ at the highest. The cross sections change slowly as a function of energy suggesting that broad features observed in the derivative electron transmission spectrum are due simply to small variations in the sum of the nonresonant scattering channels.

*Supported by NSF-CHE8417759 and NSF-CHE8507732

LA-4 Electron Collision Cross Sections for CH_4 From Measured Swarm Data, L. E. KLINE, D. K. DAVIES, W. E. BIES and T. V. CONGEDO, Westinghouse R&D Center -- Electron drift velocity and ionization coefficient values have been measured and used, together with available cross section data, to determine a consistent set of collision cross sections for CH_4. Predicted values of the drift velocity and ionization coefficient from Monte Carlo simulations agree well with our measured values. Isotropic scattering is assumed for all collision processes. A total cross section for dissociation to form neutral products is obtained by subtracting measured dissociative ionization cross section values from measured total dissociation cross section values. The measured, continuous electron energy loss spectrum of CH_4 is approximated by assuming four neutral dissociation processes with thresholds at 9, 10, 11 and 12 eV. No adjustment of these measured cross section values is required in order to obtain good agreement between predicted and measured swarm parameters. The elastic and vibrational cross sections are based on previous determinations from swarm data.
Supported in part by the U. S. Army Research Office

LA-5 Cross Section Measurements in C_3F_8 and C_2H_3Cl†.

P. J. CHANTRY and C. L. CHEN, Westinghouse R&D Center.--
Total attachment cross sections have been measured in C_3F_8 between 300 and 730 K. The room temperature data peaks at 2.8 eV with a value of 1.75×10^{-17} cm^2. This is 14 times smaller than Kurepa's[1] value, and is between two more recently reported values.[2] At 730 K the peak cross section has increased by $\sim$ 60% and the threshold is lower by 1.1 eV. Our C_3F_8 positive ion data is similar to Kurepa's in shape at higher energies, but with typically half the magnitude. Curvature makes the positive ionization threshold at 13 eV difficult to locate. At room temperature C_2H_3Cl attachment has a threshold at 0.85 eV and a peak at 1.35 eV of 3.2×10^{-17} cm^2, in good agreement with previous work. At 850 K the cross section at the peak is x 2.6 larger, and lower in energy by 0.3 eV, while at 0 eV it has reached 6×10^{-18} cm^2.

† Supported in part by the U.S. Army Research Office.

1. M. V. Kurepa, 3rd Cz. Conf. Electr. Vac. Phys. (1965), p. 107.
2. S. R. Hunter and L. G. Christophorou, J. Chem. Phys. 80:6150 (1984); S. M. Spyrou and L. G. Christophorou, J. Chem. Phys. 83:2829 (1985).

SESSION LB

9:25 AM - 11:20 AM, Thursday, October 15

Space Science and Technology Center, Room 4

HIGH INTENSITY DISCHARGE LAMPS

Chairman: H. Witting (General Electric-Corporate Research Div.)

LB-1 Arc Physics in High Intensity Discharge Lamps: The Present State of the Art and Challenges for the Future. JOHN F. WAYMOUTH, GTE Electrical Products - An overview is given of arc physics phenomena in discharge lamps such as high-pressure-mercury, high-pressure-sodium, and metal halide lamps, collectively known as High Intensity Discharge (HID) lamps. These are based on LTE arcs, generally though not always wall-stabilized, in complex mixtures of gases and vapors. Their energy balances are radiation-dominated; characteristics are affected by convective, MHD, and cataphoretic flow systems. An extensive body of literature and knowledge on phenomenology, modelling, and diagnostics will be reviewed. Gaps in that knowledge offering opportunities for future R&D will be identified.

LB-2 Cataphoresis in High Intensity Discharge Lamps, J. H. INGOLD, General Electric Co., Cleveland, OH 44112. --Cataphoresis in low pressure discharges is fairly well understood from a theoretical point of view.[1] This theory is reviewed briefly. Then the major differences between low pressure and high pressure cataphoretic theory are discussed. Finally, two examples of application of high pressure cataphoretic theory to high intensity discharge lamps are presented. First, application to a high pressure sodium lamp operated on pulsed DC is discussed, and theoretical results are shown to be in good qualitative agreement with observation. Second, application to a metal halide lamp operated on AC is discussed, and theoretical results are also shown to be in qualitative agreement with observation.

[1] C. C. Leiby, Jr. and H. J. Oskam, Phys. Fluids 10, 1992 (1967); H. J. Oskam, ibid. 12, 2449 (1969); J. H. Ingold and H. J. Oskam, ibid. 27, 214 (1984).

LB-3 Models of 2-D and 3-D Convective Effects in High Pressure Mercury Discharges without and with Additives, J.T. Dakin and W. Shyy, GE Corporate R&D - First-principles models have been developed to predict the radiation, electrical, chemistry and fluid behavior of a high pressure discharge from a specification of its arc tube geometry, Hg and additive doses, and power input. These 2-D and 3-D models assume local thermodynamic equilibrium and steady power loading. They derive from axisymmetric 1-D models which have been reported earlier.[1,2] Results are discussed for 400 W discharges and Hg pressures of several atmospheres. Calculations for vertical arc tubes with and without metal halide additives show that the convective velocity profile shapes are not significantly impacted by the additives. When the axis of the arc tube is declined from 0° through 45° to 90° relative to the vertical, 3-D convective patterns are shown to evolve which dramatically impact the discharge shape.

1 JT Dakin and RP Gilliard, J. Appl. Phys., 60, p. 1281 (1986)
2 JT Dakin and RP Gilliard, J. Appl. Phys., XX, p. XXXX (1987).

LB-4 *A Simple Lineshape Model for Radiation Transport Calculations in High Intensity Discharges*, P.A. VICHARELLI and W.P. LAPATOVICH, *GTE Laboratories Incorporated, Waltham, MA* -- We present a simple analytic model for bridging the gap between asymptotic treatments of collisionally broadened lineshapes. Such lineshapes may be expressed as generalized Lorentzians with detuning dependent widths which are well characterized in the line core and the line wings by the impact and the static approximations, respectively.[1] However, these approximations are valid only when the detunings are much less or much greater than the inverse of the characteristic collision duration. In this work we connect these asymptotic limits through switching functions. These functions turn on the proper frequency dependence in one detuning region while suppressing the other. Radiation transport calculations carried out with this model are in excellent agreement with line of sight lineshape measurements in high pressure mercury arcs.

1. G. Peach, J. Phys. B 17, 2599 (1984); J. Phys. B 20, 1175 (1987).

LB-5 Deviations from Excitation Equilibrium in the Hg 6^3P Levels in a High Pressure Arc. * D. KARABOURNIOTIS AND S.COURIS, University of Crete, Physics Department - The nonequilibrium excitation in the Hg 6^3P_1 resonance level in 50-Hz ac mercury arc (≈2 bar) has been determined vs the time and the radius during the half a period of the arc current. The spectroscopic technique proposed by Karabourniotis[1] has been used. The Hg $6^3P_{2,0}$ metastable levels have been also measured at the moments of minimum (0 ms) and maximum (5 ms) current intensity. It was found that : i) the 6^3P_1 level is in equilibrium at 0 ms and its maximum deviation occurs at 5 ms; ii) it is underpopulated on the axis and overpopulated in the periphery; iii) its density exhibits a modulation out of phase with that of the high lying 6^3D_2 level and in phase with the T_{el} and presents a maximum at ≈2 ms; iv) the $6^3P_{2,0}$ levels on the axis are overpopulated at 0 ms and underpopulated at 5 ms.

*Research supported by the Greek Ministry of R & T

[1]D. Karabourniotis, Opt. Commun., 61, 38 (1987).

LB-6 Pinpoint Laser Absorption Measurement of Sodium Density in a Metal-Halide Lamp. G. Allen, GTE Electrical Products, Danvers, MA - We previously reported measurement of the radial profile of ground state sodium atoms in a metal-halide lamp using laser absorption spectroscopy. [1] The major shortcomings of those measurements, inherent to the Abel inversion of the chord-integrated data, were the assumption of axisymmetry and the accumulation of data errors toward the axis. To avoid the Abel inversion, an improved pinpoint laser absorption technique has been developed in the metal-halide lamp using a strong, modulated pump beam to modulate the absorption signal on an intersecting, weak probe beam to measure the density of absorbers in the intersection volume. This follows the original development of the technique in a low pressure discharge. [2] The pinpoint technique has a particular advantage in the case of the hollow profile of sodium atom density where the noise on the Abel-inverted data obscured the weak signal at the discharge axis.

[1] G. Allen, L. Lagushenko, J. Maya, W. Keeffe, J. of the Illum. Eng. Soc. 16, p. 13 (August, 1987)
[2] P. Moskowitz, Appl. Phys. Lett. 50, p. 891 (1987)

LB-7 Pulsed Laser Optogalvanic Spectroscopy of Scandium and Sodium in a High Pressure Metal Halide Discharge. JERRY KRAMER GTE Labs --Pulsed laser irradiation of a high pressure metal halide discharge tuned to excite Hg and the metal additives, sodium and scandium, produced negative optogalvanic signals. Optogalvanic signals resulted from excitation of ground state Na atoms at 589 nm, from excitation of both ground and excited state Sc atoms throughout the visible, and from excited states of Hg. The optogalvanic spectrum was very similar to the emission spectrum, except for the absence of self-reversal in the optogalvanic spectrum. In contrast to Hg the optogalvanic signals for ground state Na and Sc were linearly dependent on the laser intensity. Vertical segregation of Na and Sc was evident from the axial variation of the optogalvanic signals. Increasing the envelope temperature and hence, the vapor pressures of the additives (by raising the input power to the discharge) increased the optogalvanic signals from ground state Na and Sc. This result suggests that optogalvanic spectroscopy could be developed as a diagnostic for determining the effect of fill variations on the additive concentrations which are present in the discharge.

SESSION MA

1:30 PM - 3:25 PM, Thursday, October 15

Space Science and Technology Center, Room 5

ELECTRON-IMPACT CROSS SECTIONS IV

Chairman: W. Blumberg (Air Force Geophysics Laboratory)

MA-1 Measurements of Electron-Impact Ionization Cross Sections for Ions. R.A. PHANEUF, ORNL*--The direct ejection of an outer-shell electron is the dominant mechanism for electron-impact ionization of ions in the lower ionization stages. As the initial ionic charge becomes larger, however, indirect mechanisms involving inner electron shells play an increasingly important role. For initial charge states as low as +3, inner-shell excitation followed by autoionization can dominate the total ionization cross section in some cases by more than an order of magnitude. Such effects are not included in the semi-empirical formulae widely applied in plasma modelling, and can significantly alter the ionization balance in even relatively low-temperature plasmas. Examples will be presented which illustrate the signatures and relative roles of these ionization mechanisms in total cross sections for electron-impact ionization of ions.

*Operated by Martin Marietta Energy Systems, Inc., under contract DE-AC05-84OR21400 with the U.S. Department of Energy.

MA-2 Electron-molecule Cross Sections and Temporary Negative Ion Studies*, P.D. BURROW, U. of Nebraska, Lincoln -- Temporary negative ion formation and the attendant decay processes play an important role in a number of 'gaseous electronic' environments. Recently, molecules of considerable complexity, such as hydrocarbons with halogen substituents, have been employed for various purposes in discharges. Aside from the immediate need for data about molecules of topical importance, electron scattering studies and cross section measurements are required to advance our understanding of resonances in complex species. Following a brief review of the systematics of resonances,[1] examples of temporary negative ions in several prototypical molecules will be discussed. The influence of geometry changes on resonance energies and decay channels will be emphasized.

*This work was supported by NSF.

[1]K.D. Jordan and P.D. Burrow, Chem. Rev., June 1987.

MA-3 Electron Impact Phenomena Using Quasi-Free Electrons. T.J.MORGAN, Wesleyan U.,Middletown,CT--Recent experiments using keV energy highly excited Rydberg atoms and molecules as carriers of electrons have demonstrated under a variety of conditions that a weakly bound Rydberg electron in the kinetic energy region 1-20 eV reproduces free electron scattering phenomena.[1] Absolute cross sections for total scattering have been measured in Ar, N_2, Co_2, and SF_6. The results confirm the quasi-free electron[2] picture and demonstrate incoherent scattering by the core and Rydberg electron.[3] As the excitation of the atom is decreased the core will eventually influence the electron impact collision modifying the scattering behavior.[3,4] The present experimental technique is extendable to both higher and lower electron collision regimes and may prove useful to compliment electron impact experiments.

1 L.J.Wang, M.King, and T.J.Morgan, J.Phys. B19, L623 (1986). See also P.M.Koch, P.R.L. 43,432 (1979)
2 M.Matsuzawa, J.Phys. B13, 3201 (1980)
3 J.H.McGuire, N.Stolterfort, and P.R. Simony, Phys. Rev. A24, 97 (1981); J.M.McGuire, Bull. Am. Phys. Soc. 32, 1256 (1987)
4 M.R. Flannery, Phys. Rev. A22, 2408 (1980)

MA-4 Measurements of Positron- and Electron-Alkali Atom Total Scattering Cross Sections.* T.S. STEIN, M.S. DABABNEH, W.E. KAUPPILA, C.K. KWAN, AND Y.J. WAN, Wayne State U.--A beam transmission technique[1] has been used to measure (from 4 eV to 102 eV) total cross sections for positron- and electron-potassium and for electron-sodium collisions. The measured positron- and electron-K total cross sections are observed to merge near 30 eV and above, whereas at lower energies, the positron cross sections are larger than the corresponding electron values. A merging of positron- and electron-atom total cross sections at such low energies has not been observed for any other atoms (or molecules).[2] This may be at least partially related to the relatively large polarizability of potassium which could result in the polarization interaction overwhelming the static interaction. Comparisons are made with prior electron measurements and with theoretical calculations for positrons and electrons.

*Research supported by the NSF.

[1]T.S. Stein et al., Phys. Rev. Lett. 55, 488 (1985).
[2]T.S. Stein and W.E. Kauppila, to appear in Atomic Physics with Positrons, edited by J.W. Humberston (Plenum, New York and London, 1987-88).

MA-5 Electron-Noble-Gas Spin-Flip Scattering at Low Energy*, T.G. Walker, K.D. Bonin, and W. Happer, Princeton University. The spin-exchange rates and spin-relaxation rates for thermal electrons colliding with noble-gas atoms are calculated using the orthogonalized- plane-wave approximation and via partial wave analysis. The two techniques give similar results and are in order-of-magnitude agreement with the experimental rate in Ar[1]. For most conditions the spin-exchange rates are negligible but the spin-relaxation rates can be important for optically pumped plasmas of the heavier noble gases Ar, Kr, and Xe[2].

*Research supported by ARO.

[1]H.G. Dehmelt, Phys. Rev. 109, 381 (1958).

[2]T.G. Walker, K.D. Bonin, and W. Happer, Phys. Rev. A 35, 3749 (1987).

SESSION MB

1:30 PM - 3:25 PM, Thursday, October 15

Space Science and Technology Center, Room 4

MICROSCOPIC MODELING OF DISCHARGES

Chairman: J. P. Boeuf (Universite Paul Sabatier)

MB-1 Behavior of Electron Swarms in Methane and Monosilane, H. TAGASHIRA, Hokkaido University, Japan - The electron swarm behavior in methane and monosilane was studied for E/p_0 from 0.2 to 200 V cm^{-1} $Torr^{-1}$ by a two-term Boltzmann equation method and a Monte Carlo simulation method. The results show that it is possible to find a set of collision cross sections which represents the experimental swarm parameters well for either of the gases. The value of the electron drift velocities is shown to differ for different modes of observation of electron swarms[1] at high E/p_0, and experimental characteristic energy at high E/p_0 in methane is shown to be represented well if the difference of the modes is considered. The accuracy of the two-term Boltzmann analysis is found to lower at around E/p_0=1 V cm^{-1} $Torr^{-1}$. The electron energy distribution in monosilane is found very similar to Druyvestyn distribution. In the analysis, the vibrational cross section for monosilane was assumed similar to that of methane because of no available data. A search for more appropriate cross section may be necessary.

1. H. Tagashira, Invited Papers of 15th International Conference on Phenomena in Ionized Gases, 377-394 (1981)

MB-2 Monte Carlo Calculations of Electron Transport in CH_4 with Anisotropic Scattering, L. E. KLINE, W. E. BIES and T. V. CONGEDO, Westinghouse R&D Center -- The measured differential cross sections for elastic scattering, dissociation and ionization in CH_4 are strongly forward peaked. Total and differential cross section data from the literature are used as the input data for Monte Carlo calculations of electron transport in CH_4. The differential cross section shapes are used to determine the scattering probability vs. angle and energy. The measured, continuous electron energy loss spectrum of CH_4 is approximated by assuming four neutral dissociation processes with thresholds at 9, 10, 11 and 12 eV. Cross section values which are consistent with the experimental cross section data result in predicted swarm parameter values (drift velocity, diffusion coefficient/mobility and ionization coefficient) which agree with experiment. The vibrational cross sections are based on previous determinations from swarm data which assumed isotropic scattering. A 30% increase in these vibrational cross sections is needed to correctly predict the swarm data.

MB-3 Monte Carlo Simulation of Ion Transport Through rf Glow-Discharge Sheaths, BRIAN E. THOMPSON AND HERBERT H. SAWIN, Massachusetts Institute of Technology - Ion transport was simulated to determine the distributions of ion-bombardment energy and angle of impact. Several sheath parameters were examined: 1) the type of ion-molecule scattering (hard sphere, potential-field interaction, and charge exchange), 2) the ion to neutral mass ratio, 3) the ratio of the sheath width to collision mean-free-path, 4) spatially-uniform, spatially-linear, and time-dependent (rf) electric fields in the sheath, and 5) the frequency of an rf component in the sheath. The results of the Monte Carlo simulations indicate that the type of elastic scattering does not significantly change either the impact-angle distributions or the scaled ion-bombardment energy distributions. The fully-developed distributions depend only on the ion-to-neutral mass ratio, type of ion-neutral scattering, and the dc value of the electric field-to-pressure ratio at the electrode. Fully-developed distributions are reached in approximately 3 mean-free-paths in spatially-uniform sheath fields and in about 6 mean-free-paths for spatially-linear sheath fields.

MB-4 Transient and Steady State Electron Energy Distribution Functions obtained with a Monte Carlo Flux Code,* P. HUI AND G. SCHAEFER, Weber Research Institute, Polytechnic University - Monte Carlo calculations of electron energy distribution functions have the disadvantage of a poor resolution in the wings of the distribution. These are of specific importance to calculate the onset of collision rates for inelastic processes. A significant improvement is achieved with the Monte Carlo Flux method. In this method a Monte Carlo code is used to calculate the particle flux from one phase cell to any other for a constant time interval. The resulting transition matrix can then be used to calculate steady state distribution functions and transient distribution functions starting with a given initial condition. Examples of electron energy distribution functions in Nitrogen (steady state and transient) will be presented and compared with results obtained with a conventional Monte Carlo code.

* Research supported by NSF.

MB-5 Modeling of Gas Discharges During Transients in Complex Geometries.* Mark J. Kushner, University of Illinois--Gas discharge devices, such as lasers, switches, and plasma processing reactors, are usually transient and have non-planar geometries. To accurately model these devices, methods must be chosen which are appropriate to the time and spatial scales of interest, and correlation must be made between microscopic and macroscopic processes (eg. ioni- zation and circuit parameters). In this paper, the optimum choice of modeling techniques will be discussed for transient discharges in complex geometries. Particle simulations and continuum models will be compared for appropriateness, with examples chosen from both low pressure (eg., thyratrons, RF discharges) and high pressure devices (eg., lasers, spark gaps). The importance of accurate initial and boundary conditions for such models will be discussed.

*Work Supported by NASA, ARO, DOE, and ONR

MB-6 Electron Energy and Vibrational Distribution Functions in High-Frequency N_2 Discharges*, C.M. FERREIRA AND J. LOUREIRO, Lisbon Tech.U. - The electron energy distribution function, transport parameters and excitation rates, and the vibrational distribution of $N_2(X,v)$ molecules in hf N_2 discharges at pressures 0.1-1Torr were calculated self-consistently by solving the Boltzmann equation along with the rate balance equations for the v-levels. These calculations extend those recently carried out for dc discharges[1] and the effects resulting from the changes in ω are analysed in detail. The formulation involves three independent parameters, a reduced effective field E_e/N, the ratio ω/ν_{ce}, where ν_{ce} is a representative value of the collision frequency for the bulk of electrons, and the degree of ionization, n_e/N. The values of n_e/N required to produce a given characteristic vibrational temperature, T_V, increase as ω/ν_{ce} increases. This follows from the fact that the electron fractional power transfer into vibrational excitation decreases while that into electronic excitation increases in going from $\omega/\nu_{ce} \ll 1$ to $\omega/\nu_{ce} \gg 1$.

*Work supported in part by NATO RG 105/87.

1 -J. Loureiro and C.M. Ferreira, J. Phys.D 19, 17(1986)

SESSION NA

3:45 PM - 5:15 PM, Thursday, October 15

Space Science and Technology Center, Room 5

LASER KINETICS

Chairman: K. Y. Tang (Western Research Corporation)

NA-1 UV Excimer Radiation from Dielectric-Barrier Discharges. B. ELIASSON AND U. KOGELSCHATZ, Brown Boveri Research Center, 5405 Baden/Switzerland - The current flow in dielectric-barrier discharges at about atmospheric pressure is maintained by a large number of statistically distributed microdischarges of submicrosecond duration. Each microdischarge can be described as a transient high pressure glow discharge with adjustable electron energies of the order 10 eV and gas temperature close to room temperature. These microdischarges provide a controlable environment for the formation of rare gas excimers. In pure xenon we obtained the VUV radiation of the Xe_2 excimer peaking at 172 nm (half width: 12 nm). The efficiency of the UV output was determined by O_2-and N_2O-actinometry and reached values of 7-9%. For the discharge in xenon we present a model that calculates the different physical and chemical processes in a microdischarge. It can predict UV efficiencies as a function of the discharge parameters. In other gas mixtures excimer radiation was obtained at 147 nm (Kr_2^*), 248 nm (KrF^*) and 308 nm ($XeCl^*$). Our experiments show that it is possible to build rather efficient UV sources with substantial UV output with a simple discharge device. Different discharge geometries will be discussed.

NA-2 Photoabsorption Measurement of Ar_2F Excimer at 248 nm, K. HAKUTA, S. MIKI, T. SUGOH, AND H. TAKUMA, University of Electro-Communications - In order to quantitatively design the e-beam pumped KrF laser medium, it is essential to know accurately the photoabsorption cross-section at lasing wavelength for triatomic excimers such as Kr_2F or Ar_2F. In this work, we report on the first direct photoabsorption measurement of Ar_2F at 248 nm. The photoabsorption was monitored by observing the fluorescence suppression induced by KrF laser; the same technique described for Kr_2F measurement.[1] In contrast to the results for Kr_2F, it is found that the fluorescence suppression sharply decreases by increasing the Ar pressure, which leads to a conclusion that the photoabsorption process is a photo-dissociation process and the dissociated products are rapidly converted to Ar_2F. The dissociation process and its cross-section are presented.

[1]K. Hakuta et al., J. Appl. Phys. 61, 2113 (1987).

NA-3 Electronic Structure and Photoabsorption Characteristics of Ar_3^+,* H. H. MICHELS, UTRC ---- A study of the electronic structure of the ground and low-lying excited states of Ar_3^+ and the photoabsorption characteristics of this trimer ion has been carried out using accurate quantum mechanical methods. We find that the most stable geometry for the ground state of this ion is a non-symmetric linear structure, in contrast to the symmetric linear form predicted by Wadt[1] and Turner and Conway[2], and the trigonal form predicted in our earlier studies[3]. Our new results show that Ar_3^+ has $C_{\infty v}$ symmetry with R_1 = 2.56 Å (close to Re for Ar_2^+) and R_2 = 2.79 Å, suggesting that Ar_3^+ is a cluster ion of Ar + Ar_2^+. The photoabsorption cross-section peaks near 550 nm and is predicted to be broad (450 — 700 nm) and comparable in strength to the Ar_2^+ $^2\Sigma_u^+ \rightarrow {}^2\Sigma_g^+$ transition.

*Supported in part by AFOSR under Contract F49620-85-C-0095.

W. R. Wadt, Appl. Phys. Lett. 38 1030 (1981).
D. L. Turner and D. C. Conway, J.C.P. 71, 1899 (1979).
H. H. Michels, et al, Appl. Phys. Lett. 35 153 (1979).

NA-4 Experimental Determination of the Einstein Coefficients for the N_2(B-A) Transition,* L.G. PIPER, K.W. HOLTZCLAW, and B.D. GREEN, Physical Sciences Inc., Andover, MA, 01810, and W.A.M. Blumberg, Air Force Geophysics Laboratories, Hanscom AFB, MA, 01730 -- We have used a branching ratio technique to measure the relative variation in the transition dipole moment with internuclear distance for the N_2(B-A) transitions. Our spectral observations cover the range from 500 to 1800 nm using several different detectors and excitation sources. In the regions of spectral overlap, the data are consistent from one set to another. Using well established values for the radiative lifetimes of N_2(B, v'>3) allows the relative dipole moment function to be placed on an absolute basis. From the dipole-moment function and a set of RKR-based Franck-Condon factors which we have computed, we derive Einstein coefficients covering the range v'=0-12 and v"=0-19.

* Sponsored by the Air Force Office of Scientific Research and the Defence Nuclear Agency.

NA-5 A Chemical Process Showing Laser Gain in the Visible Region. S. H. COBB, R. WOODWARD, AND J. L. GOLE, School of Physics, Georgia Institute of Technology, Atlanta, Georgia 30332 - We have been concerned with the study of sodium cluster-halogen atom reactions (Na_n + Cl,Br,I) in the low pressure "single collision" pressure regime. The Na_3 - X (Cl,Br,I) metatheses are found to produce Na_2 with sharp, bimodal, excited state vibrational distributions, the fluorescence from these states resembling that characterizing optically pumped alkali dimer lasers. Laser gain studies demonstrate the presence of a population inversion involving several excited state levels of Na_2. An explanation is provided for this extremely efficient inversion process at very low pressures.

NA-6 A Chemically Driven Visible Laser Using Fast Near Resonant Energy Transfer. R. WOODWARD, S. H. COBB, and JAMES L. GOLE, School of Physics, Georgia Institute of Technology, Atlanta, Georgia, 30332 - We report the first visible chemical laser system based on an efficient near resonant energy transfer involving metastable excited states of germanium monoxide, formed in the reaction of germanium atoms with ozone, and $X^2P_{\frac{1}{2}}$ ground state thallium atoms. This energy transfer populates the thallium $^2S_{1/2}$ excited state creating a population inversion with respect to the upper $X^2P_{3/2}$ component of the ground ^2P thallium atom configuration. We have observed superradiance associated with the thallium $7^2S_{\frac{1}{2}}$-$6^2P_{3/2}$ transition whose duration in a self-terminating system is 5ns FWHM.

SESSION NB

3:45 PM - 5:30 PM, Thursday, October 15

Space Science and Technology Center, Room 4

ARCS

Chairman: A. Bhattacharya (General Electric-Lighting Bus. Group)

NB-1 The Electrical Conductivity of Non-ideal Plasmas, R. J. ZOLLWEG AND R. W. LIEBERMANN,* Westinghouse R&D Center - Plasmas of high electron density but relatively low temperatures are called non-ideal because the Debye representation of electron screening of ionic Coulomb potentials becomes inaccurate in that domain. Such plasmas exist in some electromagnetic launch armatures, arc heaters, and MHD generators, as well as potentially other pulsed power devices. The well-known Spitzer formula for the electrical conductivity of fully ionized gases is no longer valid. We have developed a modified formula that is valid in the fully-ionized, non-ideal plasma domain. In addition, a rigorous method of calculating electrical conductivities in partially ionized gases in both ideal and non-ideal plasmas is described. These models are based on the classical Chapman-Enskog approximation with the superposition of binary collisions without the assumption of additional electron scattering mechanisms, such as scattering by plasma oscillations. Good agreement with experiment is obtained in the non-ideal region.

*Now at GTE Lighting Products Bus., Danvers, MA 01923

NB-2 On The Transition Probability Scale Modification of Ar I,* A. SEDGHINASAB and T. L. EDDY, Georgia Institute of Technology - Present transition probability data for Ar I have a scatter of about factor of 2, which is much larger than their stated uncertainties. Detailed arc experiments in argon at 30A and various pressures (0.1 - 10 bars) have been performed and analyzed using the Generalized Multithermal Equilibrium (GMTE) method to determine the extent of non-LTE, as well as the onset of the LTE condition. Numerous neutral spectral lines have been measured at each pressure to yield precise upper level excitation temperatures (T_{exp}). The intensity data are corrected for self-absorption and line wings by appropriate techniques. Results indicate that the corrections to the transition probability values are strong functions of the upper level energies. This is apparently due to the neglect of non-LTE effects in the 1-atm arc experiments used to determine the previous transition probability values.

*Sponsored in part by NSF Grant CPE 8311325.

NB-3 Transient and Quasi-Steady non-LTE Diagnostics of a Rotating Argon Arc,* R.V.Frierson and T.L.Eddy, Georgia Institute of Technology - Absolute line emission spectroscopy, Stark broadening of $H\beta$, and the generalized multithermal equilibrium (GMTE) model[1] were used in the non-LTE diagnostics of an argon DC arc. The arc was rotated around circular electrodes by a superimposed rotating magnetic field, thus creating a plasma nozzle [2,3]. Quasi-steady time averaged intensity measurements across the channel suggest a state close to LTE; however transient measurements of the arc proper as it rotates around its trajectory shows the true non-LTE state, as evidenced by discrepancies in the electron density derived from LTE and that from $H\beta$.

*Sponsored in part by NSF Grant CPE-8311325.

1. A.Sedghinasab & T.L.Eddy, 18th ICPIG, (1987)
2. R.V.Frierson, et al, Rev. Sci. Inst., 57, 2096, (1986)
3. R.V.Frierson & T.L.Eddy, ISPC8, (1987)

NB-4 An Investigation of the Pulsed Cesium-Mercury-Xenon Arc. H.L. WITTING, GE CORPORATE RESEARCH, SCHENECTADY, NY - An arc discharge was operated in a Cs-Hg-Xe gas mixture at a total pressure of approximately 40 kPa. Current pulses of 420A, 0.7 joules and 2 micro-sec were superimposed on a DC discharge. Spectral and temporal measurements were made of the light output from the discharge. An analysis of the power input and heat capacity of the discharge gas shows that at the conclusion of the current pulse the gas is essentially fully ionized. During the following 40 micro-sec, the cooling plasma radiates the absorbed energy strongly in a series of oscillations[1].

[1] H.L. Witting, Bull. Am. Phys. Soc. II, 197 (1977).

NB-5 An effect of Mixing Plenum and Hydrogen Concentration on the Downstream Temperature Profiles of DC Plasma Torch in Ar-H_2 Mixture Gas Plasmas, I.Ishii, J.S. Chang, McMaster University, F.Y. Chu, Ontario Hydro
The effect of hydrogen percent mixture and mixing plenum on the gas temperature and its profiles of an Acrax DC 80 kW plasma torch have been investigated by the relative intensity method via emission spectra. Assuming local thermal equillibrium (LTE) in a reagon studied, local temperatures were determined by means of the Abel inversion. The H_α and H_β emission lines were chosen for the determinations, where radially and axially movable OMA system located downstream of the torch exit is used for the present diagnostics. In order to study the effect of a mixing plenum, which is utilized under powder injection experiments, the emission spectra were taken with and without the plenum. The results show that: 1) Gas temperature increases with increasing torch input power; 2) Gas temperature decreases with increasing H_2 concentrations and decreasing gas flow rate; 3) The effect of gas flow on the gas temperature increases with increasing input power; 4) Relatively uniform gas temperature region has been observed near the exit of plasma torch; 5) Significant mixing plenum effect on the gas temperature and its radial profile have been observed.

NB-6 **Temperature Measurements of a Free-burning Plasma Arc by a Combination of Holographic Interferometry and Emission Spectroscopy, A. SHAH, M. S. DASSANAYAKE, AND K. ETEMADI, State University of New York at Buffalo** - **The temperatures of a free-burning, high-intensity arc have been measured spectroscopically above 8000 K while the lower temperatures have been determined by off-axis double exposure holographic interferometry. The isotherms of the atmospheric argon arc are given at an electrode spacing of 1 cm covering a 4 cm radius area around the axis of the arc. A comparison between the numerical model which is based on the solution of a set of conservation equations (continuity, momentum, energy, and electron continuity) and the experimentally obtained data is presented. The effect of a shrouding gas which is injected from a cathode port for plasma stabilization on the plasma arc is shown on interferograms.**

NB-7 INVESTIGATION OF ARC ROOT IGNITION ON OXIDIZED CATHODES K. P. Nachtigall, Ruhr-U. Bochum, FRG.- Experiments on Cu_2O- films over a thickness range of some nm up to 200nm in air at atmospheric pressure are described in this work. An arc is blown magnetically against a cathodic electrode, which is inserted into the discharge vessel.A linear voltage ramp is applied to the arc plasma in front of the electrode. The time the arc needs for igniting new arc roots on the cathode surface was registrated. Short times in the range of some us up to 200us and also very long times of more than 500us could be observed in most of the measurements. The investigations were supplied by smear camera and electron microscopical records.

NB-8 Control of Surface Melting and Ablation via the MVS Mechanism: Proof-of-Principle Device*, O. HANKINS, O. AUCIELLO, M. BOURHAM, J. GILLIGAN, and B. WEHRING, NCSU - A device to verify the Magnetic Vapor Shielding effect[1] has been constructed. Its purpose is to demonstrate a decrease in the high heat flux erosion of a material surface due to the presence of a strong parallel magnetic field. The device consists of a plasma discharge source, magnet, and vacuum system. The source is a plasma gun discharged by a high-energy-density capacitor of up to 15 kJ of stored energy. The resultant current pulse has a FWHM of 25 μs and a peak current of 100 kA. The plasma has a blackbody temperature of 1-10 eV. The magnetic field is supplied by a pulsed liquid-nitrogen-cooled solenoid which can produce pulsed (8 ms FWHM) magnetic fields of up to 20 T. Diagnostics include Rogowski coils, magnetic probes, and an optical MCA. Initial results suggest that ablation due to high heat flux is changed by high parallel magnetic fields.

*Research supported by Grant ARO DAAL03-86-K-0029.
[1]J. G. Gilligan and D. H. Hahn, Journal of Nuclear Materials, 145-147 (1987), 391-395.

PLENARY SESSION 0

8:00 AM - 9:55 AM, Friday, October 16

Space Science and Technology Center, Rooms 3-5

MACROSCOPIC MODELING OF DISCHARGES

Chairman: V. Godyak (GTE Electrical Products)

O-1 MODELING OF A D.C OXYGEN GLOW DISCHARGE: COMPARISON WITH MEASUREMENTS* , C.M.FERREIRA', G.GOUSSET,M.TOUZEAU AND M.VIALLE, Lab. Phys. Gaz et Plasmas, U.Paris-Sud, Orsay, France--A kinetic model for the Oxygen glow discharge has been developed that predicts the radially averaged concentrations of electrons,O^- ions, atoms, ozone and $O_2(a^1\Delta)$ metastables as a function of the reduced field ,E/N,and the discharge current, I. The calculated concentrations of O and $O_2(a^1\Delta)$ range from about $5\ 10^{14}$ to $5\ 10^{15}$ cm^{-3} for pR-0.2-2 torr.cm and I-10-80mA and agree very well with V.U.V. absorption measurements[1,2]. The predicted relative concentration $[O^-]/n_e$ is in the range 0.4-0.8 under the same conditions. Additonally the continuity equations for the dominant charged species, O_2^+, O^- and e were solved subject to appropriate boundary conditions and the radial density distributions of these species were consistently calculated as a function of the operating parameters. The predicted discharge characteristic of E/N vs. NR which follows from the solution to the above boundary value problem disagrees with the experiment indicating that the ionization rate in the discharge is about an order of magnitude higher than that determined in swarm experiments.

*Work supported by CNRS-PIRSEM.

'Permanent address:Centro de Electrodinamica, Lisbon Tech. U., Portugal

1-G.GOUSSET et al.-Bull. Am. Phys. Soc. 32,1154,(1987)
2-G.GOUSSET et al.-Plasma Chem. and Plasma Process(1987, to appear)

O-2 A Model for Electron Beam Sustained Glow Discharges for Plasma Etching Applications. AJIT P. PARANJPE AND SIDNEY A. SELF, Stanford University - In this continuum formulation the discharge properties are obtained for a specified electron beam current and discharge current. Continuity and Poisson's equation are reduced to a second order differential equation for the electric field, for efficient solution. The ionization rate is obtained from a self consistent solution of the electron energy balance equation.

Anisotropic etching of SiO_2 using large area electron beam enhanced etching[1] may be explained on the basis of this model. A static DC field that draws neutralizing ions from the plasma to the substrate is set up, so that the total ionization (by beam and plasma electrons) is adequate to supply the required ion flux.

[1] P.K. Boyer, T. Verhey and J.J. Rocca, Paper K3.2, Proc. MRS Spring Meeting, April, (1987).

O-3 Explicit Finite-Difference Methods for Time-Domain Modeling of Low Pressure RF Glow Discharges*, M. S. BARNES, T. J. COTLER, M. E. ELTA, University of Michigan- Two explicit finite-difference schemes have been developed for the self-consistent numerical modeling of rf glow discharges at low pressures[1,2]. These differencing schemes are based on those used to solve the transport equations for semiconductor IMPATT diodes[3,4]. Results from these models will be presented and compared for argon glow discharges at various pressures (i.e., 500 mT and below). The timestep/spacestep limitations and boundary/initial conditions necessary to incorporate each method into a self-consistent simulation will be discussed. Molecular rf glow discharge modeling using these numerical techniques will also be discussed.

*Research supported by SRC.
[1]M.S. Barnes et al, J. Appl. Phys, 61(1), 81 (1975)
[2]M.S. Barnes et al, submitted to J. Comp. Phys.
[3]P.A. Blakey et al, IEEE Trans. ED-26, 1718 (1979)
[4]R.K. Mains et al, IEEE Trans. ED-30, 1327 (1983)

O-4 Fluid Models and Diagnostics of Glow Discharges: Prospects and Problems. D.B. GRAVES, G.M. JELLUM, M. SURENDRA, and K.E. HUFFSTATER, University of California, Berkeley - Fluid models of low pressure gas discharges are becoming popular as a means of understanding the self-consistent couplings and interactions that dominate gas discharge dynamics. A brief overview of problems commonly encountered using fluid equations will be presented, including boundary conditions, obtaining stable numerical solutions and the use of a graded mesh in the finite difference or finite element solution of the equations. Emphasis will be on the likely uses of fluid equation simulations and the importance of comparing simulation results to experimental measurements. As an example of the latter, a summary of recent comparisons between simulations results and diagnostics of a dc negative glow discharge will be presented. Diagnostics employed include spatially resolved optical emission spectroscopy, laser-induced fluorescence and electrostatic probes.

O-5 A Numerical Model of rf Glow Discharges. J.-P. BOEUF, CNRS, Université Paul Sabatier, Toulouse, France. - The space time distributions of charged particles and electric field in rf discharges have been calculated self-consistently in Helium and in a model electronegative gas in the frequency range 50 kHz-10 MHz at 1 torr. The model is based on numerical solutions of the continuity and momentum transfer equations coupled with Poisson's equation. The electron kinetics is assumed to be in equilibrium with the electric field; the validity of the model is therefore limited to frequencies less than the electron energy exchange frequency. In spite of this limitation, the model simulates very well the well known properties of rf discharges, eg: oscillations of the sheaths, increase in the current-voltage phase-shift and decrease in the maximum sheath thickness with increasing frequency. Moreover, in the case of electronegative gases, the model predicts the formation of double layers at the plasma-sheath boundary, for frequencies of the order and less than the ion plasma frequency, in agreement with recent experimental measurements[1,2].

[1]R.A. Gottscho and C.E. Gaebe, IEEE Trans. Plasma Sc. PS-14, (92) 1986

[2]R.A. Gottscho, to appear in Phys. Rev. A 1987

O-6 Schottky Theory of the Rectangular Positive Column, J. H. INGOLD, General Electric Co., Cleveland, OH 44112. --Experiments show that a low pressure discharge will not fill a rectangular tube with aspect ratio (width/height) greater than 3:1.[1] Previous theoretical work relates this "contraction" to two-stage ionization, but gives little physical insight. In the present work, numerical solutions of two, coupled, partial differential equations for electrons (ions) and excited atoms in a rectangular positive column are presented. Predicted variation of mercury line intensity at 436nm with lateral position agrees with measurements for a 5cm by 2cm discharge tube. The relative half-width at half-maximum density of the lower mercury resonance state is chosen as the measure of arc spreading. Predicted variation of this measure with discharge parameters, such as aspect ratio, current, etc., is also presented.

[1] J. O. Aicher and E. Lemmers, Illum. Engng. 52, 579 (1957);55, 39 (1960).

O-7 Theory of Positive and Negative Electrical Corona in Electronegative Gases, R. MORROW, CSIRO Division of Applied Physics, Sydney, Australia.--The methods of obtaining time dependent solutions of space-charge dominated drift and diffusion equations appropriate to point plane discharges are outlined. The equations to be solved simultaneously are the continuity equations for electrons, positive ions and negative ions, and Poisson's equation. The effects included are ionization, photoionization, attachment, recombination, drift, electron diffusion and photoemission from the electrodes. Solutions are presented for both positive and negative polarity points in oxygen at 50 torr. For the negative point plane we explain the formation of the Trichel pulse with a step on the leading edge. This step is due to the independent action of secondary electrons due to photons and secondary electrons due to ions.[1] Thus we can in principle measure the parameters for these two processes independently. For the solution of the positive point plane problem we introduce a new implicit form of the F.C.T. algorithm[2], which allows the use of a very fine mesh near the anode inorder to resolve the detail of the anode sheath. Preliminary solutions show the development of a steady positive glow corona for a positive point, rather than the pulsed corona found with the negative point.

1. R. Morrow, Phys. Rev. A., 32, 3821 (1985).
2. P. Steinle and R. Morrow, to be published.

PLENARY SESSION P

10:30 AM - 12:10 AM, Friday, October 16

Space Science and Technology Center, Rooms 3-5

ELECTRON-IMPACT CROSS SECTIONS V

Chairman: L. C. Lee (San Diego State University)

P-1 Electron Collisions in Excimer Lasers, D. C. LORENTS, SRI International - Electron collisions play a key role in excimer lasers of all types whether discharge or e-beam pumped. Of particular importance are collisions with excited states that redistribute the populations, moderate the electron temperature, and lead to ionization. Cross section data for most of these excited state interactions are completely lacking even for rare gases and are urgently needed for modelling of excimer laser systems. The status of available excited state cross section information and the needs will be reviewed together with some practical methods of estimating cross sections.

P-2 Applications of Electron Cross Section Data. A.V. Phelps, JILA, NBS and U. of Colorado — We review the use of cross section data for electron collisions with atoms and molecules in models of systems and devices of interest in applied science and engineering. Applications include the understanding and prediction of the properties of the ionosphere, discharge light sources, rf plasma processors, gas discharge lasers, corona chemistry, charged particle beams, and arc discharges and switches. Traditionally, models have used total cross sections as a function of electron energy. More recently, the sophistication of models and of computers have lead to a demand for angular distribution data and for secondary electron distributions resulting from ionization. The use of halogenated molecules in applications renewed interest in electron attachment, elastic and inelastic scattering, and ionization for these species. Electron impact dissociation leading to ground state or metastable products remains a process for which there are few data and considerable need. Similarly, data are needed for all kinds of collisions of electrons with excited atoms and molecules.

P-3 Measurement of Electron-Impact Excitation and Ionization Cross Sections Relevant to Ionized Gas Systems*, DAVID SPENCE, Argonne National Laboratory - The subject of this paper is two-fold. First, we will discuss how high incident energy, forward scattering electron energy loss spectra may be used in a straightforward and direct way to obtain photoabsorption cross sections over extended energy ranges, and how angular scattering measurements may be used, with suitable calibration, to obtain the absolute differential electron scattering cross sections of specific electronic states. Systems discussed will include $HgBr_2$, XeF_2, and Si_2H_6, among others. Second, we will discuss the growing body of evidence that molecular dissociative ionization cross sections can be strongly dependent on the initial vibrational state of the molecule, and that this may be a general phenomena which is usually unaccounted for in the modeling of vibrationally hot plasmas.

*Work supported in part by the U.S. Dept. of Energy, Office of Health & Environmental Research, under Contract W-31-109-Eng-38.

P-4 Electron Collisions with Etchant Gas Plasma Constituents*. K.A. BLANKS and K. BECKER, Lehigh University. - The need to manufacture ever smaller microelectronic devices has given dry plasma etching of silicon and silicon compounds the leading edge over wet chemical etching techniques. Electron collisions with simple halogen-containing molecules, in particular dissociative collisions which produce the etch-active neutral halogen atoms as well as ionic and heavier molecular fragments play an important role in processing plasmas. A detailed knowledge of the break-up mechanisms of the main plasma constituent and of the various electron-impact cross sections for the formation of radiating, metastable and ground state fragments provide invaluable input data for the modelling of the plasma. Results for the fragmentation of NF_3, CF_4 and SF_6 will be presented and possible schemes to measure the cross section for formation of neutral ground state fluorine fragments will be discussed.

*Supported by NSF through grant CBT-8614513.

INDEX OF AUTHORS

TOTAL NUMBER OF PAPERS: 231
TOTAL NUMBER OF AUTHORS: 442